February 2022

Master's Degree Thesis

Mineral phase profiling on accelerated carbonation cured cement paste

Graduate School of Chosun University

Department of Architectural Engineering

Major: Building and Material Engineering

Gebremicael Liyew, Abitew

Mineral phase profiling on accelerated carbonation cured cement paste

급속탄산화양생된시멘트페이스트의광물상프로파일링

February 25, 2022

Graduate School of Chosun University

Department of Architectural Engineering

Major: Building and Material Engineering

Gebremicael Liyew, Abitew

Mineral phase profiling on accelerated carbonation cured cement paste

Advisor: Professor Hyeong-Ki Kim

This thesis is submitted to graduate School of Chosun University in partial fulfillment of the requirements for the degree of

MASTER OF SCIENCE

In

Architectural Engineering

October 2021

Graduate School of Chosun University

Department of Architectural Engineering

Major: Building and Material Engineering

Gebremicael Liyew, Abitew

The Master of Science thesis committee for Gebremicael Liyew Abitew certifies that this is the approved version

Committee:

Professor Chang-geun Cho, Chosun University (sign)

(Chair Committee)

Professor Taehoon Kim, Chosun University (sign)

(Committee Member)

Professor Hyeong-Ki Kim, Chosun University (sign)

(Committee Member)

December 2021

Graduate School of Chosun University

TABLE OF CONTENTS

LIST OF FIGURES

LIST OF TABLES

ABSTRACT

Mineral phase profiling on accelerated carbonation cured cement paste

Gebremicael Liyew Abitew, B.Sc.

Advisor: Prof. Hyeong-Ki, Kim, Ph.D.

Department of Architectural Engineering

Graduate School of Chosun University

Industry gas emission being an issue for many decades. Nowadays, much research has been conducted to utilize the factory's gas, and concrete carbonation curing is one of them. This paper conducted research to utilize CO_2 gas as a concrete curing agent, which will have mutual benefit for the structures as well as environmental contribution. The effect of the accelerated carbonation curing on the phase formation of the later age and early age cement paste was conducted via phase profiling. The study was conducted using quantitative x-ray diffraction (QXRD) and thermogravimetric analysis (TGA).

Mineral phase profiling of the later age and early age cement paste, subjected to accelerated carbonation; was conducted through the depth. The later age carbonation was conducted at 14 or 28 days followed by 14 or 28 days of carbonation, with a concentration of 10% CO_2. The early age carbonation was conducted at 6hr, 1day or 3 days of hydration followed by 1 day or 3 days of carbonation, four CO_2 gas concentrations (5%, 10%, 15% and 20%) were used. In addition, the mechanical (compressive and dynamic modulus) and

further carbonation resistance of the early age carbonated was investigated.

The pre-curing period has a significant effect on the formation of type and amount of calcite on the front surface and through the depth. The pre-curing period determines the concentration of the calcite on the surface. However, the calcite formation on the front surface of specimens is less influenced by the duration of the carbonation. On the other hand, the duration of the carbonation influences the formed calcite through the depth. Overall, the depth of the carbonation in the accelerated carbonation is reached 20 mm in the later age, and 12 mm at the early age. Whereas 3 days and 28 days pre-cured resulted in an approximately similar amount of calcite and vaterite on the surface, which is the maximum total amount of $CaCO_3$ reached up to 40% of the total volume of the paste. The amount of portlandite on the surface is diminished for both conditions. Whereas through the depth, early age carbonated has a relatively greater amount of portlandite which could be due to the hydration after the carbonation was completed.

The mechanical strength does not have increasing consistency as usual throughout the time. This possibly from the dehydration ultimately resulted in a lack of water for anhydrous hydration, basically for lower water to cement ratio. If there is additional further water curing after the carbonation, there will be an improvement.

한 글 요 약

급속 탄산화 양생된 시멘트 페이스트의 광물상 프로파일링

Gebremicael Liyew Abitew, B.Sc.
Advisor: Prof. Hyeong-Ki, Kim, Ph.D.
Department of Architectural Engineering
Graduate School of Chosun University

산업에서의 가스 배출 문제는 지난 수십 년간 많은 환경문제를 야기하였다. 이에 대한 해결 방법의 하나로 최근 공장 배출 가스를 산업에 재활용하기 위한 많은 연구가 진행되고 있으며 콘크리트의 탄산화 양생도 그 중 하나이다. 본 연구에서는 CO2 가스를 콘크리트 양생용 기체로 활용하는 연구를 수행하였으며, 이는 환경적 기여는 물론 구조물의 성능 확보에도 이익이 될 수 있다. 실험을 통해 가속 탄산화 양생이 후기 및 조기 시멘트 페이스트의 내부 물질의 변화에 미치는 영향을 알아보기 위해 광물계 상(mineral phase)에 대한 프로파일링을 수행하였다. 이 때 정량적 X선 회절(QXRD) 및 열중량 분석(TGA)을 사용하였다.

가속 탄산화 처리된 후기 및 조기 시멘트 페이스트의 광물상 프로파일링, 즉 깊이별 물질 분석은 다음과 같은 방법으로 진행되었다. 후기 탄산화의 경우 수화 14일 또는 28일 후 추가로 14일 또는 28일간 10% 농도의 CO_2 조건에 노출 하였다. 조기 탄산화의 경우 배합 직후 6시간, 1일 또는 3일의 수화 후 1일 또는 3일간 탄산화 하였으며, 이 때 4 단계의 CO_2 가스 농도(5%, 10%, 15% 및 20%)를 사용하였다. 조기 탄산화 된 페이스트의 기계적 특성, 즉 압축강도 및 동탄성계수 뿐 아니라, 추가 재탄산화 깊이를 측정 해 이후 가속 탄산화 양생된 콘크리트의

자연 탄산화 저항성을 평가 하였다.

실험 결과, 사전 일반양생 기간은 깊이에 따른 탄산칼슘 결정의 종류와 형성량에 큰 영향을 미치는 것으로 확인하였다. 먼저, 탄산화 양생 전의 일반양생 기간은 표면의 탄산칼슘 발생량을 결정한다. 그러나 일정 깊이 이상의 탄산칼슘 발생량은 탄산화 지속시간의 영향을 덜 받는다. 전반적으로 가속 탄산화에 의한 탄산화 깊이는, 페놀프탈레인 수용액을 이용해 확인한 바 12-20mm 수준이다. 이 결과는 탄산칼슘의 발생량과 연동되었다. 탄산칼슘의 생성량은 탄산화 표면에서 페이스트의 총 부피의 40-50%까지 도달하였다. 표면의 포틀란다이트 양은 두 조기 및 후기 탄산화 조건 모두에서 감소하였다. 한편, 조기 탄산화 시, 탄산화가 완료된 후에도 수화로 인해 포틀란다이트의 양이 추가로 발생하였다.

시간에 따른 물리적 강도 발현은 탄산화 조건에 따른 단순한 선형 변화가 아니었다. 이것은 탄산화와 동시에 발생한 건조로 인한 것으로 판단되는데, 극초기 탄산화 시 수화를 위한 물이 부족했기 때문으로 예상된다. 따라서 탄산화와 동시에 수분 공급이 된다면 물리적 성능 개선에 더 효과적일 것으로 판단된다.

1 INTRODUCTION

1.1 Background

In the ancient civilization the construction of buildings were conducted by placing heavy block of rock on top of another, held in place due to the geometric shape and friction between them. Different binders have been used in the development of Egypt, Greece and Roman civilization (Herrmann and Bucksch [2014]). Nowadays, concrete is the most widely used material in the construction industry, usually made by mixing a hydraulic cement, sand, aggregate, and water as lubricating material (Mehta and Monteiro [2014]). Produced quickly and resulted in reasonable strength and, more importantly, durability makes it a preferred construction material. Production of concrete passes through some processes, starting from preparing the material to curing and finishing works. Concrete technology is applicable in the different construction industries such as buildings, bridges, highways. It has excellent resistance to water without severe deterioration.

Binding material is one of the constituents in the concrete production, typical mix have 15-20 by wt%, and basic material in the integration of each component to function as a unit system. The hydration of the cement plays an essential role in the formation of the C−S−H (gel-like) structure that unites the materials in the concrete. The hydration of cement takes a long time and continues until there is water. Generally, cement requires around 40% by wt for the complete hydration, although half of the water will involve in the chemical reaction (Mather and Hime [2002]).

Initially, some of the water is evaporated based on the humidity, and some of them got stacked as bound water, which can't chemically react. Therefore, concrete curing is a crucial phase in the concrete production process to proceed the hydration of the cement and to create a durable, dense micro-structure (Vijai et al. [2010], Mousa et al. [2015]). There are different types of concrete curing, such as water curing, steam curing, form-work curing, and carbonation curing. Carbonation curing has been used for the precast concrete (Rostami et al. [2011]).

The primary aim of curing is to take care of the fresh concrete in a good moist condition in a suitable temperature range (Zongjin [2011]). In terms of the process of curing, carbonation curing is different from other types of curing. Because, most other curing types aim to preserve or to keep the amount of water or moisture in the cement matrix. Carbonation is the opposite of preserving the water; it evaporates the water during calcite mineral formation. Generally, other types of curing are more of preserving the physical change, but carbonation filling large porosities by chemical change.

The purpose of accelerated carbonation curing (ACC) described clearly on (Al-Kadhimi et al. [1996]). It is to create the fully carbonated dense concrete structure within a short period. The optimum process of accelerated carbonation is affected by different factors. The factors can be classified into physical and chemical; physical, which determine the diffusion process of carbon-di-oxide gas, such as water to cement ratio, microstructure and chemical factors determine the reactivity of the cement minerals and hydration phases of the concrete.

The early accelerated carbonation and later age accelerated carbonation follow a different pattern of phase development and decalcification. In early age carbonation, the anhydrous is simultaneously exposed to carbonation and hydration. Whereas, in later age carbonation, the majority percentage of anhydrous is almost consumed by the hydration and then the hydration products exposed to carbonation.

Accelerated carbonation at an early age or later age plays a vital role in the improvement of durability and mechanical strength by changing the cement microstructure. Studies showed that the formed calcite in the accelerated carbonation improves the microstructure of the cement specimens with reducing large porosity.

Although the consumed amount is small relative to the gas emission of the cement industry, the carbonation curing can have its contribution to the reduction of the gas to the environment.

1.2 Research objective

The fundamental objective of this thesis is to contribute an investigation in the utilization of industry CO_2 as a concrete curing agent. Primarily, the paper is focused on the phase changes of cement paste due to early, and later age accelerated carbonation. In addition, the study incorporates the mechanical and further carbonation resistance of carbonation curing. In detail, the study addresses:

The effect of later age concrete accelerated carbonation on the micro structural change was investigated.Evaluation of carbon capture of the accelerated carbonation cement paste. The study was conducted using phase profiling through the depth of the specimen.

For utilizing the industry CO_2 at the early age accelerated carbonation curing, an investigation was conducted to determine a preferable combination of pre-hydration and carbonation effect on the micro-structural development through phase profiling. The formation of mineral phase composition of the early age accelerated carbonation curing through the depth of concrete was determined. The paper shows the effect of the timing approach (pre-hydration plus carbonation curing) on the formation of the phases in the cement paste.

The effect of the accelerated carbonation on the mechanical and gas permeability resistance was investigated. The strength development of the accelerated carbonation curing was investigated at the age of 7, 14 and 28 days. Durability (resistance to permeability of the gas) effect of the accelerated carbonation curing was investigated. The resistance of the accelerated carbonation curing specimens were exposed to further carbonation for 28 and 56 days.

In accelerated carbonation curing, phase profiling is important because the mineral composition and the way they integrate determine the structure's mechanical and durability. In addition, the carbon capturing capacity of each curing condition.

1.3 Thesis Layout

Chapter 1 : Introduction. It gives a general introduction about concrete, curing methods, carbonation curing, and its application in terms of durability and strength development.

Chapter 2: Literature Review. Different studies regrading the mechanism of cement hydration and carbonation were reviewed.

Chapter 3 : Preliminary investigation of the later age carbonation effect on the phase formation of cement paste. The specimens were hydrated for 14 and 28 days and followed carbonation for an additional 14 or 28 days. Phase profiling were used to determine the phase composition.

Chapter 4: Early age accelerated carbonation curing and its application was investigated. Early age hydrated samples were exposed to 5%, 10%, 15% and 20% concentration of CO2. In addition, their mechanical and gas permeability resistance was addressed.

2 LITERATURE REVIEW

2.1 Introduction

In this chapter different articles related to cement hydration and accelerated carbonation is reviewed. Generally, three categories are used to classify and to sort applicable reference documents. Firstly, the fresh cement paste studies related to hydration are explored. Next, an investigation is conducted on the mechanism of natural and accelerated carbonation. They have similar phase formation, but the amount and the depth penetration is extremely different. The concentration in the natural carbonation is too much lower compared to the accelerated. Finally, the application and drawbacks of accelerated carbonation curing is addressed.

2.2 Cement hydration

2.2.1 Introduction

The mechanism of cement hydration is a complex physicochemical process; there is no full understanding yet. The hydration of cement involves some chemical reactions; the initial hydration stage starts with dissolution, surface hydrolysis, and release of ions into the solution and has a very rapid exothermic reaction. The formation of hydrate coating on the surface retarded decelerates the dissolution. After its initial setting, nucleation and growth of main hydration products accelerate and continue formation into large empty space and creates densified microstructure (CHATTERJI and RAWAT [1965]). Figure 1

shows the time dependant kinetic mechanism of cement hydration measured via calorimetry. The portlandite and C−S−H nucleation phase is going on in the acceleration and deceleration phase of cement hydration (Barnes and Bensted [2002]). Portlandite nucleation and growth become rate-controlling, indirectly the growth and development of C−S−H controlled by it (Bullard et al. [2011]).

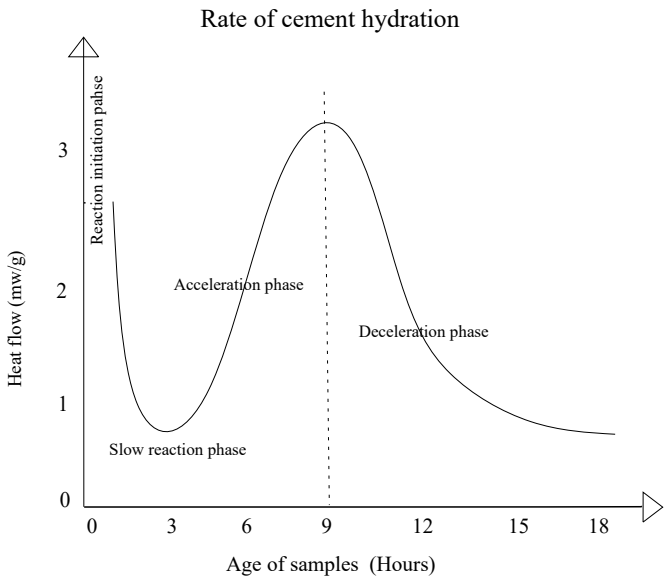

Figure 1: Heat flow of cement hydration via calorimetry measurement (Bullard et al. [2011])

Table 1 shows the typical chemical reactions during cement hydration. The hydration reaction accepts the formed principles of chemical thermodynamics and kinetics (Scrivener and Nonat [2011]).

Table 1: Typical chemical reactions during OPC hydration (Papadakis et al. [1992])

Reactants	Products
$2\,C_3S + 6\,H \xrightarrow{r_{H,C_3S}} C_3S_2H_3 + 3\,CH$	
$2C_2S + 4\,H \xrightarrow{r_{H,C_2S}} C_3S_2H_3 + CH$	
$C_4AF + 2\,CH + 2\,C\bar{S}H_2 + 18\,H \xrightarrow{r_{H,C_4AF}} C_8AF\bar{S}H_{24}$	
$C_3A + C\bar{S}H_2 + 10\,H \xrightarrow{r_{H,C_3A}} C_4A\bar{S}H_{12}$	
$C_4AF + 4\,CH + 22\,H \xrightarrow{r_{H,C_4AF}} C_8AFH_{26}$	
$C_3A + CH + 12\,H \xrightarrow{r_{H,C_3A}} C_4AH_{13}$	

2.3 Mechanism of concrete carbonation

2.3.1 Introduction

Carbonation of concrete involves gaseous, dissolved, and solid reactants. The hydration products as well as the anhydrous phases involve in the process. Solid reactants including hydration product of cement paste (Portlandite and C−S−H), main strength contributors of cement ingredients (C_3S and C_2S) (Papadakis et al. [1989]). Figure 2 shows a simple illustration of the carbonation mechanism. The CO_2 diffuses to the pores and cracks of the concrete specimen and forms H_2CO_3 by dissolving with the pore solution. The carbonic acid converts to the carbonate ion which is active to react with Ca^{2+} and forms the calcium carbonate mineral inside of the pores of the concrete (Jeong et al. [2019]).

The carbonation of C−S−H and $Ca(OH)_2$ gives a continuous declassification of the compounds and formation of Ca-modified silica gel and calcium

carbonate. The polymerization of the C−S−H to ca-modified silica gel and calcium carbonate formation increases as the concentration of the carbon-di-oxide increase.The carbonated C−S−H have a lower ca(near to tobermorite) ratio than the uncarbonated samples. For carbonation concentration with 10% and 100% was conducted, the C−S−H was completely consumed by the carbonation process and formed a polymerized Ca-modified silica gel. The carbonation with 3% is more similar microstructure formation with the environmental carbonation (0.03 % by volume) compared to concentration of 10% and 100% (Castellote et al. [2009]).

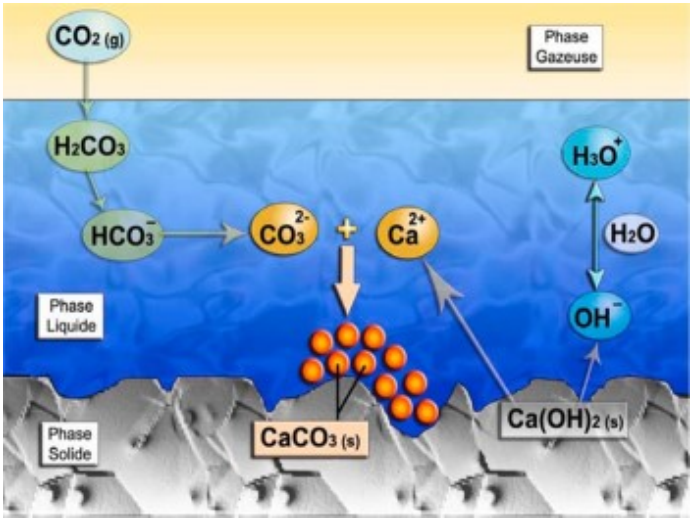

Figure 2: Typical illustration of carbonation mechanism in the pores of cement paste (Jeong et al. [2019])

Natural carbonation and accelerated carbonation curing have different mechanisms and effects of carbonation on the concrete structure. In early accelerated carbonation: a high concentration of carbon-di-oxide gas is applied to the matrix of cement paste which greatly affects the rate of cement min-

erals and hydration products composition at an early age. However, both the natural and accelerated carbonation have similar changes in phase collection and microstructure development (Shah et al. [2018]).

The CO_2 gas diffuses from the environment to the concrete through the air-filled pores of the hardened paste following the Fick's law (diffusion of the gas from high concentration to low). It dissolved with the film of water which shields the wall of a pore. The portlandite diffuses from regions of the gel phase, which have high alkaline, to the low alkaline pore water. (Papadakis et al. [1992]).

2.3.2 Chemical reactions during carbonation

The chemical reaction of the carbonation is neutralization reaction between the cement compounds which is existed in the basic state with carbonic acid (Chatterji et al. [2002]). In addition to portlandite, anhydrous (C_3S ,C_2S,C_3AC_4AF) and hydrate solid phases (C−S−H,AFt and AFm) are participated in the carbonation (Papadakis et al. [1989]). C−S−H formed from the early carbonation has similar stoichiometry with the hydration (YOUNG et al. [1974]). In stoichiometry analysis, the amount of C_3S remained after 12 hydration is equivalent to 3 min carbonation (YOUNG et al. [1974]). The predominant factor for the hydration of specimens in the pre-curing duration. The carbonation reaction in the cement paste simplified and expressed in the Table 2.

Table 2: Chemical reactions during OPC carbonation

Reactants	Products
$C_3S_2H_3 + 3CO_2 \xrightarrow{r_{C-S-H}} (3\,CaCO_3 \cdot 2\,SiO_2.\ 3\,H_2O)$	
$Ca(OH)_2 \xrightarrow{r_D} (Ca^{2+}(aq) + 2\,OH^-(aq))$	
$Ca^{2+}(aq) + 2\,OH^-(aq) + CO_2(g) \xrightarrow{r_{CH}} CaCO_3(s) + H_2O$	
$C_3S + 3CO_2 + xH_2O \xrightarrow{r_{C_3S}} SiO_2 \cdot xH_2O + 3CaCO_3$	
$C_2S + 2CO_2 + xH_2O \xrightarrow{r_{C_2S}} SiO_2 \cdot xH_2O + 2CaCO_3$	

2.3.3 Numerical modeling

Different models were developed to predict the carbon-di-oxide penetration depth during the process of accelerated carbonation. Model investigation was conducted on different cement and concrete parameters (water/cement, aggregate/cement ratio) and environmental factors (relative humidity and concentration of CO_2) to show the propagation of carbonation depth with time-dependent function (Papadakis et al. [1992]). From (Papadakis et al. [1991]) reaction model, the depth of carbonation is expressed as

$$Xc = \sqrt{(}(2[CO_2]De, CO_2, c)/([Ca(OH)_2]+3[C-S-H]+3[C_3S]+2[C_2S]))x\sqrt{(}t)$$

$$X(c) = Ax\sqrt{(}t)$$

In addition to time, the constant empirical expression also varies for each paste composition. In the Papadakis 1991 mathematical model, the rate of the

carbonation was predicted using the chemical composition of cement, porosity, pore size distribution, and the external environmental conditions including concentration of the CO_2 gas, temperature and relative humidity (Papadakis et al. [1991])

2.4 Factors affecting accelerated carbonation of cement paste

2.4.1 Properties of the material

There are different factors, which influence the rate of carbonation. Chatterji et al. [2002] listed the most important ones. Cement amount in the paste and its type are the main factors in the carbonation process and they can be categorized under the material characteristics. The porosity type and distribution of the paste is strongly affected by the water/binder ratio and binder types (Ngala and Page [1997]). Higher water to cement ratio increase the carbonation rate.

An increment of strength, density, modulus of elasticity and shrinkage was observed due to carbonation (An Jerga [2004]). This carbonation increment is proportional to the amount of cement content in the fresh mix. The concentration of the gas (up to 20%) is proportional to the relative increment of OPC cement solid volume. In OPC cement, the total porosity is reduced (Shah et al. [2018], Auroy et al. [2015]). The durability of concrete structures (shrinkage, creep, cracking and transport properties) is strongly dependent on porosity.

Binding material characteristics affect the hydration and carbonation rate as well as the mechanism of porosity reduction. The total porosity of OPC, OPC-30% of fly ash and OPC-65% ground granulated blast furnace slag was reduced due to the deposition of the calcite. The formed calcite has high volume than the hydrated phases of the cement, which used to clog the porosity of the material. The ratio of capillary pores for OPC shows no significant increment, but OPC-30%PFA and OPC-65%BFS increased by 140% and 230% respectively (Ngala and Page [1997]).

In an experiment which is conducted by (Wu and Ye [2017]), different types of binding materials were considered with blending with the OPC. In the blended cement paste the amount of the portlandite is smaller than the OPC and the carbonation is dominated by C−S−H with low ca content. The porosity of cement paste increases due to the carbonation of most C−S−H. Therefore, the change in the microstructure is mainly due to the carbonation of C−S−H with a high or low ca/si ratio. The total porosity and effective porosity of the paste are highly influenced by the amount of C−S−H involved in the carbonation.

Dilution effect and the pozzolanic reaction of supplementary cementitious materials (SCMS) reduce the amount of portlandite than the portland cement paste. In one year hydration period, the portlandite of the OPC is greater than the SCM, which leads to high production of calcite in the carbonation time (Wu and Ye [2017]).

2.4.2 Permeability of the concrete

Permeability is the transportation of gases, water, dissolved ions to the internal section of the concrete. Figure 3, shows material and environmental factors that control the transportation mechanism in the concrete structure (Bertolini and Polder). The porosity, which developed from the loss of a water, is one factor that controls the diffusion of the gas. Generally, permeability is dependent on the porosity of the material. However, permeability will not necessarily be reduced by lowering the porosity (Matschei et al. [2007]).

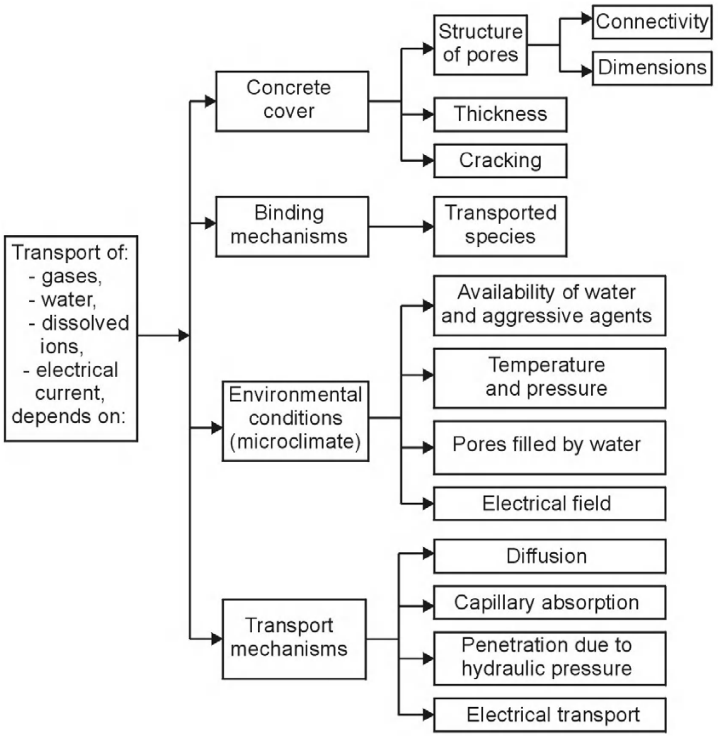

Figure 3: Basic factors that affect the transportation process in concrete (Bertolini and Polder)

In addition, shrinkage cracking due the carbonation also influence the transportation process. The consumption of CO_2 increases when the water to cement ratio gets higher. It may be due to the evaporation of the water that ultimately causes pores and shrinkage in the cement matrix.

The diffusion rate of the CO_2 is also affected by the presence of aggregate (Papadakis et al. [1989]). In the concrete, the availability of the aggregate will influence the rate of gas diffusion, which indirectly affects the rate of carbonation.

2.4.3 Carbon di-oxide concentration and relative humidity

Concentration of CO_2 and relative humidity has an essential factor in accelerated carbonation (Ashraf [2016]). The rate of the reaction increase as the CO_2 pressure increases. The compressive strength doubled when the pressure of the gas doubled. However, the increment of the gas pressure to 4 atm had a small effect (YOUNG et al. [1974]). In addition to concentration, relative humidity has a significant impact. For the early age carbonation, the amount of aqueous or water content of the specimen influences the diffusion of the gas. The diffusion CO_2, basically at an initial stage, is influenced by losses of the water(An Jerga [2004]).

It has been well known that the aqueous content in the specimen pore highly depends on the relative humidity. The reaction of CO_2 is promoted in some amount of water. However, low relative humidity limited the hydration reaction and the carbonation, but high relative humidity limited the carbona-

tion reaction by preventing the diffusion of the gas. The study by Phung et al. [2013] shows that fully saturated samples has slow rate of carbonation and the permeability decreases by one order of magnitude.

The required optimum water in the pores should have enough amount to provide a medium for a reaction between the portlandite and CO_2 . On the other side, it should not be exceeded to block the diffusion of the gas. At low relative humidity, the pores are dried which the CO_2 gas diffuses very fast; however, the rate of carbonation is very slow due to the lack of moisture in the pores. On the other hand, high relative humidity filled the pores with water, blocking the diffusion of the gas. The diffusion coefficient depends on the pore humidity and highly decreased for the pore humidity from 0.9 to 0.6, but it is almost constant below 0.6 (Bavzant and Najjar [1971]).

Based on (Al-Kadhimi et al. [1996]) investigations, two steps were involved in controlling the uncertainty regarding the rate of carbonation: (a) Preconditioning to lower the relative humidity could be used to shorten the diffusion time of the carbon-di-oxide, dissolve in the pore water and react with hydration product and anhydrite minerals. (b) Carbon di-oxide at high pressure increases the solubility of the carbon-di-oxide in water. Except the lag period, C_3S and C_2S follows similar behavior in the carbonation process (YOUNG et al. [1974]).

2.5 Application of accelerated carbonation for concrete

2.5.1 Introduction

Accelerated carbonation has been used for production of sustainable construction materials such as recycled aggregate production, industrial wastage management by changing in to solid forms and used as a curing agent for pre-cast concrete production. Studies shows that, carbonation curing has an enhancement in the durability, and strength.

2.5.2 Durability

Different studies have been conducted on the application of carbonation regarding durability improvement. The accelerated carbonation cured concrete revealed resistance to chloride attack, sulphate attack, ion migration, and freeze-thaw damage (Rostami et al. [2012]). The SEM-EDS and Thermodynamic model investigated by (De Weerdt et al. [2019]) shows that the decalcification of C−S−H increases the uptake of alkali metals to the formed carbonation solid. Accelerated carbonation concrete gives a better improvement on the surface property (sorptivity, water absorption, abrasion resistance) of concrete (Sharma and Goyal [2020]). Carbonation decreases the surface fractal dimension, whereas the specific surface area changes based on the composition of the binder (Arandigoyen et al. [2006]).

Studies from (Wu and Ye [2017]) shows that, the level of permeability reduction of the carbonated cement paste strongly depends on the cement type. Although, the carbonated OPC cement and blended cement decrease the effective capillary porosity. Whereas the total porosity decreases for P100 and F30 (30% fly ash) replacement approximately by 5% hence, the portlandite involves in the carbonation than C−S−H. The OPC cement pore diameter reduces to medium capillary pore (0.04um), whereas the blended cement pore diameter is larger (0.4-0.5) um (Wu and Ye [2017]). The carbonated OPC cement shows a reduction in total porosity, whereas due to the lack of portlandite in Pozzolanic Portland Cement (PPC) and Limestone Calcined Clay Cement (LC3) the porosity is increased. Figure 4, shows that the carbonation effect in the reduction of the porosity. However, the crack propagation will increase proportionally with the degree of carbonation(Han et al. [2013]).

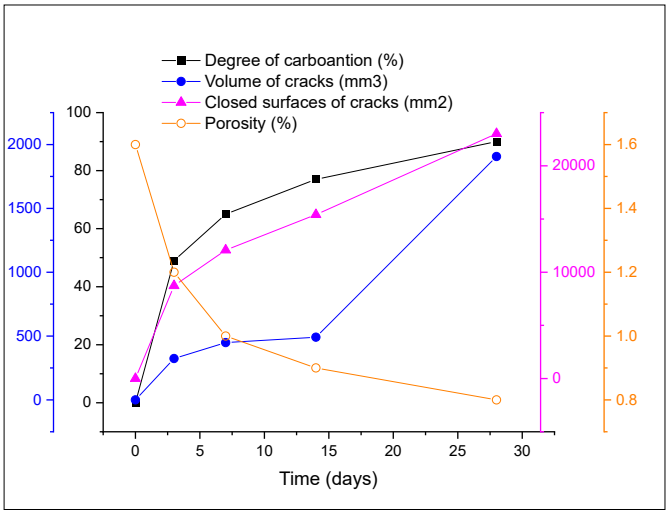

Figure 4: Degree of carbonation and its effect on the cracks and porosity (The data used from (Han et al. [2013]))

The carbonation reduces the porosity around 10%, the amount of portlandite carbonated was proportional with the decreased pores (Vol%.) (Arandigoyen et al. [2006]). The carbonation results increasing in solid volume until all portlandite in the cement matrix is consumed (Shah et al. [2018]). The carbonation of most C−S−H species will increase the cement paste porosity, and its porosity is significant when the C−S−H have low Ca, which is why the blended cement pastes have relatively high porosity in case of carbonation curing than the OPC. The porosity of the blended cement has an increment when the replacement percent is increased (Wu and Ye [2017]).

2.5.3 Mechanical strength

Concrete is a heterogeneous composition of different materials; its strength is affected by many factors: Generally, they can be classified as internal and external factors. Internal factors include the composition of materials (raw materials, proportion between the raw materials, and additional admixtures) and the interface between them. External factors include curing time, curing type, and duration (Zongjin [2011]).

Based on the study of (Raheem et al. [2013]), the effect of curing on density and compressive strength of concrete was investigated using six methods of curing such as water submerged, air curing, spray curing, polythene curing, moist sand curing, burlap curing. The study shows that moist sand curing resulted in the highest strength, whereas air curing produced the lowest strength of all types. However, the correlation between density and compressive strength is weak.

Exposing C_3S and β-C_2S to CO_2 leads to rapid strength development (YOUNG et al. [1974]). The effect of early age carbonation curing on the lightweight concrete was investigated (El-Hassan et al.). The samples which don't initially cure absorb around 8.5 % while the 4 hr initial curing specimen absorbs around 22 to 24 % CO_2 and the four-day initial curing absorbed around 35 %. Based on their investigation, the carbonated specimen shows higher early-age strength, but due to the water loss, the strength reduced on its 28th day relative to the steam and hydrated specimens.

2.6 Drawbacks of accelerated carbonation

2.6.1 Shrinkage

The shrinkage and volume stability due to carbonation depends on paste maturity, aggregate compressibility, water to cement ratio, and relative humidity (Kamimura et al. [2015]). Based on the (An Jerga [2004]) investigation, the shrinkage increment due to carbonation is reached 35%.

2.6.2 Corrosion

Corrosion decreases the reinforcement bar available cross-section area, which decreases its strength. The pH value reduction of pore water below 9 results dissolution of the protective layer and activation of the bars to corrosion (Papadakis et al. [1992]). When the volume of corrosion product is greater than corroding material, it causes an internal pressure which results in the rapture of the concrete and ultimately causes a crack, spalling, and loss of bond

between the concrete and the bar (Papadakis et al. [1989]). The alkalinity (pH) of the inner part of the concrete recovered from the later hydration reaction. While on the surface, all the mineral compositions of cement and the hydrated phases are totally carbonated, which it creates stable calcite that can't undergo any hydration or chemical reaction with the environment.

3 LATER-AGE CARBONATION OF CEMENT PASTE

3.1 Introduction

In this chapter results from the later age hydrated cement paste carbonation is discussed. The cement pastes were initially cured for 14 or 28 days. After completed their hydration period, the samples were exposed to 10% CO_2 concentration for further 14 and 28 days. Phase profiling was used to determine the composition of the paste through the depth with 5mm interval. In each layer of the paste, the remained amount of water, the amount of water absorbed, the initial phase formation from the reference, the change in their phase after carbonation which is basically the increment of $CaCO_3$, mono-carbonate and, and hemi-carbonate is discussed. On the other hand, the reduction $Ca(OH)_2$, $C-S-H$,C_2S, C_3S other cement minerals were quantified through the depth. [1]

3.2 Experimental program

3.2.1 Material and specimen preparation

The paste was prepared using commercial portland cement, which Blaine fineness of 3,430 cm2/g and has a specific gravity of 3.12. The performance of cement (including strength and setting time) has satisfied Korean Standard (KS) L 5201, as well as ASTM C 595 Type I(SM) and CEM II/B-S 42.5. The

[1] This chapter reproduced from the submitted article on Journal of Case studies in construction materials with title of "Phase profiling of carbonated cement paste: quantitative x-ray diffraction analysis and numerical modeling"

initial and final setting of the cement is 3.5h and 6.0h, respectively. The cement has a compressive strength of 41.1 MPA, 47.2 MPa, and 58.0MPa, which is measured according to ISO 679:2009 at 3, 7, and 28 days respectively. The chemical composition of cement detected by Quantitative X-ray Diffraction (QXRD) and X-ray Fluorescence (XRF) is described by weight percentage in the tables below.

Table 3: Oxide composition of cement obtained from XRF.

Composition	**wt.-%**
CaO	64.50
SiO_2	17.30
Al_2O_3	4.36
Fe_2O_3	3.70
MgO	2.51
Na_2O+ K_2O	1.23
SO_3	3.25
Cl	0.06
Loss on ignition	2.16
Etc.	0.83

Table 4: Phase composition of commercial cement obtained from QXRD.

Phase	**wt.-%**
C_3S	40.9
C_2S	10.8
C_4AF	8.4
C_3A	3.9
Calcite	4.6
Gypsum	1.6
Hemihydrate	1.3
Anhydrite	0.5
Thernadite	0.1
Ettringite	0.1
Amorphous	25.0

The cement paste was prepared using deionized water with a water to ce-

ment ratio of 0.5. The agglomeration of the cement particles was controlled by adding water slowly until the cement lumps were fully dispersed. In addition, the bleeding of the paste was managed by continuously mixing the mixture for more than 1.5h. Four types of specimens were prepared based on the permutation of two types of hydration and two types of carbonation. Two types of hydrations were 14-day hydration or 28 hydration. Following the end of hydration, two types of carbonation proceeded, those are 14-day carbonation or 28-day carbonation for each hydration condition. The naming of the specimens were referred as "14H-14C","14H-28C","28H-14C", and "28H-28C". As a reference, one specimen from each hydration condition without accelerated carbonation was prepared. The 40X40X160 mm3 prism samples were prepared and coated with epoxy at the age of one day. The specimens were cured at a temperature of 20°C for 14 or 28 days and then cut using a diamond saw in half. The cut samples were exposed in the carbonation chamber with 10% CO2 gas concentration, 20°C temperature, and 55% relative humidity. It was exposed for 14 days and 28 days in accelerated carbonation. After completing the carbonation, the specimens were submerged into isopropanol to prevent further hydration until profiling. The hardened cement paste specimens were drilled using a 12 mm mechanical drill bit.

The specimens were drilled and collected approximately 10-20gm of cement powder at every 5±1 mm depth. The depth was measured using a digital meter. The powder was collected from two similar prism specimens and sieved with a 0.75 mm sieve. The prepared powder was submerged in isopropanol again for three days. The submerged powder samples were dried using a vac-

uum chamber at 50°C for 2-3 days to evaporate the isopropanol prior to the material characterization tests. The vacuum chamber has a 65 L capacity and 60L/min vacuum pumping speed. In the chamber, a pressure of 5.9 X 10^-5 atm was maintained.

3.2.2 Phase characterization test

The material characterization test was conducted using QXRD and Thermograivmetric analsysis (TGA). QXRD test was conducted by X'Pert PRO MDP (PAN analytical). The test was conducted at 40 kV and 30 mA. The specimens were scanned from 5 to 65 in a 2 θ range at a step size of 0.013°/step. The scanning time for the QXRD was 1.5 hr. External standard method using rutile (Jansen et al. [2011]) was used to quantify the amorphous content in the specimens. The powder sample's mineralogical composition was determined using a scale factor of the rutile and mass absorption coefficient (MAC). The Rietveld refinement was conducted using HighScore Plus ver. 4.8 software (Pananlytical B.V). Structures of the phase used for the refinement are attached in the Appendix B section. The determined result of the QXRD was re-normalized based on the bound water, TGA test was conducted for each depth of the specimen to determine the amount to the bound water and it was expressed per unit mass of anhydrous (gm/100gm OPC). The TGA test was conducted using the DTG-60H model (Shimadzu Corp.). The temperature was ranged from room temperature up to 1000℃, and the temperature rate was increased by 10℃/min. Figure 5 shows the TGA test result of the OPC and hydrated paste and Figure 6 shows the carbonated paste up to the

depth of 20 mm.Hence, after 20 mm they have approximately similar TGA loss.

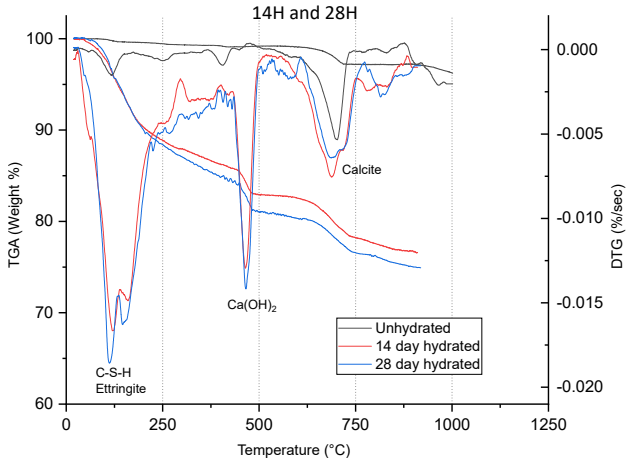

Figure 5: TGA result of unhydrated and hydrated at 14 and 28 days

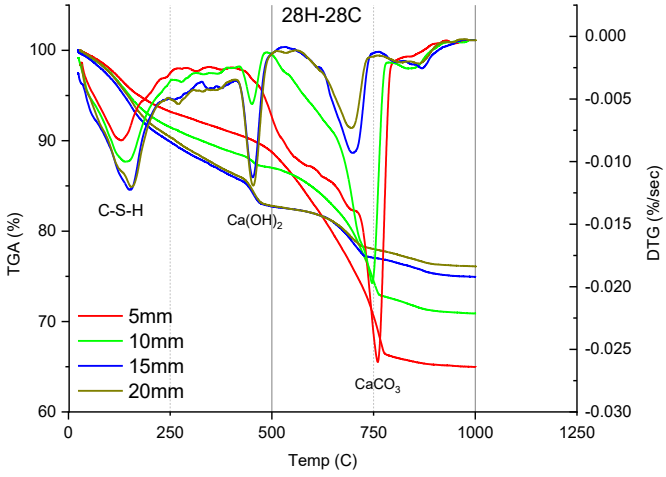

Figure 6: TGA result of 28 days hydration and 28 days carbonation

The Axios-minerals model (PANalytical B.V) X-ray Fluorescence (XRF) was used to determine the oxide composition of the commercial cement. The

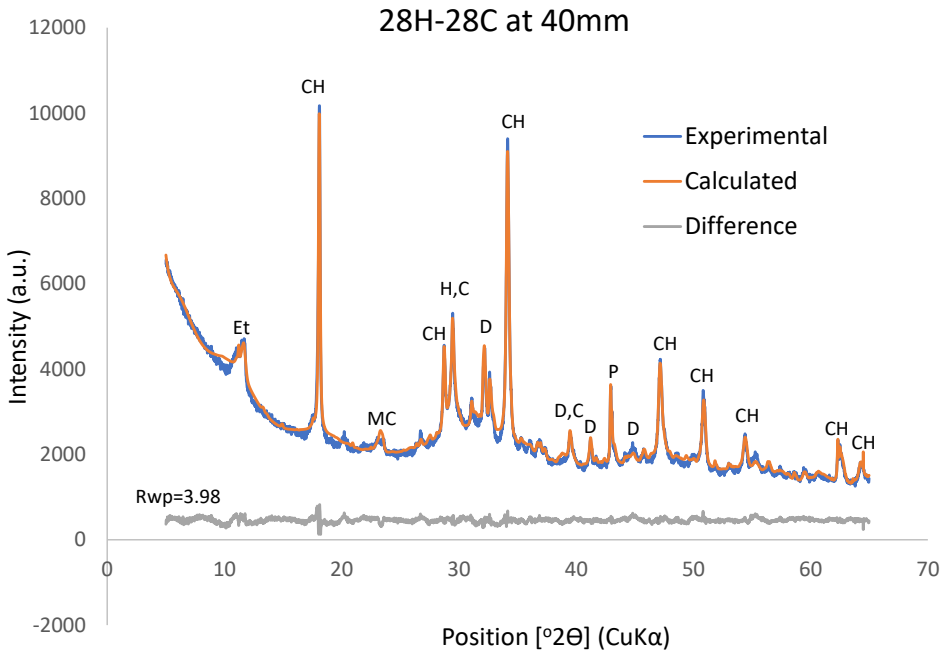

Figure 7: QXRD of 28H-28C at 40 mm depth (Et= Ettringite, CH= Portlandite, MC= Monocarbonate, H= Hatrurite, C= Calcite, D= Dicalcium silicate, P= Periclase)

X-ray generator has 60KV and 125mA, and the detector has the flow counter 13°to 148°2θ and a scintillation counter 8°to 104°2 θ, 22Ti $\sim$ 92U were used.

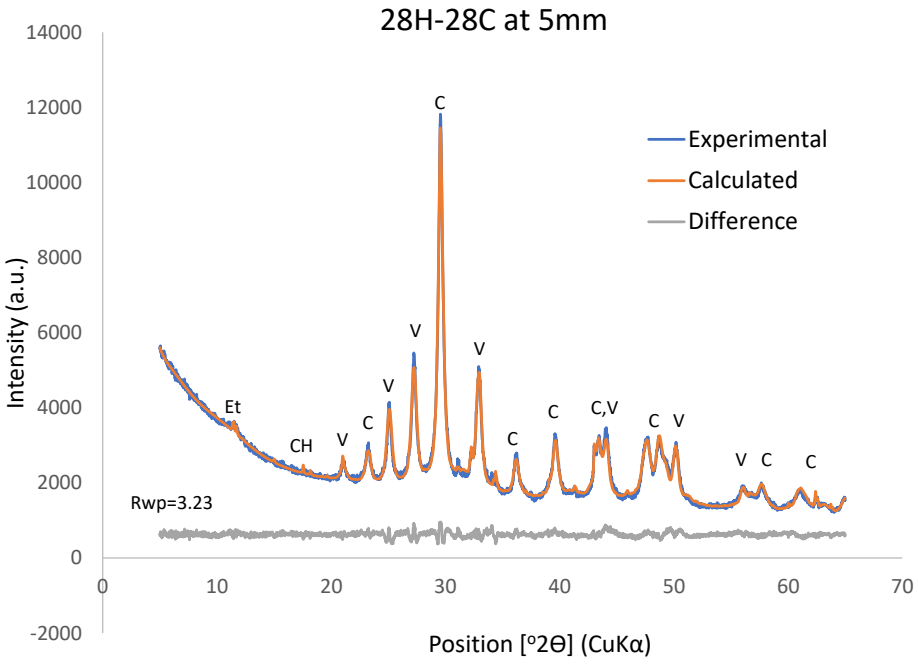

Figure 8: QXRD of 28H-28C at 5 mm depth ((C= Calcite, Et= Ettringite, CH= Portlandite, V= Vaterite)

3.3 Result and discussion

The profile of various phases by the depth of the carbonated specimens determined from QXRD analysis is described below. The free water and the acquisition of the gas strongly depend on the depth. The formed calcite evaporates the water as well as reduces the large porosity, which will affect the diffusion of the gas. In addition, the removal of water on the surface will decrease the relative humidity of pore structures and the rate of the reaction on the surface. The analysis begins from the summary of each curing condition regarding their gas absorption capacity. Figure 9 shows the free water remained

after hydration and calcite formation,and Figure 10 shows the amount of CO_2 absorbed in each curing conditions. As the graph shows, on the surface the amount of water is evaporated and replaced with CO_2, where this reduces logarithmic-ally through the depth. The calcite concentration on the carbonation front surface was reached to 56 % (gm/100gm OPC) in 14H-14C, 62.6% in 14H-28C, 61.3% in 28H-14C, and 61.1% in 28H-28C. Overall amount absrobation was estimated on Figure 11 show that the total amount of CO_2 gas absorbed in the 40 mm depth of specimen per meter cubic. Overall, specimens that were carbonated for 28 days absorbed a greater amount. Especially, 14H-28C has a higher amount of cumulative gas acquisition of all other conditions. On the other hand, specimens that are hydrated for 28 have better resistance. The formed dense C-S-H in the system could reduce the diffusion of the gas. In addition, the calcite formation of the C-S-H depends on the concentration of Ca, which is high or low.

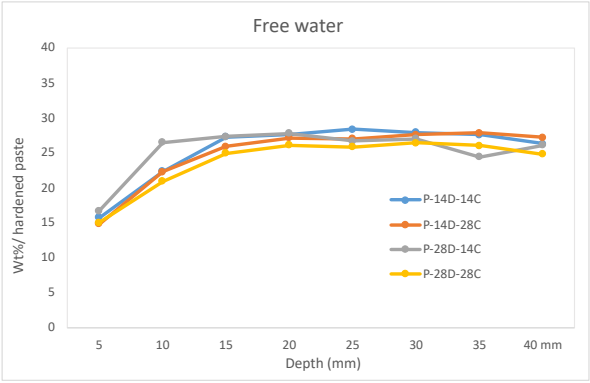

Figure 9: Free water content in the carbonated specimens

The remaining amount of C_3S and C_2S was detected, the remaining amount of anhydrous based on the QXRD analysis is approximately 6% vol. However,

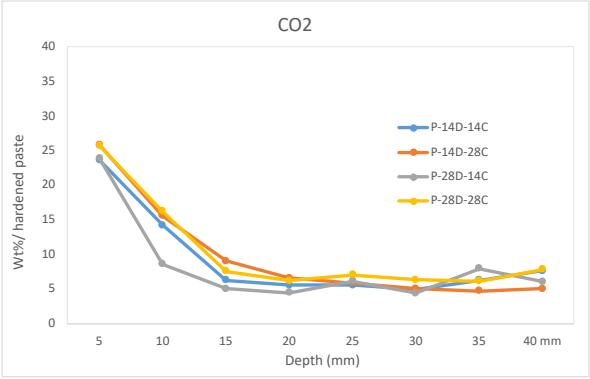

Figure 10: CO2 acquisition through the depth

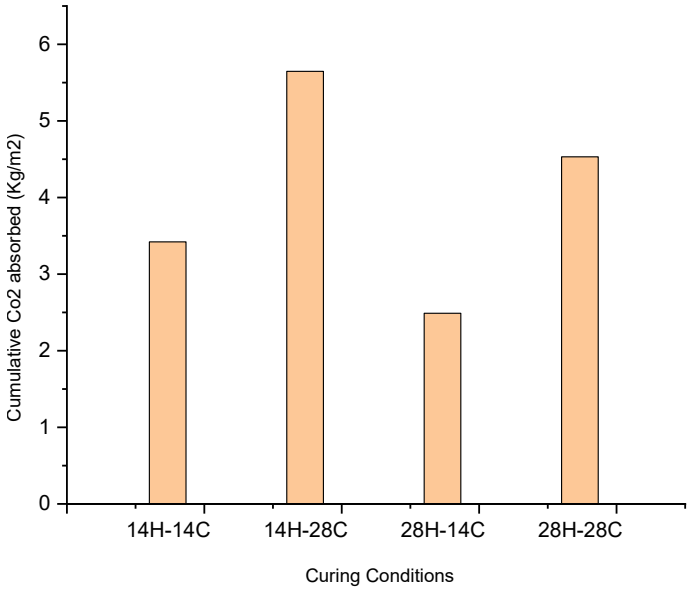

Figure 11: Cumulative CO2 gas acquisition through the specimen

it is barely available on the carbonation front surface due to the hydration and carbonation. In addition, the residual amount of C_3A and C_4AF is nearly empty throughout the depth due to enough amount of cement hydration. anhydrous show the remaining amount of unhydrated phases. The amount of C_2S obviously relatively reduced during 28 days of hydration than 14 days.

The amount of C_3S consumed both on the surface and through the depth, nearly totally consumed during the hydration period, it shows independence of C_3S on the carbonation period in the later age carbonation.

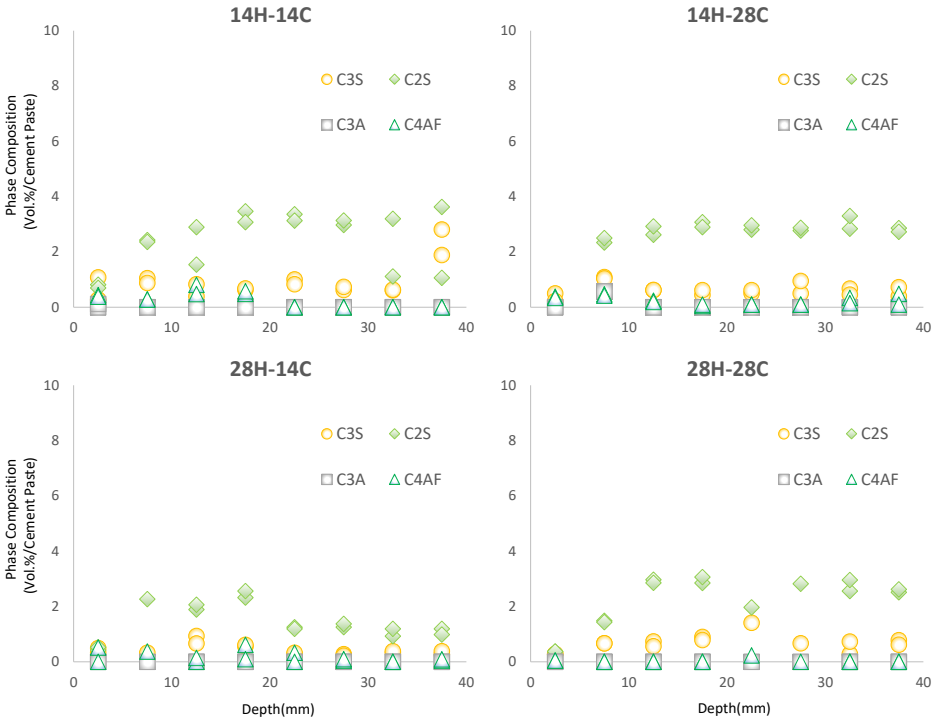

Figure 12: Anhydrous phase composition

The initial amount of $CaCO_3$ in the cement was less than 3%. In the carbonation front, both calcite and vaterite were clearly observed in a large amount.28 day hydration has higher amount of vaterite formation than 14 days. As studies of (Auroy et al. [2018]) shows that, the formation of the Vaterite is from the carbonation of C-S-H. In natural carbonation, calcite is mainly precipitated from the carbonation, whereas in accelerated carbonation, vaterite and aragonite, which is a polymorph of calcite is also formed.

Figure 13 illustrates the formed calcite polymorph for each curing conditions. The domination of the calcite and vaterite is clearly visible on the graph. The duration of the carbonation has slight effect on the surface of 14 days hydration and almost negligible impact on 28 days hydration. However, up to 20 mm the depth of the carbonation was highly depends on the duration of the carbonation in both curing types. After the depth of 20 mm, the amount is reduced and barely available. In addition, some amounts of mono-carbonate and hemi-carbonate were determined with less than 3% and slightly decreased on the surface.

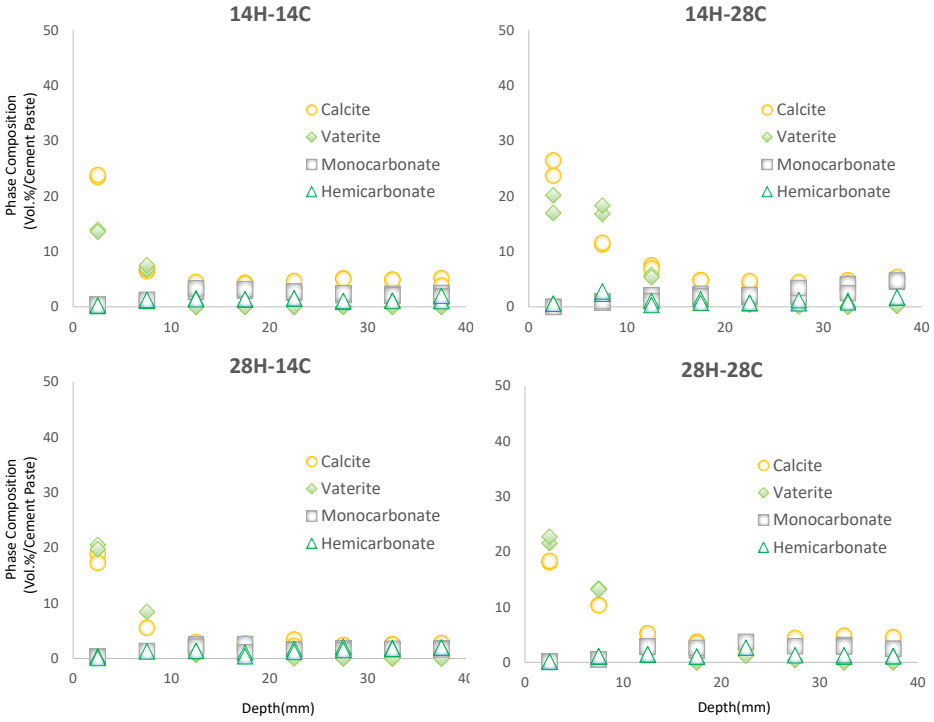

Figure 13: Calcite formation at different condition of curing

Figure 14 shows the trend of the amorphous and portlandite, reduced on

the surface. The amount of portlandite was diminished on the surface for all types. On the top surface (within 5mm) reduced to nearly 0% and at the depth between 15mm-40mm, the concentration of the portlandite is between 10%-15%. The duration of the carbonation reduced the amount on the next layer. The amorphous was consumed and reached to 20-30%. The duration has higher influence in 14 days than 28 days of hydration. The amorphous in this cement paste contained three types: these are C-S-H, anhydrate slag, and unidentified trace minerals. The amount of the slag could be considered negligible. The degree of hydration of slag in slag cement is almost similar to that of cement (Feng et al. [2004],Yio et al. [2014]). Based on the common knowledge of cement chemistry, the amount of unidentified minerals by QXRD could have an insignificant effect. As a result of these considerations, the amount of C-S-H amorphous, which is estimated from 30% to 70% was resulted from clinker hydration and reaction between slag and $Ca(OH)_2$.

Figure 15 shows summary of the amount of portlandite, calcite, C-S-H, and CO_2 in all curing conditions. Overall, all show similar characteristics. Portlandite is not available on the surface and reached approximately 10% by vol%. The amount of the C-S-H reduced to between 20 and 30% on the surface. In contrast, the calcite formed around 40% of the total volume.

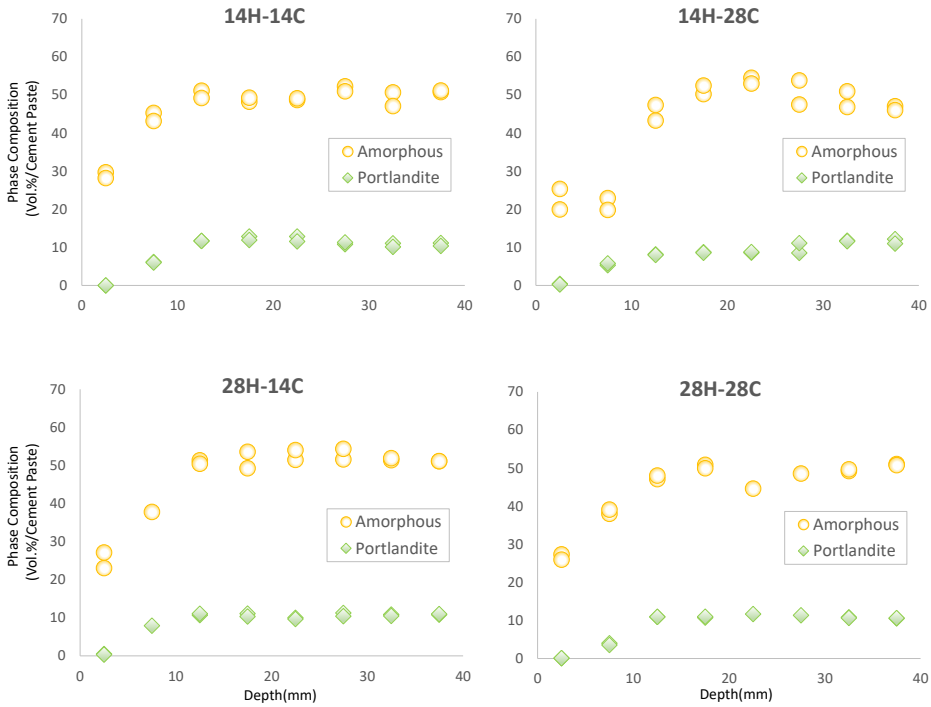

Figure 14: Amorphous and portlandite phase composition

3.4 Chapter summary

This chapter investigates the cement paste phase formation, which is cured with a high concentration of CO_2 via phase profiling. The cement paste was prepared into two hydration groups, 14 or 28 days. The carbonation was conducted with 10%CO2 for an additional 14 and 28 days. The phase analysis was conducted using QXRD and verified by comparing the TGA test result.

The hydration effect on the 14 and 28 days has a slight effect, initially before carbonation all have a higher amounts of C−S−H and $Ca(OH)_2$. However, the followed carbonation for those duration has a significant difference in the

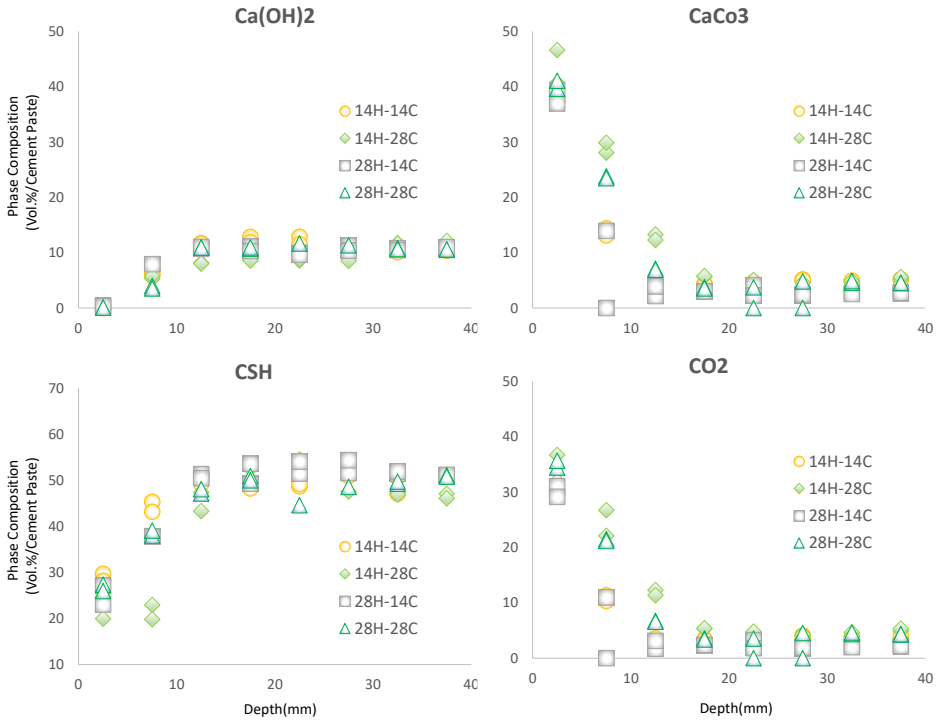

Figure 15: Summary of each curing condition

acquisition of the CO_2 and consumption of anhydrous and cement hydration products. The amount of $Ca(OH)_2$ on the surface reached null. However, on the second layer some amount of it is determined, which also depends on the duration of carbonation. The absorption amount of CO_2 is directly related to the amount of water evaporated and $CaCO_3$ formation. 14H-28C resulted in higher amount of calcite formation whereas 28H-14C produced a lower amount from all conditions.

Overall, the concentration of calcite is exponentially related to the depth of the carbonation and reached up to 20mm. However, this takes 14 and 28 days. This study shows that 14H has higher absorption than 28H for the

same period of carbonation. The carbonation is more effective in the low pre-curing periods. The early age carbonation is recommended to maximize the absorption capacity of the CO2 and to accelerate the reaction of the minerals in a short period of time.

4 EARLY-AGE ACCELERATED CARBONATION CURING OF CEMENT PASTE

4.1 Introduction

This chapter presents the phase change of cement due to the early age carbonation curing with the combination of pre-curing, carbonation, and post carbonation hydration and its effect on the mechanical strength and further carbonation resistance. The mineral phase composition of the carbonation cement paste specimen was determined through profiling. In addition, the mechanical and further carbonation resistance of the accelerated carbonation curing was determined using cement mortar.

The formed hydration products (at 1 day and 3 day) have different influences on the diffusion of the gas and water. The growth of C−S−H is a highly dominated product in the peak heat evolution of hydration reaction (Scrivener et al. [2019]). For typical cement, which is expected after 6 hr of cement and water contact. The growth of C−S−H thickness of reaches to 1um decelerates the rate of hydration because of the rection needs time to diffuse through the layer. In addition, the reduction of the available space and concentration change also have a significant role in decreasing the rate (Scrivener and Nonat [2011]). Then, a hydration reaction is based on the diffusion of the water into the cement matrix, whereas calcite formation depends on the diffusion of the gas through it. Which is faster to penetrate through the complex cement matrix.

At the early age of carbonation, the pre-curing has a significant role in the calcite formation on the surface of a specimen; however, the carbonation duration has a slight effect on the depth of carbonation. Ngala, Page 1997 studied the effect of carbonation on cured hydrated cement paste in its pore structure and diffusion resistance. Materials diffusion resistance was highly affected by the pre-drying and carbonation (Ngala and Page [1997]).

4.2 Experimental program

4.2.1 Materials and specimen preparation

Phase profiling of early age accelerated carbonation curing was conducted using clinker as binding material. The chemical composition of the clinker and the calcite content were determined using XRF, QXRD, and TGA. Purified distilled water was used to control undesirable chemical reactions which will come from the water minerals. For the paste mix, the water to cement ratio was 0.5 by weight. The oxide and crystal-chemical composition of clinker cement used for the phase profiling are expressed by the weight percentage in Table 5 and Table 6 below.

Cement paste samples were prepared using a mechanical mixing machine. In the paste preparation, bleeding was the problem due to the high amount of water used. The paste was agitated every 30 min for around 3 hr. The plastic mold helps to prevent water from leaking and to control the consistency of the experiment. Plastic cube mold (50x50x50mm) for the profiling and mechanical test samples, and the prism molds were used for the modulus of elasticity

Table 5: Oxide composition of cement obtained from XRF.

Oxide Composition	**wt.%**
CaO	63.17
SiO_2	19.92
Al_2O_3	4.22
Fe_2O_3	3.73
MgO	2.32
K_2O	1.32
Na_2O	0.36
SO_3	4.29
Loss on ignition	1.2

Table 6: Phase composition of commercial cement obtained from QXRD.

Phase Composition	**wt.-%**
C_3S	59.23
C_2S	20.99
C_4AF	13.98
C_3A	2.36
Calcite	0.21
Gypsum	0.01
Bassanite	2.14
Periclase	1.02

(15X15X80 mm). Figure 16 shows the cube and prim molds. The paste was cast to the molds and vibrated manually.

The first phase is pre-curing; the samples were kept covered with plastic in the chamber until the carbonation. The samples were pre-cured for six-hr (0.25H) or one day (1H), or three-day (3H). The second phase is carbonation; one surface of the samples was exposed and cured using accelerated carbonation. After carbonation curing, the samples were sealed and kept in the chamber up to their testing date. Figure 17 below illustrates the arrangement of the specimens to curing and carbonation at different carbonation concentrations.

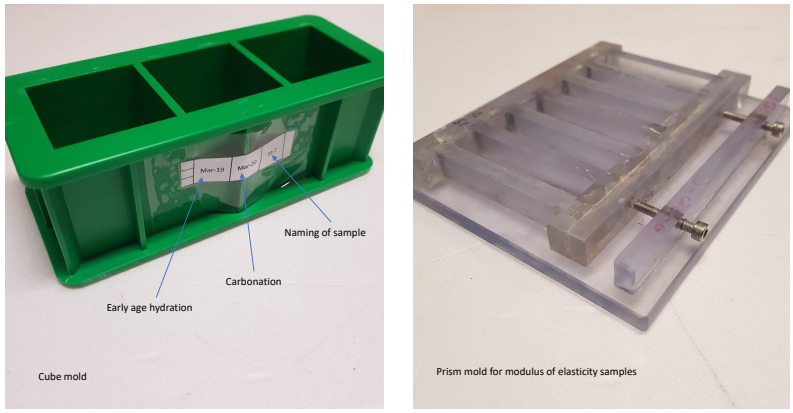

Figure 16: Plastic cube and prism mold

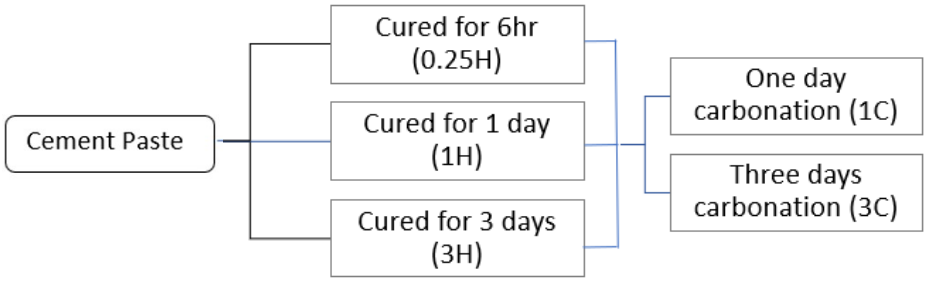

Figure 17: Specimen hydration-carbonation plan

Each sample was transported to a carbonation chamber and carbonated with a concentration of 5%, 10%, 15% or 20 %, for one-day (1C) or three-day (3C). The specimen's naming was given as follows; prior hydration period, and carbonation period respectively. The specimens were prepared with 6hr curing with 1 day or 3-day carbonation ("0.25H-1C", "0.25-3C"), 1 day curing with 1day carbonation or 3-day carbonation ("1H-1C", "1H-3C"), 3 days curing with following 1 day carbonation or 3-day carbonation ("3H-1C", "3H-3C").

Where H stands for hydration and C stands for carbonation. All samples were kept in a similar temperature and relative humidity environment, both in the humidity and carbonation chamber. After carbonation, the phase profiling samples were kept under the same condition until 28 days.

The carbonation chamber used Nova digital controlling system (Nova series-SP590) to control the flow of the gas. It has an accuracy of ±1 on the concentration controlling. TEMI1300 programmable temperature and humidity controlling system was used. It has an accuracy of ±2% on relative humidity and temperature.The chamber has a capacity of 64L, it can accommodate around 56 cube molds at the same time without any overlap and congestion that will clog the flow of the gas to the surface of the samples. In addition, most of the samples are cured with different combinations of pre-curing and carbonation curing. This decreases the number of specimens to the carbonation chamber at the same time. Setup the carbonation chamber and prepare it for the experiment including a backup carbon di-oxide gas cylinder to control any interruption in the curing process. The pressure of the gas to chamber was adjusted to 0.1Mpa. Figure 18 shows the carbonation chamber and its setup.

The specimens were covered with a plastic sheet and kept in the other humidity chamber with the same temperature and humidity as the carbonation chamber in their post carbonation curing period. The humidity chamber was prepared to keep the samples before and after carbonation with a temperature of 25℃and 55% relative humidity. It has a similar environmental condition to the chamber where samples were carbonated. Following completing the hydra-

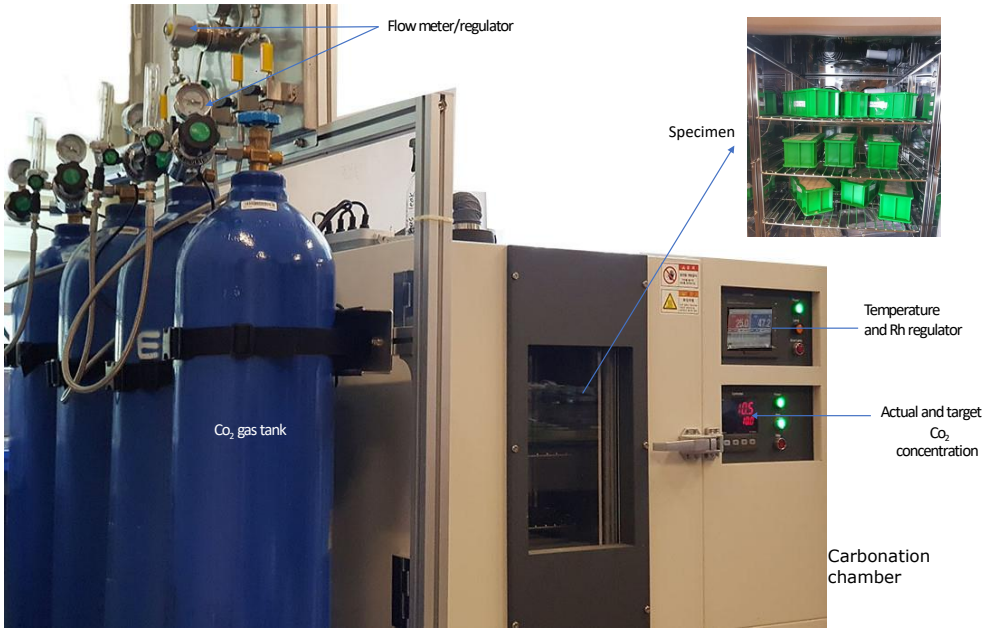

Figure 18: Carbonation chamber and specimens

tion (the pre-curing, carbonation, and later hydration), the specimens were submerged to isopropanol to stop the further hydration. Then, isopropanol followed by vacuum drying was used to remove the free water in the paste with preserving the formed phase (Scrivener et al. [2016]).

4.2.2 Phase profiling

The samples were prepared for four carbonation concentrations (5%,10%,15%, or 20%) with repeated similar experimental conditions. The profiling of the samples conducted after the samples cured for 28 days using drill pit which has a diameter of 15 mm. It was conducted starting from the carbonation front layer of the specimen and profiled up to 21 mm depth through the interval

of 3 mm depth. The profiled powder of each sample was prepared and soaked again to isopropanol. The prepared paste was dried using a vacuum prior to the QXRD and TGA test.

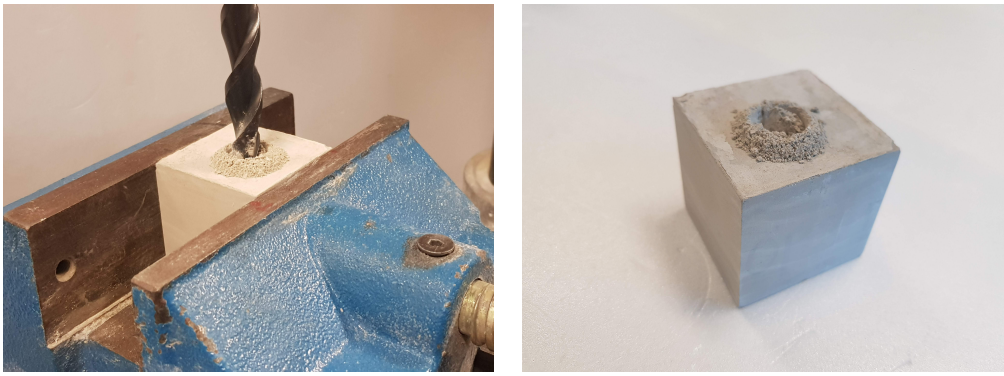

(a) (b)

Figure 19: Powder preparation through the depth the specimen : (a) drilling the sample ; (b) drilled specimen and the powder.

Mineralogical characterization was conducted for the prepared powder samples in each depth using a similar QXRD and TGA machine that was used for later age test. For the early age test, approximately around 400 sample tests were used. QXRD test was conducted using X'Pert PRO MPD, which is manufactured by PAN analytical. The x-ray radiation of the model Cu2KW (conducted at 40kV, 30mA) and it has Micro-capillary diffraction to analyze the microscopic areas to 0.1 precision. The scanning angle is from 5 to 65 in a 2 θ range at a step size of 0.013°/step. The scanning time for the QXRD was 1 hour. External standard method using rutile –samples mineralogical composition were determined using a scale factor of the rutile and mass absorption coefficient (MAC) was used to normalize the result.

The Rietveld refinement was determined using the High Score Plus software (4.8 version number), which is produced by the Malvern Panalytical B.V Almelo the Netherlands. Structures of the phase used for the refinement is attached in the Appendix B section. The determined result of the QXRD was re-normalized based on the bound water to express per paste.

X-ray fluorescence (XRF) test was conducted using AXIOS minerals mode. The generator of the x-ray has 60KV and 125mA, and the detector has the flow counter 13°to 148°2θ and a scintillation counter 8°to 104°2 θ, 22Ti $\sim$ 92U were used.

The TGA test was conducted to determine the bound water. The test was conducted using the DTG-60H model (Shimadzu Corp.). The temperature was ranged from room temperature up to 1000℃. The temperature rate was increased by 10℃/min. The phases in the TGA test were expressed by the weight percentage of the dried cement paste. In the analysis, for the clinker cement paste, the mass changes from 100°C to 300°C is responsible for C−S−H, and some monocarbonate, the mass changes from 300°C to 400°C is due to hydrogarnet, from the 400°C up to 550 °C the portlandite was determined and from 550°C to 1000°C is due to the calcite decomposition.

4.2.3 Compressive strength

The mechanical compressive test was conducted as per (ASTM C-109/109M-16a [2016]) standard. The experiment was investigated in a similar condition with the profiling, with three different curing periods (combination of pre-

curing, carbonation, and post-curing conditions). OPC cement which is available on the market used for the test. Table 7 shows the phase composition of the OPC cement. The river sand, which passes a sieve size of 4.75 mm, was used to prepare the mortar paste for the strength development, modulus elasticity, and further carbonation resistance. The ratio between OPC and river sand was prepared with 1:1. Tap drinking water was used to mix with the water to cement ration of (w/c) = 0.5 and 0.4.

Table 7: Oxide composition of opc cement obtained from XRF.

Oxide Composition	**wt.-%**
CaO	58.75
SiO_2	21.205
Al_2O_3	6.56
Fe_2O_3	3.81
MgO	2.89
K_2O	1.27
Na_2O	0.27
SO_3	4.42
Loss on ignition	3

The mortar was prepared and cast in the plastic cube molds, and when the samples completed their prior curing period, un-de-molded samples were exposed to the concentrated carbonation. The plastic used to prevent the other sides from carbonation which has a dimension of 50X50X50 mm was used for casting the mortar. The samples were cured under two conditions :

1. Reference specimens, uncarbonated
2. Accelerated carbonation curing.

The samples were covered with plastic until their carbonation. The curing

temperature is 25°C, and humidity 55% have kept constant using the humidity chamber. The compressive strength has been conducted on the 7th, 14th, and 28th days of casting.

4.2.4 Dynamic modulus measurement

The specimens for the dynamic modulus test were prepared with mortar in a similar mix design and condition with the compressive strength. The water to cement ratio was 0.5, curing temperature and humidity were 25°C and 50%, respectively. Figure 20 shows the experimental setup for the modulus of elasticity test.

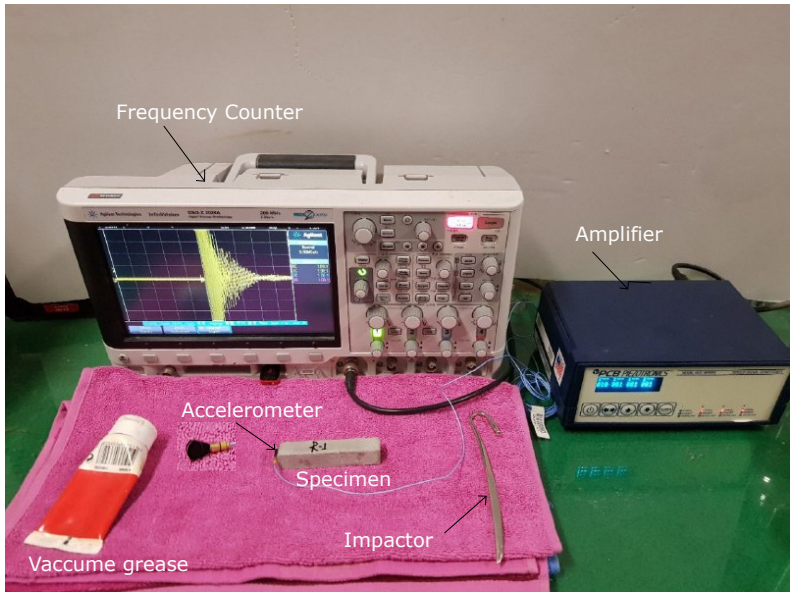

Figure 20: Experimental setup for impact resonance test

The specimens with a dimension of 15X15X80 mm were prepared, and the test was conducted as per (ASTM Standard C215 [2008]) on 3rd,7th,14th, and

28 days. The test of non-destructive dynamic young's modulus test was conducted by impact hit the side of the prism using impactor. The accelerometer was attached longitudinally on the other side of the specimen using grease. The frequency received by the accelerometer was transferred to the amplifier and recorded by the frequency counter. The result of the recorded frequency was saved on the flash and analyzed using Matlab to determine the natural frequency of the specimen.

4.2.5 Further carbonation measurement

The mortar for the further carbonation was prepared in a similar proportion with the compressive specimens. The specimens were pre-cured for 6-hr or, 1-day or 3-days before accelerated carbonation. Then, the specimens were directly transferred and cured with only 20% concentration for 1-day or 3-days, similarly to the other samples. It has been kept for 28 days after completing its carbonation period. After 28 days, specimens were exposed to a lower concentration of CO_2 than the previous, 10 % was used, for additional 28 or 56 days. After completing further carbonation, the samples were split in the vertical axis of carbon-di-oxide exposure using simple splitting wedge and compressive machine. Slices were taken from cube specimens, and phenolphthalein solution was sprayed to the fresh surface to determine the carbonation depth. The solution was prepared with a proportion of 0.5% of phenolphthalein powder mixed with 70% of ethanol and dissolved it with 30% of distilled water.

The measurement was conducted using a caliper and binary image analysis and resulted in approximately similar depth. However, the image processing

is more accurate than the visual inspection (Choi et al. [2017]). For the image analysis, the picture was taken after drying the sprayed solution. Red, green and blue (RGB) image was converted to the binary image. Then, the binary image was segmented into a carbonated and uncarbonated section and analyzed by a number of pixels. The thresholding on the gray image was converted to a binary image using Otsu's method (Otsu [1979]). The percentage or index of carbonation was determined by counting the pixels of the carbonated surface and divided by the total amount of pixels in the image (Auroy et al. [2018]).

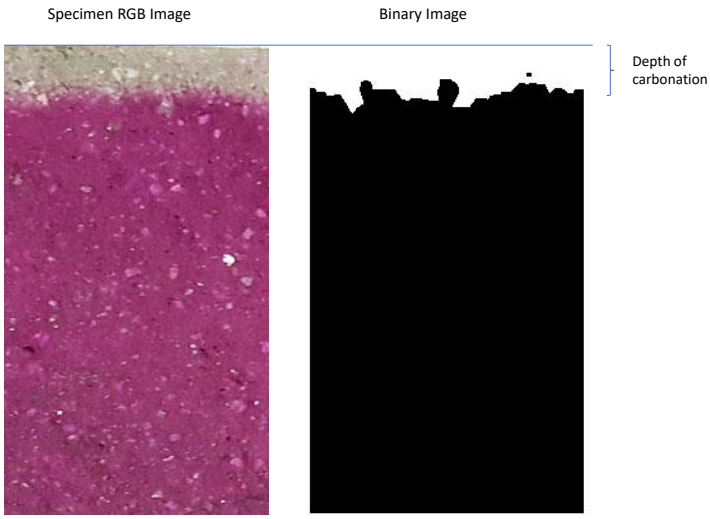

Figure 21: Specimen RGB image converted to binary image

$$Carbonation\ (\%) = \frac{Number\ of\ pixel\ on\ the\ carbonation\ surface}{Total\ number\ of\ pixel\ on\ the\ specimen}$$

$$Depth\ of\ carbonation\ (mm) = Carbonatio(\%) * Depth\ of\ the\ specimen(mm)$$

The average depth of the carbonation was determined by multiplied by the total depth of specimen with the index.

4.3 Result and Discussion

4.3.1 Phase analysis of early age accelerated carbonation curing

Generally, two competitions were going on in the consumption of the ingredients of cement paste. It is between the water and the carbon-di-oxide gas. However, different advancements were taken to see their effect on the phase formation. At six-hour procuring, most of the ingredients will not get a chance to hydrate. As the study shows that, the morphology of the cement paste after 6 hr hydration, ettringite is formed on the surface of the cement grain, but most areas of the grain are not covered by ettringite or C−S−H (Scrivener and Nonat [2011]). The growth and development of C−S−H are on the surface of the cement grain. At the end of the induction period, the degree of hydration is 2-4% (Scrivener et al. [2015]). Which gives an equal probability of the ingredients to hydrate and carbonate at the same time. However, 1H and 3H, it becomes a different situation due to the change combination of the anhydrous and hydration products percentage in the cement matrix.

The result was analyzed based on each pre-curing following different carbonation concentrations and duration effect on the phase formation. The carbonation result of the paste on the respective days was described based on the anhydrous, hydrated, and carbonated phase of the cement paste. The initial amount of clinker was described in the material preparation, Table 6; it

has 0.2% of calcite, 0.01% of portlandite, 59.22% of C_3S, 20.99% of C_2S and 13.98% of brownmillerite.

The phase composition of the specimens, which is hydrated for 1, 3, and 28 days will be presented below as reference in Figure 22. As the initial benchmark to analyze and see the changes in the carbonated specimens, the unhydrated specimen's phase composition was evaluated. 1H and 3H, has a slight change due to the hydration. C_3S was reduced from 4.85 to 3.9, and the C-S-H has an increment from 28.75 to 29.75. The other phases,$Ca(OH)_2$, Ettringite and Brownmillerite, show almost insignificant change in the 2 days hydration period difference.

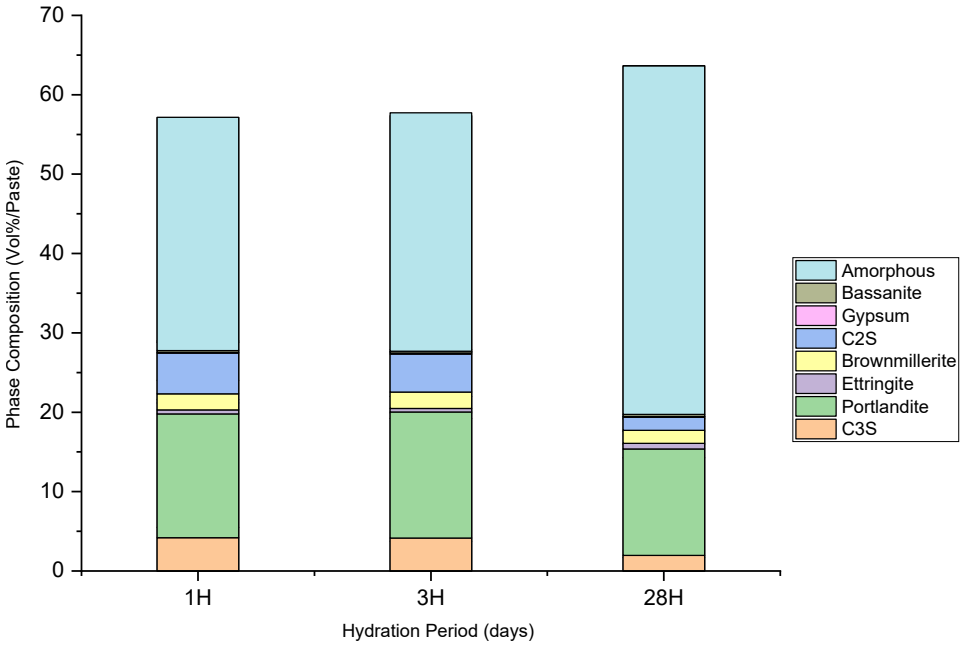

Figure 22: Hydrated specimens phase composition at 1, 3 and 28 days

Overall, based on the QXRD as well as TGA test result confirmed that all

specimens after the depth above 12mm have approximately equivalent phase composition with the uncarbonated specimen, not significantly affected by the early age carbonation. The analysis shows, the chemically bound water is 17±1%, the CO_2 gas content is 3±1%, and free water is 30±1%. However, on the front surface, the amount of free water is low. The concentration of the free water, pre-cured for 1H and 3H, lowered to approximately 8% by the weight of cement on the front face of carbonation. Thus, the amount of water is decreased by half relative to the reference. Whereas, six-hour pre-curing has around 12% by weight of cement and followed the same logarithmic pattern through the depth of the cement paste. Note that the chemically bound water for the reference is approximately 16% by weight percentage. I believe that the amount of anhydrous on the front surface was retarded, which is possibly from the lack of water; hence the water is consumed by the carbonation process. The total volume of cement paste on the surface reduced approximately to around 60%. For 5%, 10%, and 15%, the volume percentage of the paste increased through the depth nearly to 62-65% per volume of paste. However, for 20% carbonation, the volume reached 65-68%.

The TGA test result shows that, the chemically bound water followed a logarithmic pattern through the depth. The calcite concentration on the front surface of the 1H and 3H samples was doubled to the chemically bound water. While for 0.25H, the calcite amount is approximately equivalent to the chemically bound water by weight. The formed calcite uses the water both from the chemically bound water and the free water of the specimen. Although it depends on the pre-curing period, almost 1/3 of the calcite uses

the water from the free water. It is the water that will evaporate and cause pores, but now some portion is replaced with the precipitated calcite.

The specimens which have been pre-cured for 6 hr and were exposed with different concentration and carbonation curing period conditions will be described. Generally, the carbonation duration doesn't show any variation throughout the depth of the specimen. However, in this pre-curing period, except 5% other concentration carbonation develop shrinkage and cracking due to high loss of water in the early age, and it greatly depends on the duration of the carbonation. The progress and evolution of carbonation, a special distribution of crack, and parameters of pore structure of the hardened paste were studied by (Han et al. [2013])—cracks developed in the direction of carbonation due to the carbonation shrinkage. In addition, the duration of the carbonation affects the volume and depth of cracks. The phase analysis of 0.25H is presented from Figure 23 to Figure 26.

The anhydrous phases show approximately similar characteristics through all gas concentrations and the duration of carbonation curing. However, throughout the depth of the specimen, the carbonation front surface has a slightly greater amount of anhydrous than the inner section of the paste. For 5% and 10% concentration, the duration of carbonation curing slightly decreased on the front surface. However, at 15% and 20% concentration, the duration (1C or 3C) has no effect. The amount of basanite and tricalcium silicate doesn't show any dependence in concentration as well as duration. It has been almost totally consumed through the depth.

The amount of portlandite up to the depth of 3 mm is diminished in almost

all precuring and carbonation duration. However, specimens that are pre-cured for 0.25H have approximately above 5% portlandite on the carbonation front surface. The mass loss of the accelerated carbonation specimens has higher in the temperature range of 600 to 900 °C whereas both conditions have a similar mass loss in 400 to 460°C. It shows the continuous hydration reaction after the accelerated carbonation (Sharma and Goyal [2020])

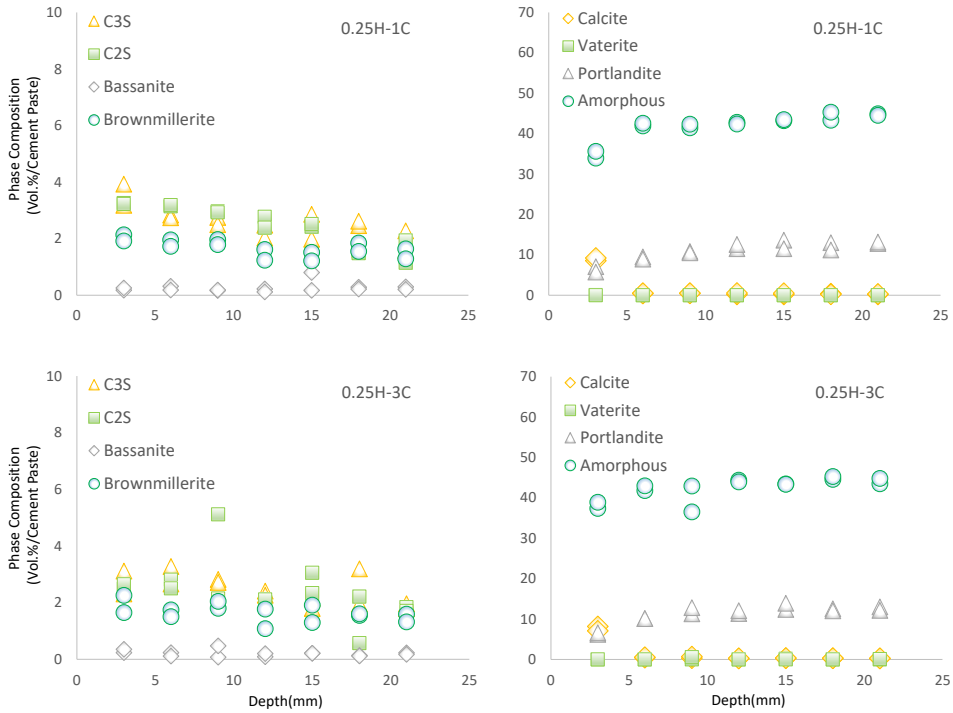

Figure 23: Phase analysis of "0.25H-1C" and "0.25H-3C" carbonated with 5%.

For 5% concentration, all carbonation conditions show a similar pattern of calcite formation. In 1C and 3C, there is high calcite formation on the surface. At the same time, the depth of carbonation is almost limited only to 6mm depth. The higher calcite formation is recorded by 10% carbonation

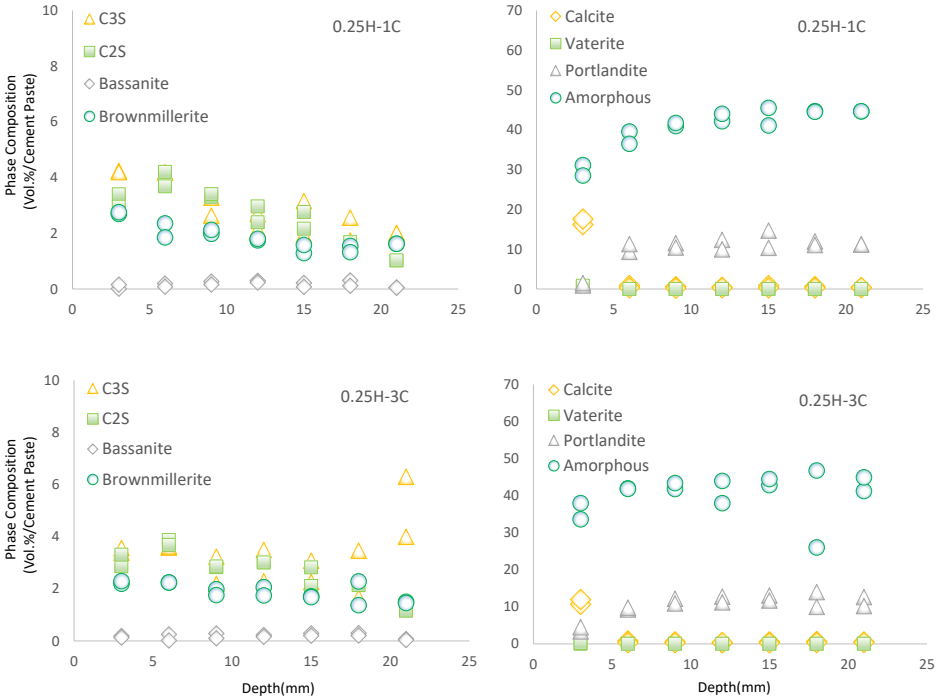

Figure 24: Phase analysis of "0.25H-1C" and "0.25H-3C" carbonated with 10%.

with 17% in 1C. Even though 3C has more time for calcite formation, 1C has less amount of amorphous, and relatively greater calcite formation was recorded. In 10% carbonation, specimens which were carbonated for 3-day were lowered amount of calcite and higher amount of amorphous by 6% than 1C. In this pre-curing condition, the amount of vaterite, mono carbonate, and hemicarboante was negligible.

Generally, the hydration products (portlandite and C-S-H) decreased on the front surface in all combinations. In the inner section of the paste, the amorphous content reached 42 to 45%, and the portlandite was approximate 10 to 13%. On the other hand, in the front section surface, the amorphous

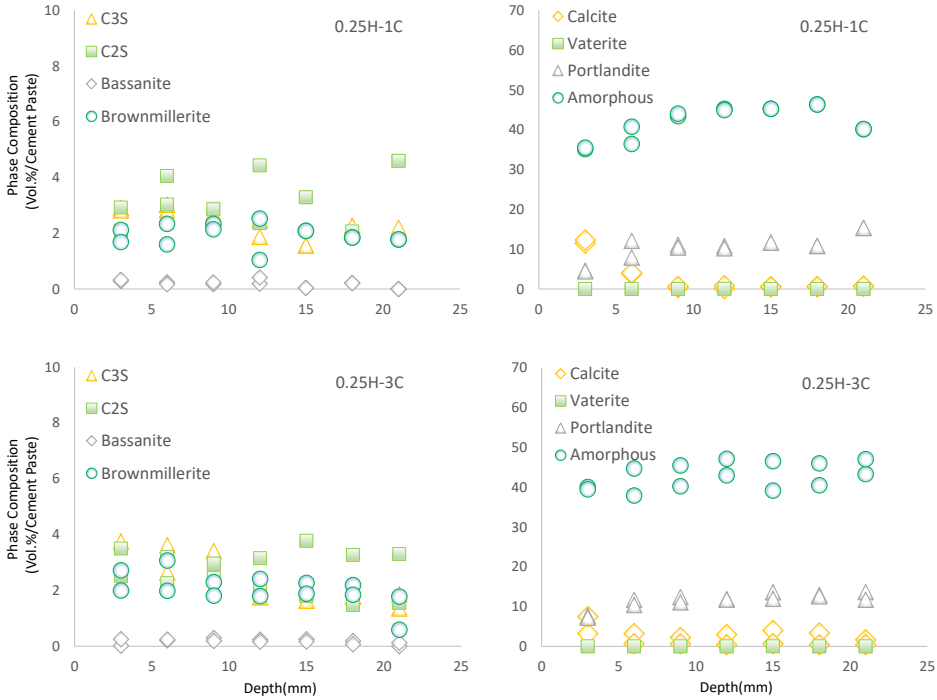

Figure 25: Phase analysis of "0.25H-1C" and "0.25H-3C" carbonated with 15%.

and calcite show an unexpected pattern for the duration of the carbonation curing.

The portlandite in 0.25H condition is not significantly affected by the carbonation duration as well as the concentration of the CO_2 gas. In addition, a higher percentage of portlandite was determined on the surface of the 5% and 20% carbonation with around 7%. This is more strongly justified due to late hydration after carbonation was completed, the concrete recovered the portlandite. Note that both of them have similar calcite formation on the surface. The portlandite percentage at 6 mm depth is not affected by the concentration of the carbonation. They have approximately the same amount

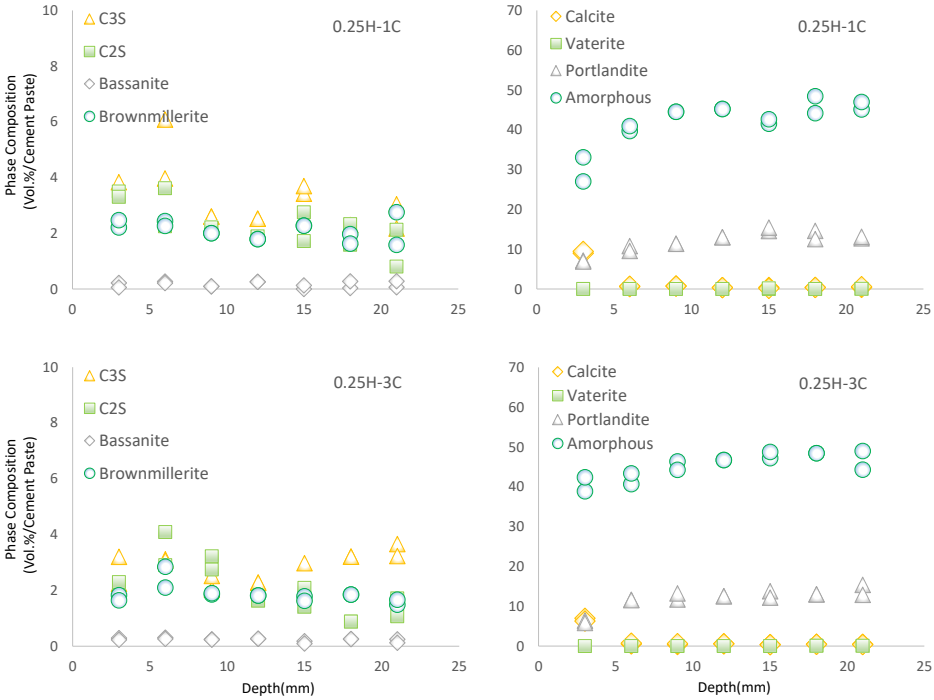

Figure 26: Phase analysis of "0.25H-1C" and "0.25H-3C" carbonated with 20%.

of portlandite throughout the other depth.

In 1H, except C_2S other anhydrous phases, show a similar pattern with the 0.25h curing condition concerning depth. C_2S in 1H is highly consumed on the carbonation front than 0.25H. The other anhydrous phases do not show significant variation due to carbonation curing duration or the concentration. The dissolution of C_3S increase the concentration of portlandite in the aqueous solution and create environment that inhibits the solubility of C_2S(Scrivener and Nonat [2011]). The carbonation reduced the amount of portlandite in the system, which increases the rate of the consumption of C_2S relatively early age. This increases the rate of conversion of the ingredients to a product in

the hydration or in the carbonation form. Accelerated carbonation accelerates the formation of products in addition to calcite precipitation. The result of 1H phase analysis presented from Figure 27 to Figure 30.

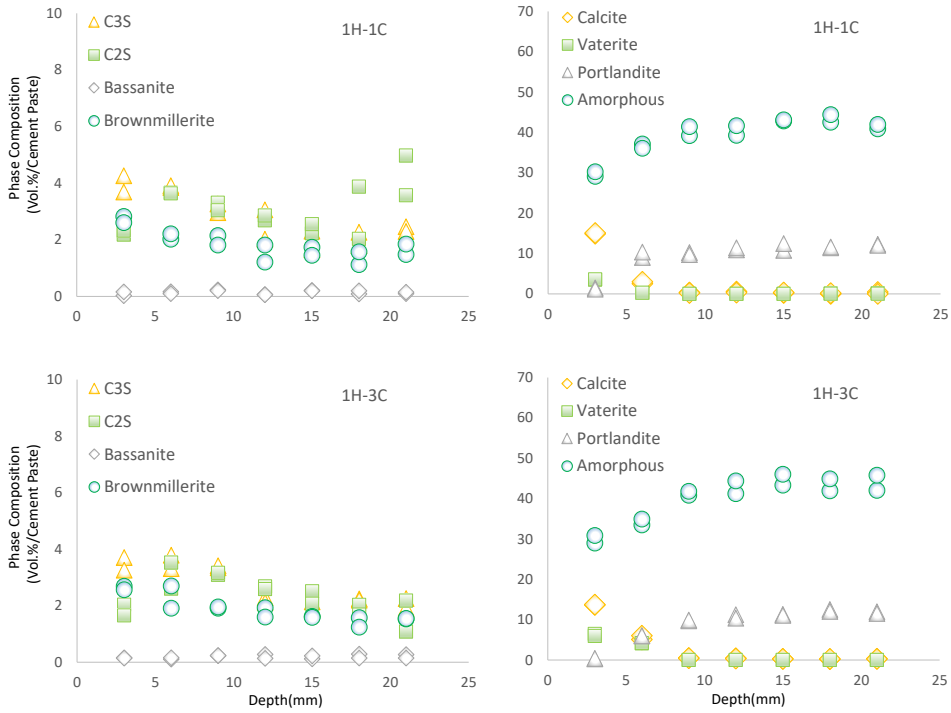

Figure 27: Phase analysis of "1H-1C" and "1H-3C" carbonated with 5%.

50% of the OPC hydrates at one day (Scrivener and Nonat [2011]). For specimens that carbonates after one day of hydration have the composition of 50% anhydrous and 50% hydration products. Excluding the chemical reactivity of the anhydrous and hydration product phase, the calcite precipitation has equal quantitative probability.

The hydration products of 1H followed a different pattern from the 0.25 H pre-curing condition. The 5% carbonation of 1H has approximately similar

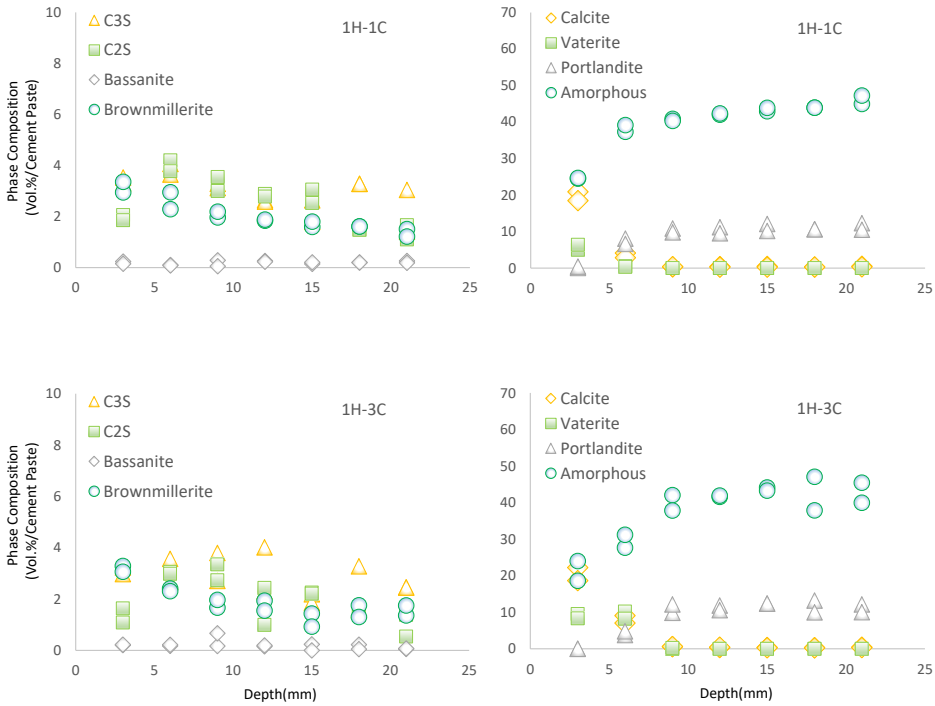

Figure 28: Phase analysis of "1H-1C" and "1H-3C" carbonated with 10%.

or equivalent results with the 10% of 0.25H , with some increment of vaterite. Thus, the carbonation duration does not significantly affect the phase composition of hydration products, except for some transformation of calcite to vaterite.

In addition to calcite, a high amount of vaterite formation was recorded, especially for 5% and 10% carbonation. In 5% carbonation, 1C and 3C resulted in a similar amount of calcite formation, around 14%. However, the vaterite formation in the 3-day carbonation is somehow more remarkable than the 1-day. The vaterite formation in the 15% and 20% concentration is lower than others.

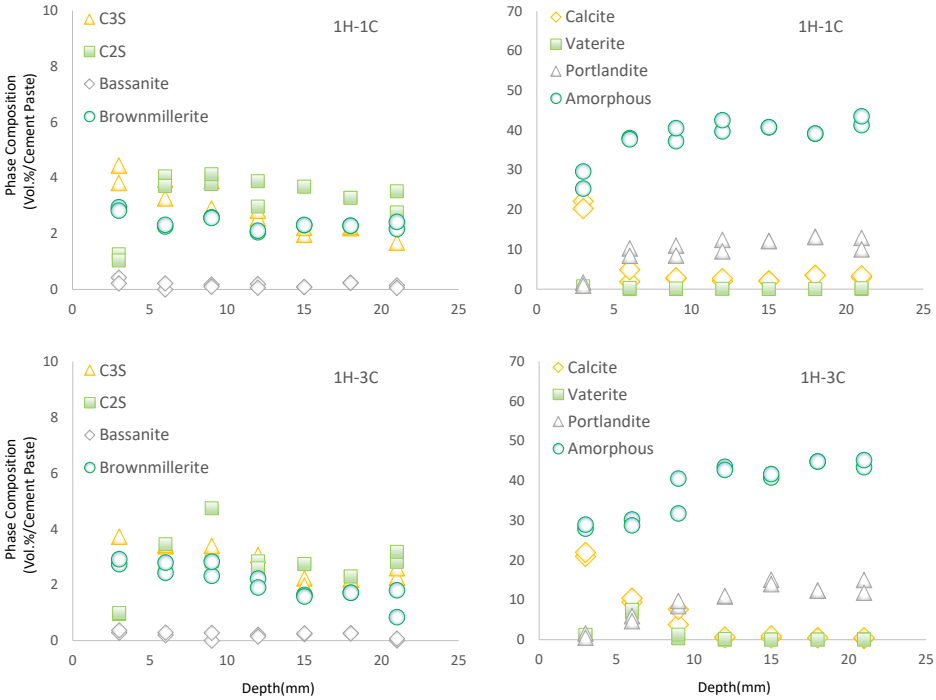

Figure 29: Phase analysis of "1H-1C" and "1H-3C" carbonated with 15%.

At 6mm depth, the duration of the carbonation and concentration of the gas influenced the amount of calcite and vaterite formation. A high amount was recorded for 10% and 15% concentration, 9% of calcite and 8% of vaterite. The portlandite percentage of 1-day pre-curing at 6mm depth, the concentration of the gas doesn't significantly affect. However, the duration of the carbonation does. 1H-3C specimens with 15% and 20% have a similar amount of calcite and amorphous formation.

In 10% CO_2, calcite and amorphous contribute similar quantity proportion, in three-day carbonation even higher amount of volume percentage in the cement matrix with some vaterite is formed. The carbonation duration re-

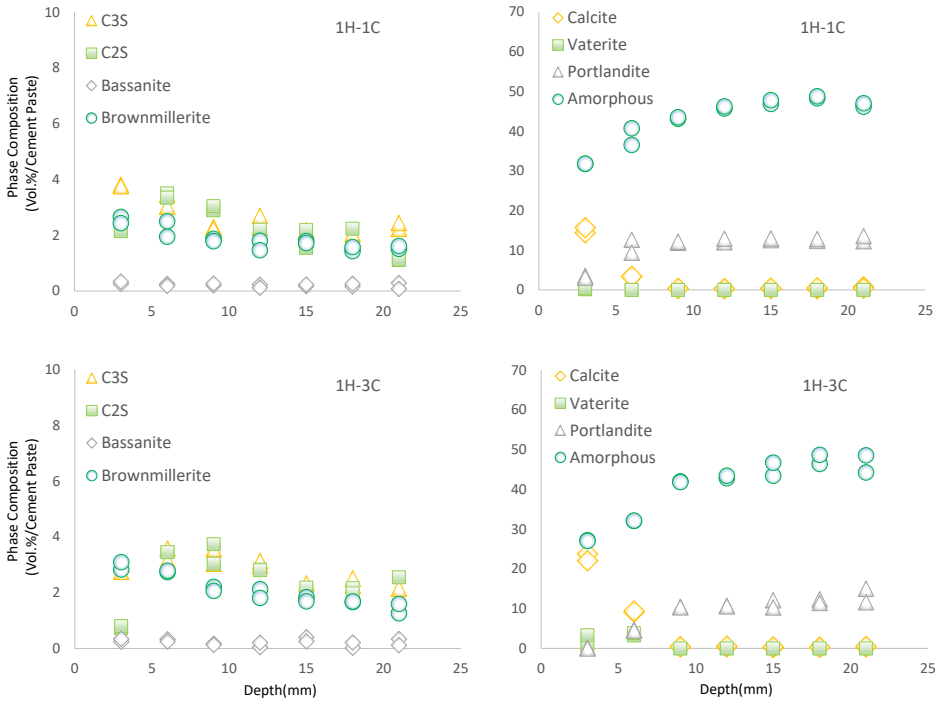

Figure 30: Phase analysis of "1H-1C" and "1H-3C" carbonated with 20%.

sulted in an increment in the calcite and vaterite, whereas there is a reduction in the amorphous content.

In 3H, almost the maximum amount of hydration product is formed relatively, and the carbonation targeted the hydration products of C-S-H, which reduces its amount than the other pre-curing days. In this pre-curing, the duration of the carbonation does not significantly affect the phase formation on the front layer. However, the duration increases the calcite and vaterite formation through the depth. On the other hand, portlandite also reduced through the depth up to 12mm, and it became constant. The result of 3H phase analysis presented from Figure 31 to Figure 34

The formation of vaterite significantly dominates in this pre-curing. Based on a study of Auroy et al. [2018], the carbonation of C-S-H, which has a higher Ca/Si ratio resulted in vaterite formation. A low amount of amorphous with high amount of vaterite was recorded in 3 days pre-curing. Anhydrous phases are independent of the carbonation concentration and duration; however, C_2S is slightly affected on the front surface.

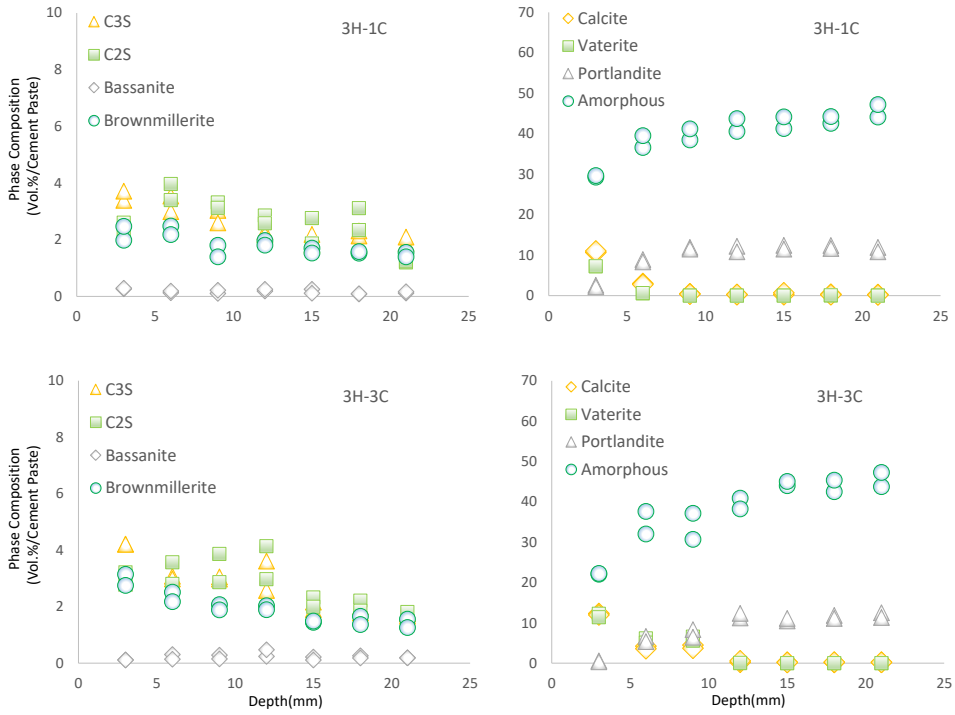

Figure 31: Phase analysis of "3H-1C" and "3H-3C" carbonated with 5%.

The formation of the vaterite depends on the duration of the carbonation as well as the pre-curing condition. Especially, at 10% concentration was resulted in a more significant amount both on 3mm and 6mm depth.

Three-day carbonation has a higher depth of carbonation formation and

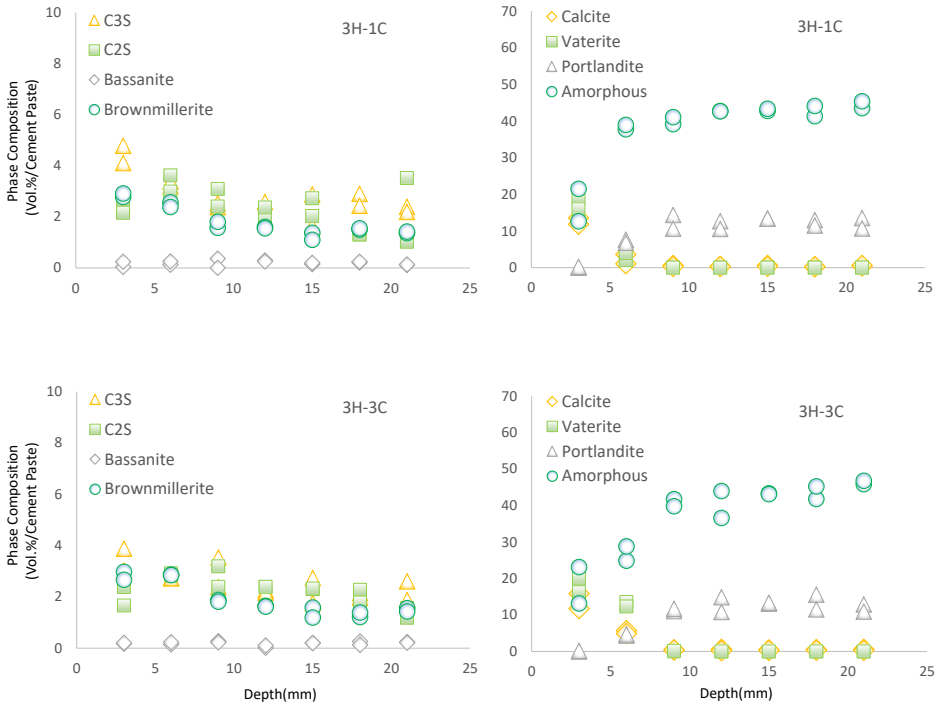

Figure 32: Phase analysis of "3H-1C" and "3H-3C" carbonated with 10%.

a greater percentage of vaterite than all other types. In 5%, an equal amount of calcite and vaterite was formed, 12%, and the C-S-H was around 22%. The calcite formation was reached 9mm with 4% of calcite and 6% of vaterite. In 10%, 13-15% of calcite and 16-19% of vaterite were formed. Which is a higher amount of calcite and vaterite combination of all conditions. In 15 and 20% of concentration, approximately a similar amount of calcite and vaterite was formed on the surface as well as throughout the depth of the specimen.

Based on the QXRD test result, the brownmillerite phase is not completely consumed. The hydration rate of brownmillerite is depends on the addition of gypsum, and its peak is proportional with the peak of the Hydro-garnet

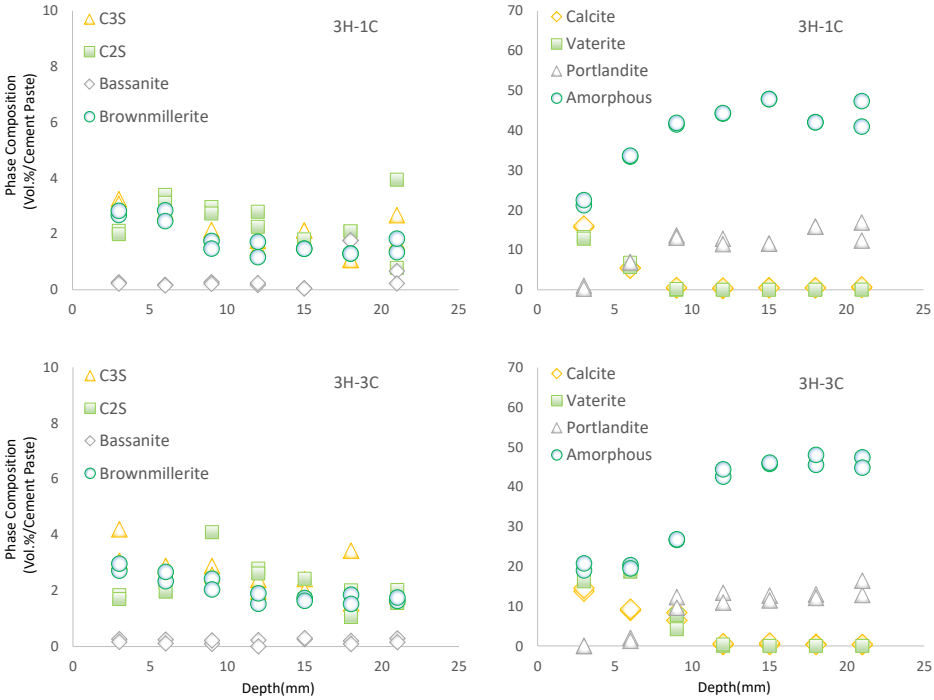

Figure 33: Phase analysis of "3H-1C" and "3H-3C" carbonated with 15%.

Meller et al. [2004]. The absence of gypsum and scarcity of portlandite strongly affect the consumption rate of brownmillerite and the formation of ettringite. At the temperature of 30°C with the absence of gypsum, the rate of hydration of C4AF is too slow. In similar studies, in the early reaction of cement, in the absence of sulphate or gypsum, the aluminate and ferrite phase undergo rapid hydration and leads to false or flash set. Tricalcium aluminate is the main phase that undergoes reaction in the induction phase (Scrivener and Nonat [2011]).

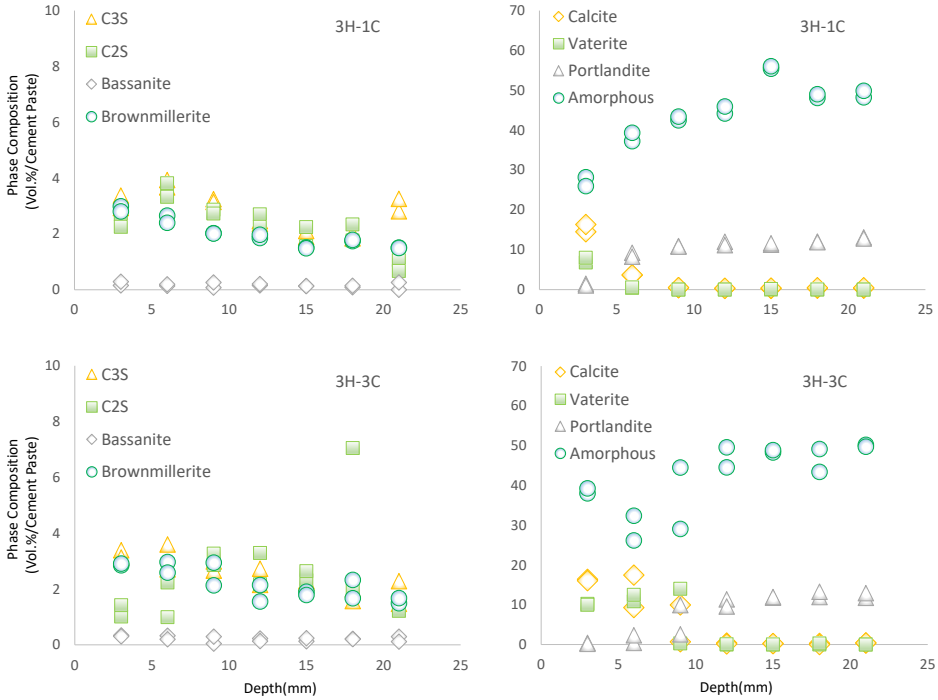

Figure 34: Phase analysis of "3H-1C" and "3H-3C" carbonated with 20%.

Summary of C_3S, C_2S, vaterite, calcite , $C-S-H$, $Ca(OH)_2$ phase formation in different carbonation concentration and curing condition is presented from Figure 35 to Figure 38. Figure 35 reveals that the amount of anhydrous phases is found in small amount; and approximately has similar characteristics through all gas concentrations and duration of carbonation curing. Unlike later age carbonation, higher amount of anhydrous is remained on the front surface of carbonation. This may be due to lack of water for the hydration of the phases on the front surface. Figure 36 shows, vaterite formation in all 0.25H pre-curing periods is almost null. 5% and 10% concentration has some vaterite fromation in 1H precuring. Maximum vaterite formation is formed

in 3H, and the duration of carbonation increased the amount. 1H has higher amount of calcite formation.Figure 37 indicates, C-S-H has higher amount in 0.25H and lower amount in 3H. In pre-curing period comparison, 3H formed higher amount of C-S-H. However, 20% concentration shows higher remained amount than other concentrations and independent to all pre-curing conditions. On the other hand 10% resulted lower amount. Figure 38 illustrates, the remain amount of portlandite followed logarithmic path through the depth and resulted similar amount after 6 mm depth from the carbonation front surface.

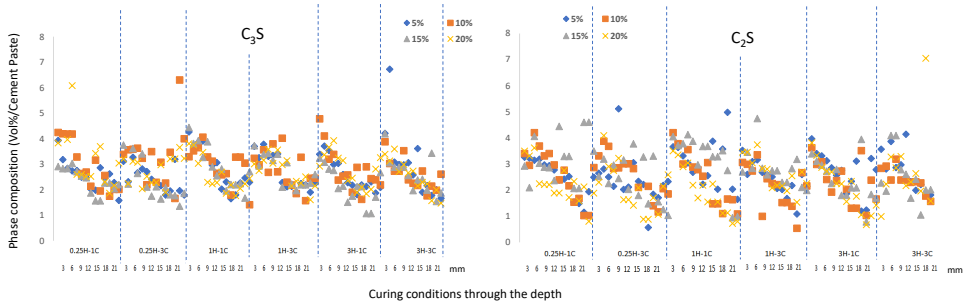

Figure 35: Summary of anhydrous phases through the depth in early age accelerated carbonation at 4-CO_2 concentrations

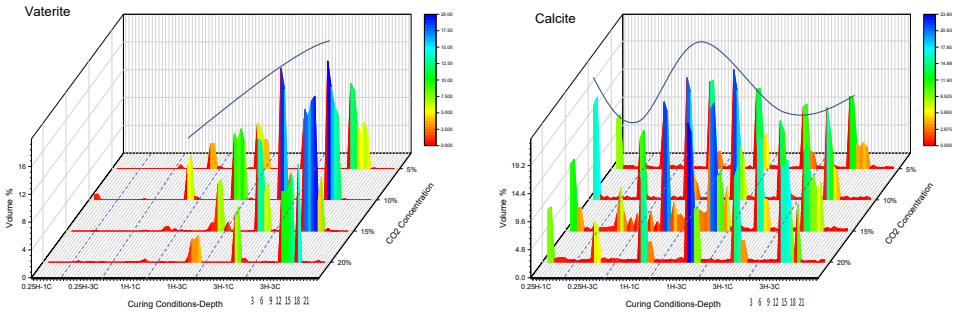

Figure 36: Summary of vaterite and calcite formation through the depth in early age accelerated carbonation at 4-CO_2 concentrations

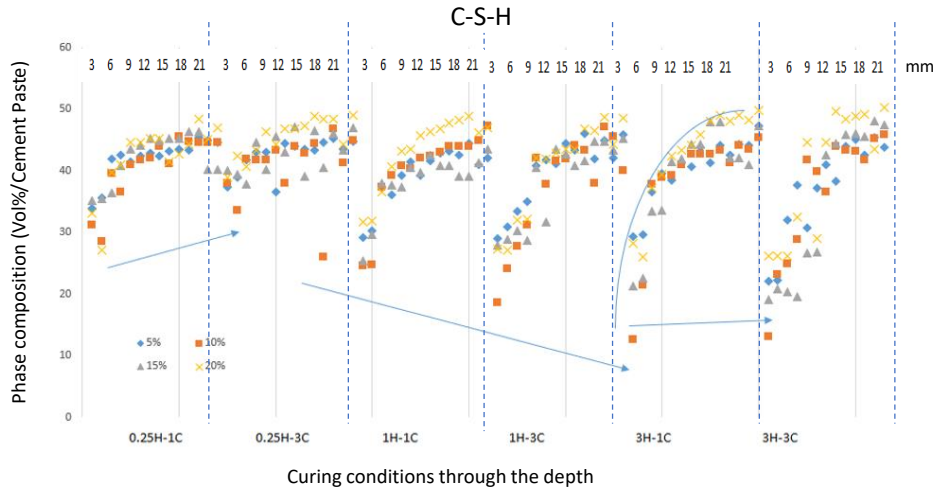

Figure 37: Summary of amorphous phase through the depth in early age accelerated carbonation at 4-CO_2 concentrations

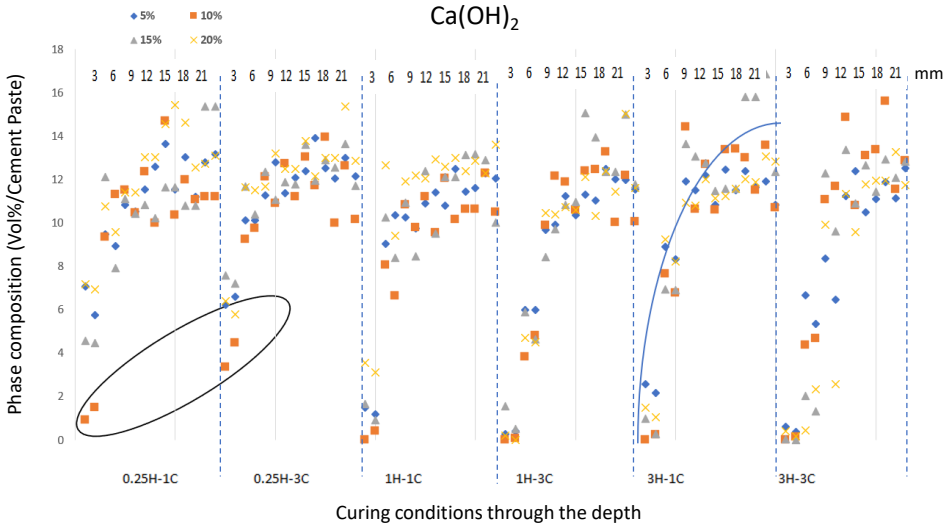

Figure 38: Summary of portlandite through the depth in the early age accelerated carbonation at 4-CO_2 concentrations

4.3.2 Mechanical properties

In the case of carbonation curing, the compressive strength of the concrete is highly influenced by binder content and type, the initial mix proportion, the curing method and period before and after the carbonation, the concentration of CO_2 and the moisture in the specimen (relative humidity). The amount of water which are essential for the aid compaction and activate the reaction of CO_2 is required (YOUNG et al. [1974]).

At an early age, the water to cement ratio has the usual effect on the mechanical property of concrete. However, on the 28th day, the specimens with different water to cement ratios yielded approximately similar strength for 1H and 3H. Therefore, the removal of water due to carbonation in the lower water to cement ratio may decrease the rate of strength development in the ultimate age.

The compressive strength result of the specimens which has water to cement ratio of 0.5 and 0.4 presented from Figure 39 to Figure 41. In 0.5 water to cement ratio, the 7th-day mechanical property of the concrete shows almost similar result for all types of pre-curing and carbonation conditions. On the 14th day, 3H, has a better compressive strength result. At 28 th day, specimens pre-cured for one day (1H) have relatively greater than other conditions. The lack of water of 3H specimens until the 28th day may retard back its compressive strength after 14 days. However, specimens that were pre-cured for 6 hr showed lower compressive strength throughout the period. This possibly, the dehydration of the specimens at an early age and causes of an additional

crack in the specimens may lower its compressive strength.

On the other hand, for specimens with a water to cement ratio of 0.4, the strength development has an increment up to 14th day in all pre-curing and carbonation conditions. However, the strength of all specimens were dropped on the 28th day. The reference average compressive strength for w/c ratio 0.5: 40.56, 41.47, and 39.84, which is the green part of the bar and and for w/c 0.4: 39.44, 43.17, and 45.28 for 7, 14 and 28 days respectively. The modulus of elasticity of all specimens is presented in the Figure 42. Specimens pre-cured for 6 hr resulted in a lower modulus of elasticity due to the crack was propagated through the specimens. However, other specimens ultimately achieved approximately similar elasticity. For 1H and 3H, the carbonation concentration (up to 20%) or duration does not have any significant effect on the modulus of elasticity.

The phenolphthalein spray test conducted in the samples after the compressive strength test, there is no color change after the $1mm$ depth from the top surface. TGA and QXRD result implies after the carbonation of the mortar/paste, following hydration recovers the concentration of the portlandite. The color change was observed when the percentage of the portlandite is below 2% (De Weerdt et al. [2019]). While based on QXRD and TGA analysis, the percentage of portlandite at a depth above 3 mm recorded is greater than the minimum.

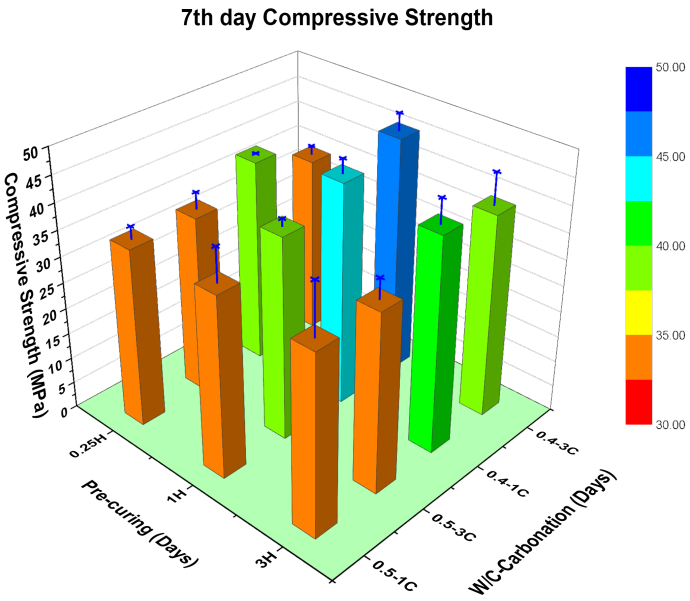

Figure 39: 7th day compressive strength

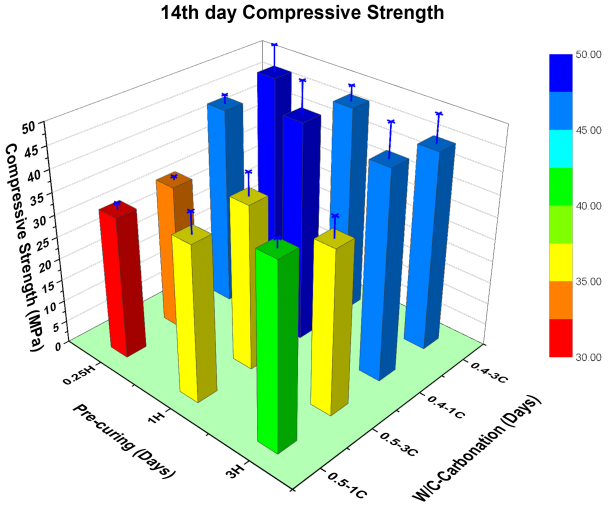

Figure 40: 14th day compressive strength

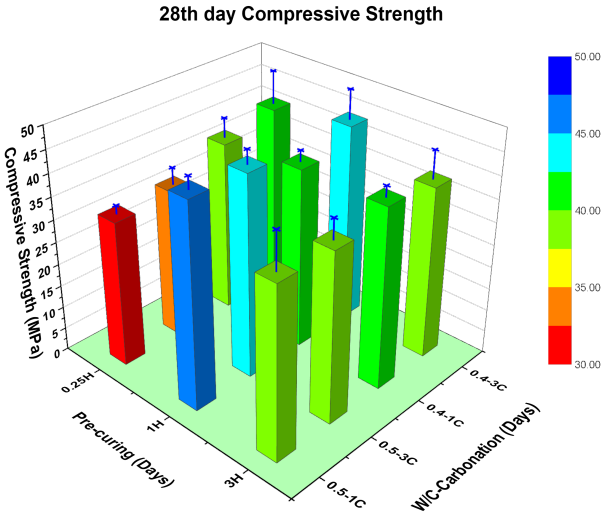

Figure 41: 28th day compressive strength

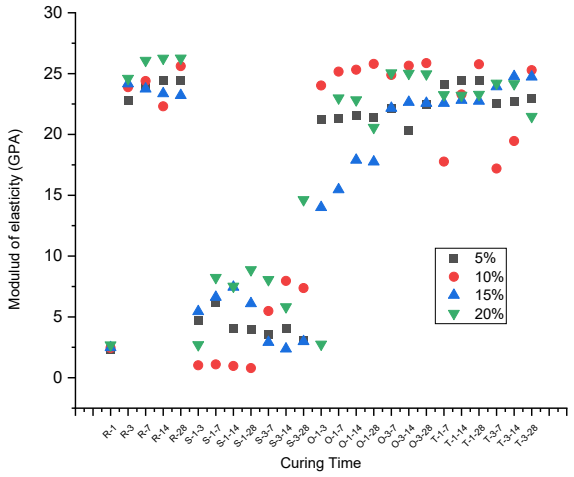

Figure 42: Moldulus of elasticity of the carbonated mortar specimens

4.3.3 Resistance of ACC to further carbonation

The result of the phenolphthalein spray test shows that specimens which is pre-cured for 3H-1C and 0.25H-1C have lower carbonation depth in the early age of carbonation. This specimen resulted in better carbonation resistance for 56 days of further carbonation. At the 28th day of further carbonation, specimens pre-cured for 0.25H-3C and 1H-3C resulted in lower carbonation resistance. Figure 43, show phenolphthalein spray test of the specimens after 28 days further carbonation and Figure 44 shows the results.

Figure 43: Phenolphethalein sprayed image of specimens

Overall, 3H-1C have a better carbonation resistance at 28 and 56 days of further carbonation. Approximately, it resulted in the same amount of depth at additional 28 and 56 days. However, the effect of carbonation can be deeper than the depth determined by the phenolphthalein spray test. This can be justified from the phase profiling test result. The experimental result from (Wu and Ye [2017]) proved this too. The weight percentage of the OPC cement carbonated specimen has 40 % of calcite and 0% of portlandite on the surface.

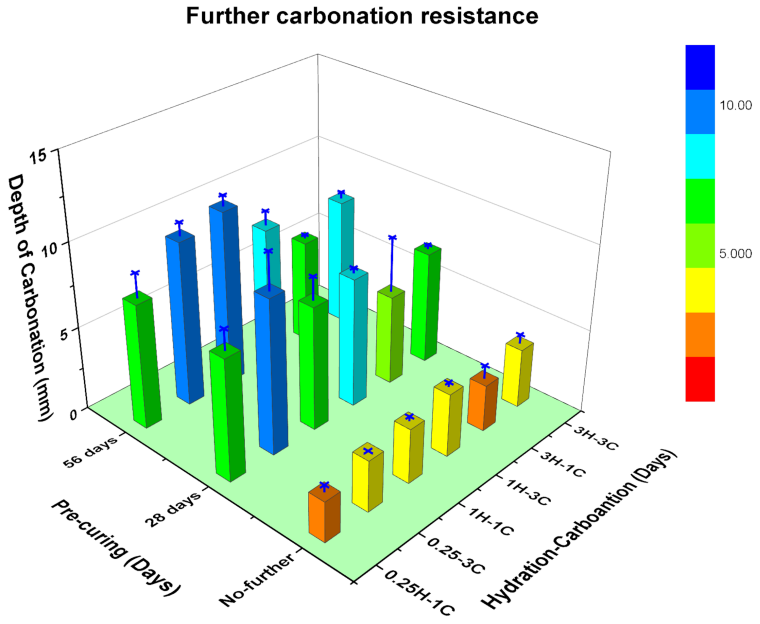

Figure 44: Depth of carbonation from the carbonation front surface

The depth of carbonation from the surface is between 2.5 and 5 mm was evaluated using the Phenolphthalein spray test(Wu and Ye [2017]) .

Durability is the most crucial parameter in concrete structures. Corrosion due to environmental carbonation, sulphate attack, and other deleterious and durability problems are indirectly related to the porosity of the material. The alkaline environment from portlandite is used to protect the reinforcement bar from corrosion. The standard concrete ph is between 12.5 and 13.5, which is from the concentration of the portlandite with dissolved alkali hydroxide, moreover the precipitation of the sodium-calcium hydroxide from the hydration reaction. However, the portlandite and the C-S-H phase react with carbon

dioxide and precipitate the calcite, some amorphous silica gel, and water which drops the value of the ph to 8.5 (Al-Kadhimi et al. [1996]).

The alkalinity (pH) of the inner part of the concrete may recovered from the later hydration reaction. While on the surface, all the mineral compositions of cement and the hydrated phases are totally carbonated, which it creates stable calcite that can't undergo any hydration or chemical reaction with the environment. Although, it needs an investigation on the corrosion effect of the accelerated carbonation curing. Even a very small amount of solid portlandite dissolution in the pore water of hardened cement paste keeps the ph value greater than 12.5 (Papadakis et al. [1992]). Corrosion resistivity of the concrete will develop from later age hydration after carbonation, especially if additional water for curing is provided to the specimen after completing the carbonation period.

4.4 Chapter summary

The calcite formation depends on the pre-curing period and carbonation duration. The pre-curing period directly affects the diffusion of the gas and phase types, which will be used as a source of calcite formation. 1H and 3H have greater calcite formation than 0.25H. Despite the curing period variation, specimens that were pre-curing for one day and three days resulted in the same amount of calcite, free water, and chemically bound water on the surface. Up to the depth of 3mm, 1H and 3H have an approximately equivalent formation of calcite. Hence, both of them has initially similar hydration products prior to carbonation.

However, the accelerated carbonation curing duration and concentration significantly affect the depth of the carbonation. For 1H and 3H, the carbonation duration has more effect on the calcite formation through the depth of the specimen. 1H-1C and 1H-3C show a similar concentration of calcite on the surface. Nevertheless, the concentration of calcite in the 3C doubled that the 1C in the next layer (at 6mm depth) after the surface. In conclusion, the result shows that the carbonation duration determines the depth of calcite formation for 1H and 3H pre-curing periods.

The mechanical property shows that in the 7th day, 1H has a better compressive strength with directly related with the carbonation duration and as usual the water to cement ratio. At 28th day, 1H has a greater strength relative to the others, however, the relation with the carbonation and water to cement ratio is somehow inversely proportional. For both further carbonation conditions, 3H-1C has a better resistance.

5 CONCLUSION

5.1 Summary

The pre-curing period and followed carbonation duration have a significant effect on the phase formation of cement paste at the surface and through the depth. The period of pre-curing directly affects the gas permeability due to the saturation of water and the formation of hydration products. Whereas the type of phase formation or minerals are the same in all conditions, but there is variation in consumption of phases or product formation amount.

Overall, the calcite formation on the surface reached up to 40-50% of the initial paste volume. In the early age one day and three days of hydration resulted in approximately a similar amount of calcite formation on the surface. In addition, 3H and 28H of pre-curing have an approximately a similar amount of vaterite and calcite formation compared to 14H. In contrast, there is a variation in the depth of the carbonation. Which should be considered regarding the corrosion of the reinforcement bar. In addition, on the surface, CO_2 gas absorption capacity of the one day and three days hydration has approximately similar with the 28H latera age carbonation.

The depth of the carbonation in the later age carbonation is reached to 20 mm, and in the early age carbonation it reached to 12mm. In early age carbonation, the calcite formation highly depends on the combination of pre-curing and carbonation duration than the later age. The amount of the portlandite is totally consumed on the surface for both conditions, whereas its available

on other depth with calcite even the amount is small near to surface. The portlandite at an early age is relatively higher, which could be recovered from the hydration after the carbonation is finished.

The anhydrous phases were totally consumed on the surface of the later age carbonation, while there was some remaining in the early age carbonation. This may be due to the shortage of water for the hydration of the anhydrous. For 3H and 3C, the amount of free water is too low. Most of the water was consumed by the carbonation process and cement hydration, which implies that additional water curing after carbonation will create a denser structure. Hence the amount of C_2S remained is estimated to be an average of 20% by weight of its initial amount.

One day hydrated samples show that an increment of calcite due to additional carbonation both through depth and on the surface. However, In an appropriate combination of pre-curing, carbonation curing and followed curing post carbonation period, accelerated carbonation curing is a promising method for durability and strength development as well as for sequestration of the CO_2.

5.2 Limitation

This research incorporates and passes through a lot of experiments. There were some challenges and limitations in the process. One of the limitation, specimens which are pre-cured for 6 hr not reached in its setting time. This could result in some disturbance during transportation. The second is unable

to quantify the amount of shrinkage cracks in the lab. The shrinkage cracks depend on the carbonation curing period and have small size distributed unevenly. This makes it hard to quantify.

5.3 Suggestions for further research

In future accelerated carbonation research, the studies should incorporate more on the durability, including a mechanism for protecting the reinforcement bars from corrosion. Hence, the depth at the later and early reached or consumed some percent of portlandite protective areas. Further research will be conducted regarding durability improvement of the early age accelerated carbonation curing in the long-term carbonation and their effect on the corrosion of the reinforcement bar.

From this study, there was a clear shortage of water in the late hydration period after carbonation curing was completed and shrinkage was also another problem. An investigation by providing additional water after carbonation and providing fiber to decrease the shrinkage phenomena may result a better result in regarding strength and durability improvement.

The new studies should suggest and guarantee with studying long-term effects in the propagation of the gas. In addition, including the economic feasibility with comparing the steam curing will show how much this method is worth. Moreover, investigations in the practical industry should be conducted to provide more reasonable and practical results.

6 Appendix

6.1 Appendix A. Modeling and simulation of hydration and carbonation of cement paste

Modeling and simulation of cement hydration and carbonation: The proposed modeling is first hydration and consumption of the C_2S, C_3S, C_4AF, and C_3A and provide portlandite and C−S−H. Following this, during the specimens exposed to the CO_2 carbonation, C−S−H, portlandite, C_2S, and C_3S were considered for the reaction with CO_2. However, the remaining amount of C_4AF and C_3A were too small at the end of cement hydration. The model considers four carbonation processes:

1. The CO_2 gas diffusion to the pores of the pore-water phase.
2. Dissolution of the clinker and hydrated phases with CO_2.
3. Precipitation of the calcite from carbon nation of the hydrates and clinker.
4. Change in gel porosity related to hydration and carbonation.

The first three mechanisms were already considered in previous works of (Jeong et al. [2019, 2021]), and the last one was newly introduced. In the following two subsections, hydration and carbonation, the analytical model of these phenomena is presented. [2]

[2]This appendix 6.1 is from submitted article on Journal of Case studies in construction materials "Phase profiling of carbonated cement paste: quantitative x-ray diffraction

6.1.1 Hydration model

The hydration model and its chemical reactions are explained in this section. Cement hydration reaction is summarized in Table 8.

Table 8: Chemical reaction during cement hydration Papadakis et al. [1989].

Type of reaction	**Rate of reaction**	**Formulas**
Hydration	$\mathrm{r_{H,C_3S}}$	$2\,\mathrm{C_3S} + 6\,\mathrm{H} \xrightarrow{r_{\mathrm{H,C_3S}}} \mathrm{C_3S_2H_3} + 3\,\mathrm{CH}$
	$r_{\mathrm{H,C_2S}}$	$2\,\mathrm{C_2S} + 4\,\mathrm{H} \xrightarrow{r_{\mathrm{H,C_2S}}} \mathrm{C_3S_2H_3} + \mathrm{CH}$
	$r_{\mathrm{H,C_4AF}}$	$\mathrm{C_4AF} + 2\,\mathrm{CH} + 2\,\mathrm{C\bar{S}H_2} + 18\,\mathrm{H} \xrightarrow{r_{\mathrm{H,C_4AF}}} \mathrm{C_8AF\bar{S}H_{24}}$
	$r_{\mathrm{H,C_3A}}$	$\mathrm{C_3A} + \mathrm{C\bar{S}H_2} + 10\,\mathrm{H} \xrightarrow{r_{\mathrm{H,C_3A}}} \mathrm{C_4A\bar{S}H_{12}}$
	$r_{\mathrm{H,C_4AF}}$	$\mathrm{C_4AF} + 4\,\mathrm{CH} + 22\,\mathrm{H} \xrightarrow{r_{\mathrm{H,C_4AF}}} \mathrm{C_8AFH_{26}}$
	$r_{\mathrm{H,C_3A}}$	$\mathrm{C_3A} + \mathrm{CH} + 12\,\mathrm{H} \xrightarrow{r_{\mathrm{H,C_3A}}} \mathrm{C_4AH_{13}}$

The rate of hydration reaction for each component of cement clinkers $r_{H,i}$ is expressed as follows: Papadakis et al. [1992, 1989, 1991]:

$$\mathrm{r_{H,i}} = -\frac{d[i]}{dt} = k_{H,i}\,\frac{[i]^{n_i}}{[i]_0^{n_i-1}} \tag{1}$$

where $[i]$ is the molar concentration of cement clinker component $i = \mathrm{C_3S}, \mathrm{C_2S}, \mathrm{C_4AF}$, and $\mathrm{C_3A}$, and $[i]_0$ is the initial concentration of each component. The coefficients n_i, rate hydration $k_{H,i}$, and molar weight for each component are given in Table 9.

analysis and numerical modeling" Model and simulation conducted by Dr.Jena Jeong, Université Gustave Eiffel, Institut de Recherche en Constructibilité, ESTP, 28 Avenue Président Wilson, 94234 Cachan, 94234 Cachan cedex, France and Dr. Hamidréza Ramézani, École Polytechnique de l'Université d'Orléans, Université d'Orléans, ICMN, UMR CNRS 7374, Interfaces, Confinement, Matériaux et Nanostructures, 8 rue Léonrad de Vinci, 45072 Orléans, France

Table 9: The coefficients, rate of hydration, and molar weight of the clinker and gypsum Jeong et al. [2019, 2021].

Mineralogy	$\mathbf{C_3S}$	$\mathbf{C_2S}$	$\mathbf{C_4AF}$	$\mathbf{C_3A}$	$\mathbf{C\bar{S}H_2}$
n_i	2.65	3.10	3.81	2.41	N/A
$k_{H,i}$ $(\times 10^{-5}\,\frac{1}{sec.})$	1.17	0.16	1.00	2.46	N/A
Molar weight $(\times 10^{-3}\,\frac{kg}{mol})$	228.3	172.2	485.9	270.1	172.17
N/A stands for not applicable.					

The analytical solution resulted to the following relation in modeling of the chemical kinetics:

$$\mathrm{F}_i(t) = 1 - \frac{[i]}{[i]_0} = 1 - \left(1 - k_{\mathrm{H},i}\,(1 - n_i)\,t\right)^{\left(\frac{1}{1-n_i}\right)}$$

or,

$$[\mathrm{i}]{=}[\mathrm{i}]_0\,\left(1 - k_{\mathrm{H},i}\,(1 - n_i)\,t\right)^{\left(\frac{1}{1-n_i}\right)} \tag{2}$$

The initial concentration of each clinker component $[i]_0$ and the one of gypsum concentration $[\mathrm{C\bar{S}H_2}]_0$ can be calculated in Equations (3) and (4) as below:

$$[i]_0 = \frac{m_i\, m_{cl}\, \rho_c\, (1 - \varepsilon_{air})}{MW_i \times \left(1 + \frac{w}{c}\,\frac{\rho_c}{\rho_w} + \frac{a}{c}\,\frac{\rho_c}{\rho_a}\right)} \tag{3}$$

$$[\mathrm{C\bar{S}H_2}]_0 = \frac{m_{gy}\, \rho_c\, (1 - \varepsilon_{air})}{MW_{gy} \times \left(1 + \frac{w}{c}\,\frac{\rho_c}{\rho_w} + \frac{a}{c}\,\frac{\rho_c}{\rho_a}\right)} \tag{4}$$

where m_i is the weight fraction of component $[i]$ in the clinker, and m_{cl} in the OPC. The end time consumption of gypsum $t = t^*$ is calculated as follows

$$t^* = \frac{1}{k_{H,C_3A}\,(1 - n_{C_3A})} \times \left(1 - \left(1 - \frac{[C\bar{S}H_2]_0}{[C_3A]_0}\right)^{1-n_{C_3A}}\right). \tag{5}$$

The time consumption of gypsum in the cement pastes after mixing, $t = t^*$, was calculated as approximately 7 days after mixing.

Based on the chemical reaction kinetics of cement from Equations (2) and (5), the molar concentration carbonated components of cement is summarized in Table 10.

Table 10: Cement components molar concentration during the hydration Papadakis et al. [1992, 1989, 1991]

Molar Concentration	Analytical formulas
$[Ca(OH)_2]$	
if $t \in [0, t^*]$	$= \frac{3}{2}[C_3S]_0\,F_{C_3S} + \frac{1}{2}[C_2S]_0\,F_{C_2S} - 2[C_4AF]_0\,F_{C_4AF}$
if $t \in]t^*, \infty]$	$= \frac{3}{2}[C_3S]_0\,F_{C_3S} + \frac{1}{2}[C_2S]_0\,F_{C_2S} - 4[C_4AF]_0\,F_{C_4AF} - 2[C_3A]_0\,F_{C_3A} + [C\bar{S}H_2]_0$
$[CSH]$	$= \frac{1}{2}[C_3S]_0\,F_{C_3S} + \frac{1}{2}[C_2S]_0\,F_{C_2S}$
$[C_3S]$	$= [C_3S]_0\,(1 - F_{C_3S})$
$[C_2S]$	$= [C_2S]_0\,(1 - F_{C_2S})$
$[C_4AF]$	$= [C_4AF]_0\,(1 - F_{C_4AF})$
$[C_3A]$	$= [C_3A]_0\,(1 - F_{C_3A})$

6.1.2 Carbonation model

Based on the hydration model result, the cement clinker components were reduced in to four minerals C−S−H gel, portlandite, C_2S, and C_3S, whereas C_4AF and C_3A were not considered in the model hence, their amount is low. The chemical reactions related to the carbonation of each compound are summarized in Table 11. The numerical expression for carbonation rate is described as follows:

$$r_i = k_i\, a_s\, [i]\, \bar{V}_i\, [CO_2] \quad \text{where} \quad i = \text{CSH}, C_3S, C_2S. \tag{6}$$

where k_i is the rate constant for the reaction of i with CO_2, and a_s is the specific surface area of the cement matrix pore in contact with water, and its expression is as follows:

$$a_s = S\, \phi_s\, (1 - \varepsilon(t)) \tag{7}$$

where S is the total pore surface area per unit weight of the cement paste, and ϕ_s is the density of the solid phase. Finally, $\bar{V}_i$ is the molar volume of each component i in Table 12

Table 11: Simplified reaction of cement components during carbonation Papadakis et al. [1992, 1989, 1991].

Type of Reaction	**Rate of Reaction**	**Formulas**
Carbonation	r_{CSH}	$C_3S_2H_3 + 3CO_2 \xrightarrow{r_{CSH}} (3\,CaCO_3 \cdot 2\,SiO_2.\ 3\,H_2O)$
	r_D	$Ca(OH)_2 r_D Ca^{2+}(aq) + 2\,OH^-(aq)$
	r_{CH}	$Ca^{2+}(aq) + 2\,OH^-(aq) + CO_2(g) r_{CH} CaCO_3(s) + H_2O$
	r_{C3S}	$C_3S + 3CO_2 + vH_2O \xrightarrow{r_{C3S}} SiO_2 \cdot\ vH_2O + 3CaCO_3$
	r_{C2S}	$C_2S + 2CO_2 + vH_2O \xrightarrow{r_{C2S}} SiO_2 \cdot\ vH_2O + 2CaCO_3$

Table 12: Carbonation model coefficients and molar weight of the clinker Jeong et al. [2019, 2021].

Mineralogy	$\mathbf{C_3S}$	$\mathbf{C_2S}$	**C−S−H**	**Portlandite**
$\bar{V}$ $(10^{-6}\ m^3/mol)$	71.3	52.2	150	3.37×10^3
k (m/sec)	1.10^{-9}	1.10^{-9}	1.10^{-9}	1.10^{-9}

The carbonation process of portlandite passes through two reactions. The first reaction is the dissolution of calcium ions in a pore solution, and the

second is the reaction between CO_2 and $[OH^-]_{aq}$. The reaction rate r_{CH} and dissolution rate r_D can be estimated as follows:

$$r_{\mathrm{CH}} = H\,R\,T\,k_2\,[\mathrm{OH}^-]_{eq}\,[\mathrm{CO}_2]. \tag{8}$$

$$r_{\mathrm{D}} = 0.5\,\varepsilon(t)\,f_w\,k_s\,a_s\,[\mathrm{Ca(OH)_2(s)}]\,\bar{V}_{CH}\,([\mathrm{OH}^-]_{aq} - [\mathrm{OH}^-]). \tag{9}$$

where H is Henry's constant, R is the gas constant, T is the temperature in Kelvin, k_2 is the rate constant for the reaction of CO_2 and OH^-, $[OH^-]_{eq}$ is the equilibrium value at saturation, $\varepsilon(t)$ is the porosity change, and k_s is the mass transfer coefficient for the dissolution of portlandite. These parameters are introduced in Table 13.

Table 13: Parameters related to the carbonation of portlandite (Jeong et al. [2019, 2021]).

Henry's constant in $\frac{mol}{m^3.atm}$	**Gas constant** in $\frac{m^3.atm}{mol.K}$	**Temperature** in ℃	k_2 in $\frac{m^3}{mol.s}$	k_s in $\frac{m}{s}$	$[OH^-]_{eq}$ in $\frac{mol}{m^3}$
34.2	8.2×10^{-5}	25	8.3	5.1×10^{-5}	43.2

There are three phenomena in the carbonation process, including CO_2 gas diffusion, its reactions with the Ca containing components, and dissolution of $Ca(OH)_2$ can be handled using a nonlinear system of time-dependent partial

differential equations in Equation (10).

$$\int_{\Omega^{\mathrm{CP}}(t)} \frac{\partial\left(\mathrm{P}\,(1-\mathrm{f})\,[\mathrm{CO_2}]\right)}{\partial t}\,dV = \int_{\Omega^{\mathrm{CP}}(t)} \left(-\,\mathrm{Div}\left(-D_{\mathrm{e,CO_2}}\nabla\left([\mathrm{CO_2}]\right)\right) - S_R\right)\,dV$$
$$\text{on} \quad \Omega^{\mathrm{CP}}(t) \in R^3 \times [0,\mathcal{T}] \quad \text{where} \quad S_R = \mathrm{P_0\,f_w r_{CH}} - 3\,\mathrm{r_{C-S-H}} - 3\,\mathrm{r_{C_3S}} - 2\mathrm{r_{C_2S}} \tag{10a}$$

$$\int_{\Omega^{\mathrm{CP}}(t)} \frac{\partial[\mathrm{Ca(OH)_2}]}{\partial t}\,dV = \int_{\Omega^{\mathrm{CP}}(t)} \left(r_{\mathrm{H,CH}} - \mathrm{P_0\,f_w\,r_{CH}}\right)\,dV \quad \text{on} \quad \Omega^{\mathrm{CP}}(t) \in R^3 \times [0,\mathcal{T}] \tag{10b}$$

$$\int_{\Omega^{\mathrm{CP}}(t)} \frac{\partial[\mathrm{CSH}]}{\partial t}\,dV = \int_{\Omega^{\mathrm{CP}}(t)} \left(-\mathrm{r_{CSH}} + \mathrm{r_{H,CSH}}\right)\,dV \quad \text{on} \quad \Omega^{\mathrm{CP}}(t) \in R^3 \times [0,\mathcal{T}] \tag{10c}$$

$$\int_{\Omega^{\mathrm{CP}}(t)} \frac{\partial[\mathrm{C_3S}]}{\partial t}\,dV = \int_{\Omega^{\mathrm{CP}}(t)} \left(-\mathrm{r_{C_3S}} + \mathrm{r_{H,C_3S}}\right)\,dV \quad \text{on} \quad \Omega^{\mathrm{CP}}(t) \in R^3 \times [0,\mathcal{T}] \tag{10d}$$

$$\int_{\Omega^{\mathrm{CP}}(t)} \frac{\partial[\mathrm{C_2S}]}{\partial t}\,dV = \int_{\Omega^{\mathrm{CP}}(t)} \left(-\mathrm{r_{C_2S}} + \mathrm{r_{H,C_2S}}\right)\,dV \quad \text{on} \quad \Omega^{\mathrm{CP}}(t) \in R^3 \times [0,\mathcal{T}] \tag{10e}$$

Using these equations, the molar concentrations of each clinker component, including $[CO_2]$, $[C_2S]$, $[C_3S]$, [CSH], and $[Ca(OH)_2]$ can be calculated.

Here, the initial coefficient of CO_2 diffusion D_{e,CO_2} was estimated as a function of the effective porosity of hardened cement paste ($P_P(t)$) and relative

humidity (HR) as follows (Papadakis et al. [1992, 1989, 1991]):

$$D_{e,CO_2} \approx 1.68 \times 10^{-7} \left(P_P(t)\right)^{1.8} \left(1 - \frac{HR}{100}\right)^{2.2} \tag{11}$$

$P_P(t)$ can be expressed based on cement hydration and carbonation as follows:

$$P_P(t) = P_0 - \Delta P_H(t) + \Delta P_C(t) \tag{12}$$

where $P_P(t)$, P_0, $\Delta P_H(t)$, and ΔP_C. are current porosity, initial porosity, porosity reduction due to hydration, and porosity change due to the carbonation, respectively (see Jeong et al. [2019] for more details). The initial porosity can be well estimated by (Papadakis et al. [1989, 1991]). The change of porosity due to the carbonated cement introduced the densification of the porosity due to the precipitation of the $CaCO_3$ as follows:

$$\Delta P_C = [Ca(OH)_2]\,\Delta \bar{V}_{CH} + [CSH]\,\Delta \bar{V}_{CSH} - [CaCO_3]\,\Delta \bar{V}_{CaCO_3}. \tag{13}$$

where the difference in the molar volume value for each mineral phases is presented in Table 14. The parameter $P_P(t)$ presents a porosity change during carbonation. It is important to note that this parameter does not take into account the volume change of skeleton in the cement matrix (Papadakis et al. [1989, 1991]). The molar concentration of $CaCO_3$ precipitated, which was proposed herein, was estimated in Equation (14).

$$[CaCO_3] = 2[C_2S] + 3[C_3S] + 3[CSH] + [Ca(OH_2)] \tag{14}$$

where [C_2S], [C_3S], [CSH], and [$Ca(OH)_2$] can be calculated using a nonlinear system of time-dependent partial differential equations (Equation (10)).

Table 14: Molar volume difference of the solid products, $Ca(OH)_2$, C−S−H, and $CaCO_3$ in the carbonation Jeong et al. [2019].

Mineralogy	$\Delta\bar{V}_{CaOH_2}$	$\Delta\bar{V}_{CSH}$	$\Delta\bar{V}_{CaCO_3}$
$\Delta\bar{V}$ $(10^{-6} \quad m^3/mol)$	3.85	15.39	36.9

6.1.3 Simulation

The FEM simulation (Conducted by using Virtual cloud computing) of the hydration was conducted based on the determined chemical reaction of cement hydration. The amount of amorphous phases prior to carbonation was assumed to be determined using semi-emperical method. Initially, the anhydrous clinker phase compositions, portlandite, calcite, and amorphous phases in the hardened cement paste at 14th and 28th days of hydration, obtained from the QXRD analysis as a reference.Figure 45 presents the phase composition of the specimens before carbonation detected by QXRD. The sum of other mineral phase compositions, including C_3A, C_4AF, ettringite, and monosulfates in the specimens before carbonation was almost totally consumed, less than 1 %. Next, determined values from QXRD were adopted as the initial phase compositions of the cement matrix in the numerical simulation of carbonation. Then, a time-dependent simulation was conducted based on this initial phase composition for carbonation and further hydration. The content of water evaporated from the specimens were determined from TGA analysis. The amorphous content obtained from specimens hydratd for 14 and 28

days through QXRD was 62±3% and 67±4% respectively, its before carbonation. The experimental investigation reveals that, this phase included both the anhydrous slag and the C−S−H gel, and the anhydrous slag could not be separately calculated from the C−S−H by QXRD analysis. Although studies from (Feng et al. [2004]; **?**) shows that the degree of slag reaction in the slag cement was almost similar to that of cement. In addition, the hydration period followed by the carbonation for our samples reached from 14 days to 28 days which gives time for slag to involve in the process as hydration product. The studies from (Monkman and Shao [2010]) shows that OPC cement and blend cement with 75%-OPC/25%-slag, carbonated for 2hr resulted similar mass gain and water lost. Therefore, it was reasonable to assume that most of this amorphous content was occupied by C−S−H gel as specimens that has been hydrated sufficiently. Therefore, simulation doesn't consider the reaction of the anhydrous slag from 14 days and 28 days of hydration.

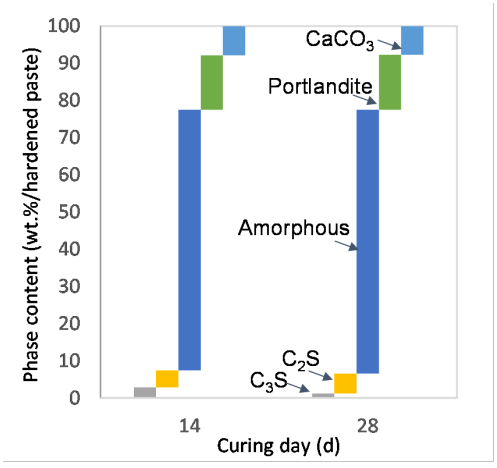

Figure 45: Specimens phase composition before carbonation detected by QXRD.

With respect to the experiments, as shown in Figure 19, a numerical sam-

ple of 40 mm × 40 mm × 40 mm was prepared using Matlab-Comsol MP user-written code (Jeong et al. [2014, 2016, 2017, 2013]; Ramézani et al. [2012, 2013]; **?**). The mesh density was improved to obtain 695 × 252 degrees of freedom, and the computation lasted up to more than 3 h [3]. The numerical sample was subjected to uniaxial CO_2 gas diffusion with a 10 vol.% of CO_2 (100,000 ppm or 4.4 $[mol/m^3]$). By applying the FEM (Oh et al. [2013]; Zienkiewicz et al. [2005]), the multi-reactive carbonation model in Equation (10) was solved considering the Neumann and Dirichlet boundary conditions on the outer surface and the rest of the numerical sample, respectively, (Jeong et al. [2019]; Ramézani and Jeong [2011]). The Dirichlet boundary condition is applied on the outer surface as below:

$$\begin{cases} [CO_2] = [CO_2]_0 \text{ on } \quad \partial\Omega^{\text{outer}} \subset R^2 \\ \quad \text{where } \quad \partial\Omega^{\text{outer}} = \{S \in R^2 |\, x = 0\} \cup \{S \in R^2 |\, y = 0\} \cup \{S \in R^2 |\, z = 0\} \end{cases} \tag{15}$$

where $[CO_2]_0$ signifies the initial molar concentration of carbon dioxide (4.4 $[mol/m^3]$) at the outer surface of the numerical sample. The Neumann boundary condition was applied to the remaining surfaces of the sample for [j]=[$Ca(OH)_2$(s)],

[3] Virtual cloud computing service offered 128 GB of RAM and 16 processors for the simulation.

[CSH], [C_3S], and [C_2S]:

$$\begin{cases} -\dfrac{\partial[\mathrm{j}]}{\partial x} = 0 \quad \text{on} \quad \partial\Omega^{\mathrm{yz}} \subset R^2, \\ \qquad\qquad \text{where} \quad \partial\Omega^{\mathrm{yz}} = \{S \in R^2 |\, x = 0, 0y40, 0z40\} \\ -\dfrac{\partial[\mathrm{j}]}{\partial y} = 0 \quad \text{on} \quad \partial\Omega^{\mathrm{xz}} \subset R^2, \\ \qquad\qquad \text{where} \quad \partial\Omega^{\mathrm{xz}} = \{S \in R^2 |\, y = 0, 0x40, 0z40\} \\ -\dfrac{\partial[\mathrm{j}]}{\partial z} = 0 \quad \text{on} \quad \partial\Omega^{\mathrm{xy}} \subset R^2, \\ \qquad\qquad \text{where} \quad \partial\Omega^{\mathrm{xy}} = \{S \in R^2 |\, z = 0, 0x40, 0y40\} \end{cases} \tag{16}$$

The initial conditions can be denoted as below:

$$\begin{cases} [\mathrm{CO_2}](\mathbf{x}, 0) = 0 & \text{on} \quad \partial\Omega^{\mathrm{CP}} \subset R^3 \\ [\mathrm{Ca(OH)_2(s)}](\mathbf{x}, 0) = [\mathrm{Ca(OH)_2(s)}]_0 & \text{on} \quad \partial\Omega^{\mathrm{CP}} \subset R^3 \\ [\mathrm{CSH}](\mathbf{x}, 0) = [\mathrm{CSH}]_0 & \text{on} \quad \partial\Omega^{\mathrm{CP}} \subset R^3 \\ [\mathrm{C_3S}](\mathbf{x}, 0) = [\mathrm{C_3S}]_0 & \text{on} \quad \partial\Omega^{\mathrm{CP}} \subset R^3 \\ [\mathrm{C_2S}](\mathbf{x}, 0) = [\mathrm{C_2S}]_0 & \text{on} \quad \partial\Omega^{\mathrm{CP}} \subset R^3 \\ \mathrm{P}(\mathbf{x}, 0) = \mathrm{P}_0 & \text{on} \quad \partial\Omega^{\mathrm{CP}} \subset R^3 \end{cases} \tag{17}$$

where $[\mathrm{Ca(OH)_2(s)}]_0$, $[\mathrm{CSH}]_0$, $[\mathrm{C_3S}]_0$, $[\mathrm{C_2S}]_0$, and P_0. are the initial molar concentrations of [$\mathrm{Ca(OH)_2(s)}$], [CSH], [C_3S], [C_2S], and initial porosity, respectively.

These initial cement paste concentrations relied on the hydration equations in ([Papadakis et al., 1991]); therefore, the hydration outcomes before

the carbonation experiments were calculated and applied as initial conditions. Hydration and carbonation were fully coupled for all carbonation computations herein. Figure 46 shows the remained clinker estimation of the experimental and numerical model, due to lower amount there is flactuation on the experimental result on the remaining anhydrous phases. Figure 47 confirmed the experimental and numerical model of portlandite and calcite.

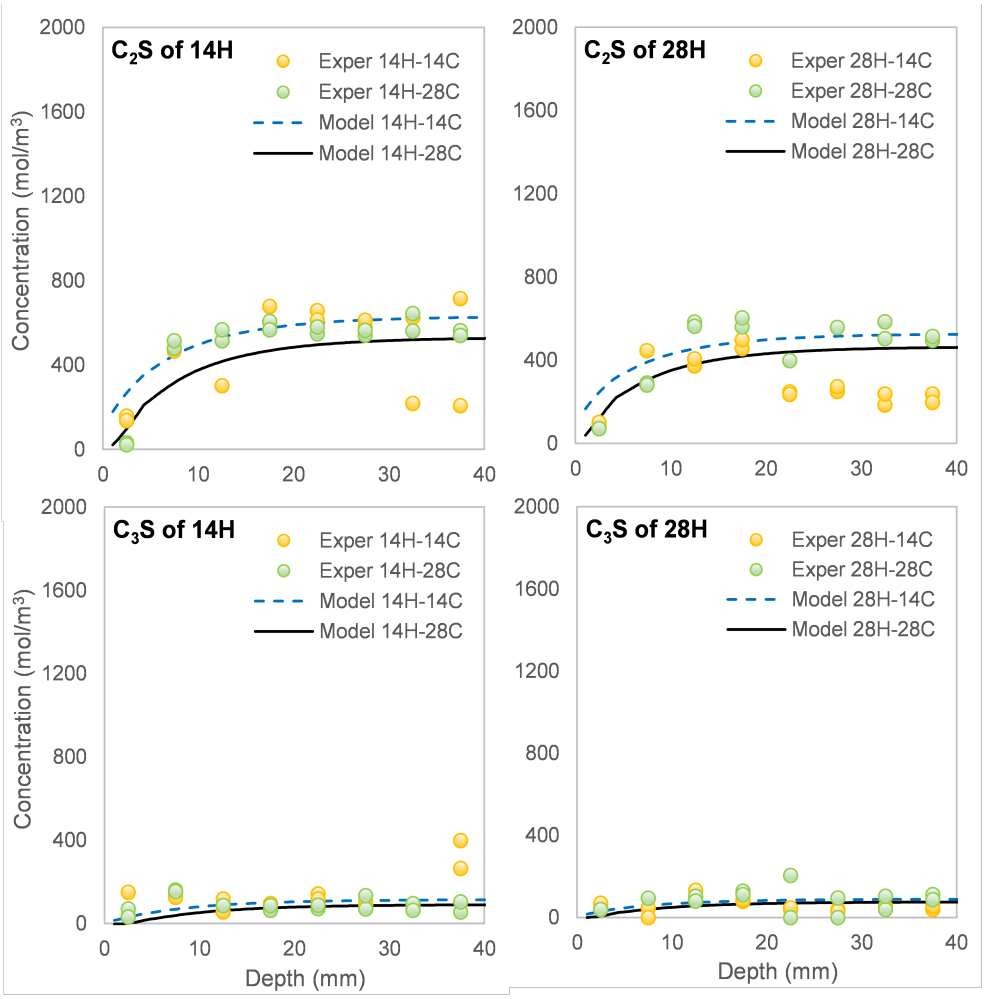

Figure 46: Profiling of anhydrous clinker minerals (Molar concentration per unit volume of hardened paste specimens) (experimental and simulation results).

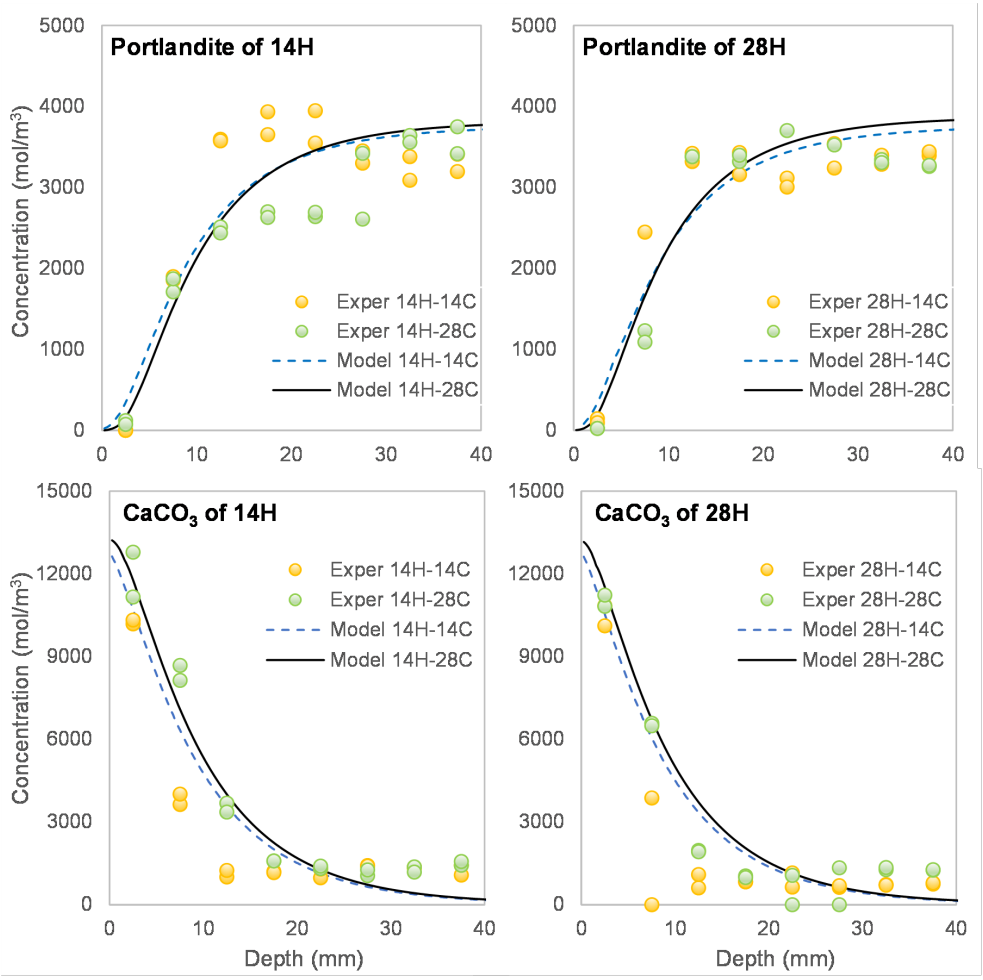

Figure 47: Profiling of $CaCO_3$ and $Ca(OH)_2$ (Molar concentration per unit volume of hardened paste specimens) (experimental and simulation results).

6.2 Appendix B. Phase structures of cement minerals used in Rietveld refinement

Table 15: Phase structures used in the Rietveld refinement and their respective references.

Phases	Formula	Crystal system notation	ICSD codes	Ref.
Anhydrite	$CaSO_4$	Orthorhombic	15876	Cheng et al. [1963]
Hemihydrate/Bassanite	$CaSO_4 \cdot 0.5\,H_2O$	Monoclinic	79529	Bezou et al. [1995]
C_4AF	$Ca_8Fe_{4\cdot06}Al_{3\cdot94}O_{20}$	Orthorhombic	98836	Redhammer et al. [2004]
Brucite	$Mg(OH)_2$	Cubic	34401	ROTHBAUER et al. [1967]
Calcite	$CaCO_3$	Hexagonal	73446	Maslen et al. [1993]
Vaterite	$CaCO_3$	Hexagonal	15879	Kamhi and IUCr [1963]
C_3A	$Ca_{8\cdot25}Na_{1\cdot5}Al_6O_{18}$	Monoclinic	100221	Takéuchi and Nishi [1980]
C_2S	Ca_2SiO_4	Monoclinic	81096	**?**
Ettringite	$Ca_6Al_2(SO_4)_3(OH)_{12}(H_2O)_6$	Hexagonal	251756	Norman et al. [2013]
Gypsum	$CaSO_4 \cdot 2\,H_2O$	Monoclinic	409581	Boeyens and Ichharam [2002]
C_3S	Ca_3SiO_5	Hexagonal	22501	Ll'Inets et al.
Periclase	MgO	Hexagonal	9863	SASAKI et al. [1979]
Portlandite	$Ca(OH)_2$	Hexagonal	202220	Chaix-Pluchery et al. [1987]
Monocarbonate	$Ca_4Al_2O_{20}CH_{22}$	Anorthic	59327	François et al. [1998]
Hemicarbonate	$Ca_{12}Al_6O_{55\cdot2}C_{2\cdot4}$	Hexagonal	263123	Runvcevski et al. [2012]
Thenardite	Na_2SO_4	Orthorhombic	28056	**?**
Rutile	TiO_2	Tetragonal	16636	Baur and IUCr [1956]

6.3 Appendix C. Phase of minerals in early age carbonated through the depth

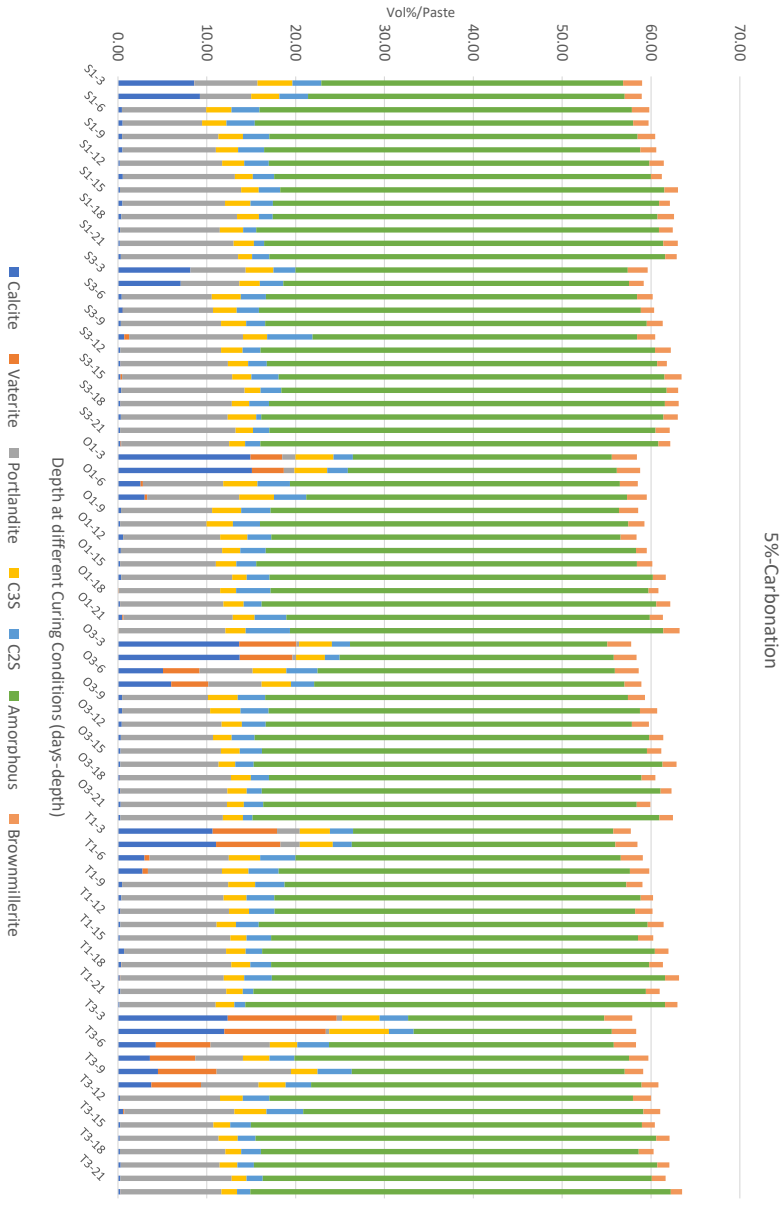

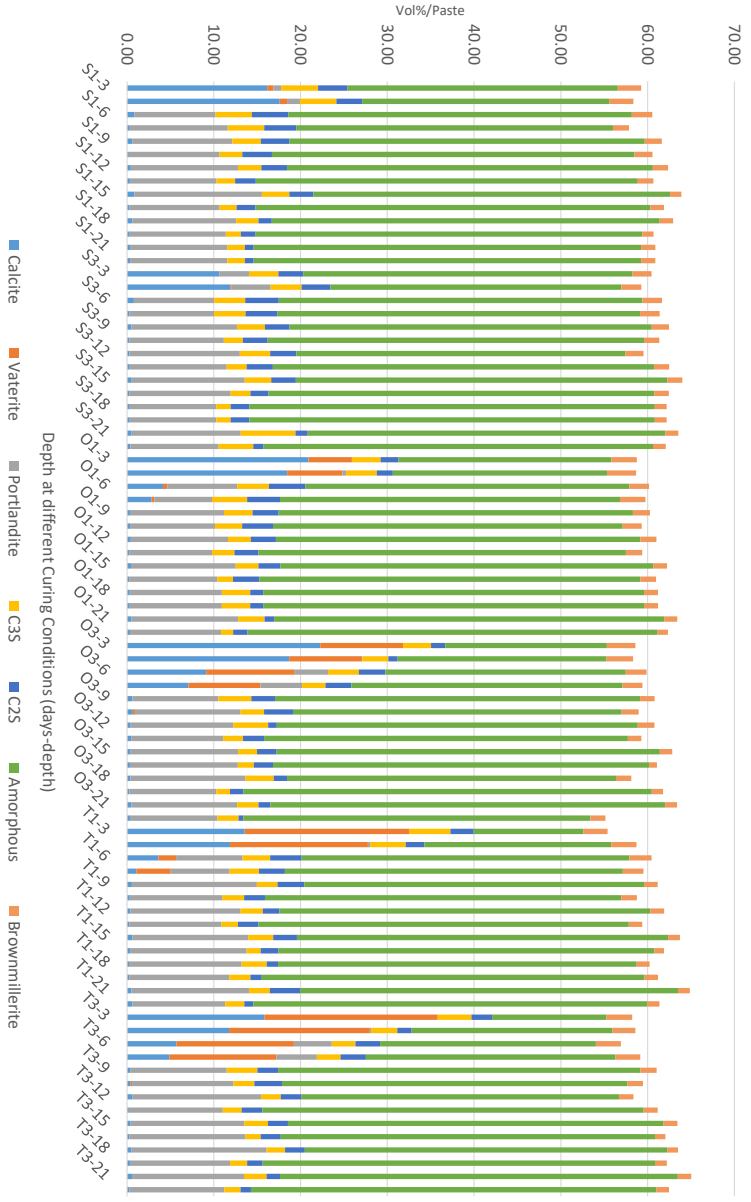

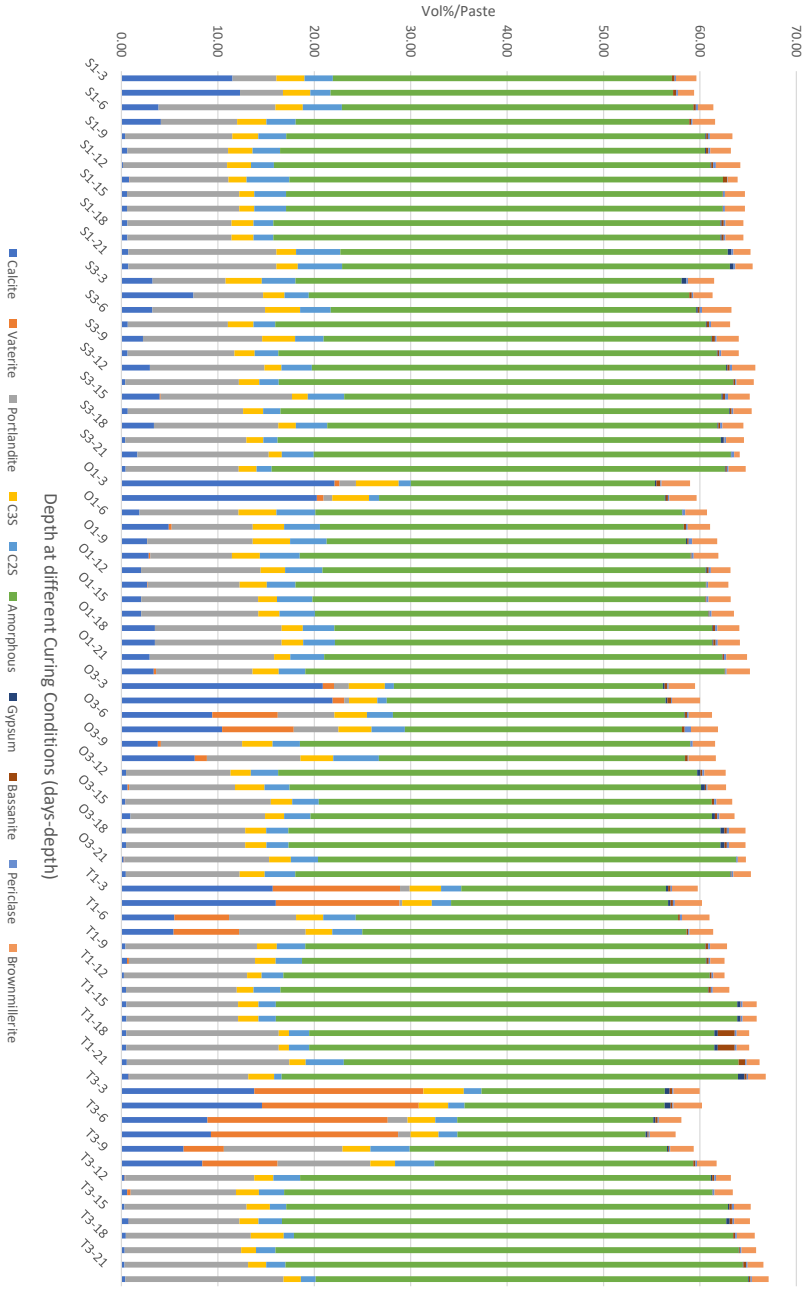

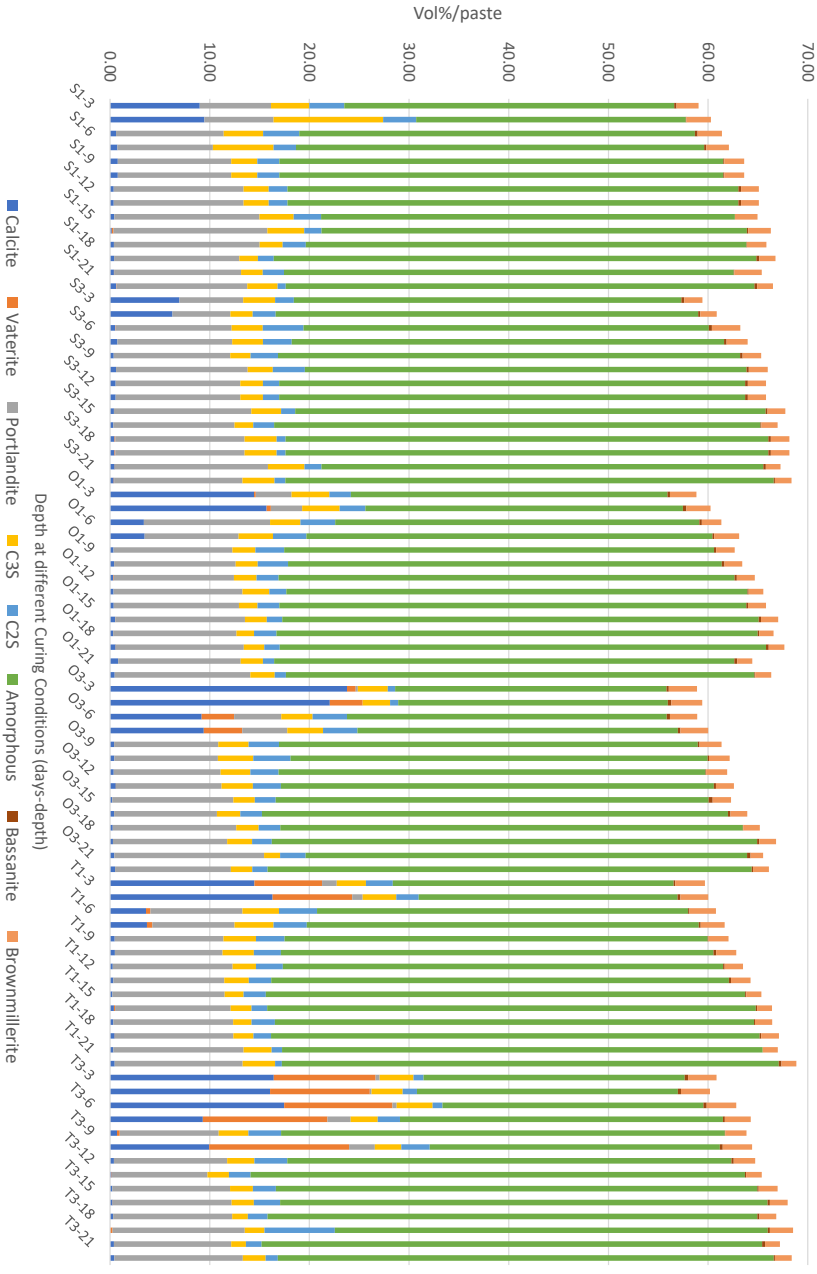

PUBLICATION

1. Jena Jeong, Abel Shiferaw Alemu, Solmoi Park, Hyo Kyoung Lee, Gebremicael Liyew, Hamidréza Ramézani, Vagelis G. Papadakis, and Hyeong-Ki Kim (2021) On Phase profiling of carbonated cement paste: quantitative X-ray diffraction analysis and numerical modeling (Submitted)

REFERENCES

[1] Al-Kadhimi, T.K.H., Banfill, P.F.G., Millard, S.G., Bungey, J.H., 1996. "An accelerated carbonation procedure for studies on concrete." Advances in Cement Research 8, 47–59. doi:10.1680/adcr.1996.8.30.47.

[2] An Jerga, J., 2004. "Physico-mechanical properties of carbonated concrete." URL: www. elsevier.com/locate/conbuildmat, doi:10.1016/j.conbuildmat.2004.04.029.

[3] Arandigoyen, M., Bicer-Simsir, B., Alvarez, J.I., Lange, D.A., 2006. "Variation of microstructure with carbonation in lime and blended pastes." Applied surface science 252, 7562–7571.

[4] Ashraf, W., 2016. "Carbonation of cement-based materials: Challenges and opportunities." Construction and Building Materials 120, 558–570. URL: http://dx.doi.org/10.1016/ j.conbuildmat.2016.05.080, doi:10.1016/j.conbuildmat.2016.05.080.

[5] ASTM C-109/109M-16a, A., 2016. "Standard test method for compressive strength of hydraulic cement mortars (Using 2-in. or cube specimens)."Annual Book of ASTM Standards , 1–10doi:10.1520/C0109.

[6] ASTM Standard C215, 2008. "Standard Test Method for Fundamental Transverse , Longitudinal , and Torsional Resonant Frequencies of Concrete Specimens." ASTM standard , 1–7URL: http://www.astm.org/Standards/C215.htm.

[7] Auroy, M., Poyet, S., Le Bescop, P., Torrenti, J.M., Charpentier, T., Moskura, M., Bourbon, X., 2015. "Impact of carbonation on unsaturated water transport properties of cementbased materials." Cement and Concrete Research 74, 44–58. URL: http://dx.doi.org/10.1016/j.cemconres.2015.04.002, doi:10.1016/j.cemconres.2015.04.002.

[8] Auroy, M., Poyet, S., Le Bescop, P., Torrenti, J.M., Charpentier, T., Moskura, M., Bourbon, X., 2018. "Comparison between natural and accelerated carbonation (3% CO2): Impact on mineralogy, microstructure, water retention and cracking." Cement and Concrete Research doi:10.1016/j.cemconres.2018.04.012.

[9] Barnes, P., Bensted, J., 2002. "Structure and performance of cements." CRC Press.

[10] Baur, W., IUCr, 1956. "Uber die Verfeinerung der Kristallstrukturbestimmung einiger¨ Vertreter des Rutiltyps: TiO2, SnO2, GeO2 und MgF2. urn:issn:0365-110X 9, 515–520. URL: //scripts.iucr.org/cgi-bin/paper?a01727, doi:10.1107/S0365110X56001388.

[11] Bavzant, Z.P., Najjar, L.J., 1971. "Drying of concrete as a nonlinear diffusion problem." Cement and Concrete Research 1, 461–473. doi:10.1016/0008-8846(71)90054-8.

[12] Bertolini, L., Polder, R., . “Green Corrosion Chemistry and Engineering Corrosion Handbook – Corrosive Agents and Their Interaction with Materials Corrosion Resistance of Aluminium and Aluminium Alloys Structural Stability of Steel Managing Performance in Construction Plasma Spray Coa. ”

[13] Bezou, C., Nonat, A., Mutin, J.C., Nørlund Christensen, A., Lehmann, M.S., 1995. “Investigation of the Crystal Structure of γ-CaSO4, CaSO4 · 0.5 H2O, and CaSO4 · 0.6 H2O by Powder Diffraction Methods.” Journal of Solid State Chemistry 117, 165–176. doi:10.1006/JSSC.1995.1260.

[14] Boeyens, J.C.A., Ichharam, V.V.H., 2002. “Redetermination of the crystal structure of calcium sulphate dihydrate, CaSO4 · 2H2O. Zeitschrift fu¨r Kristallographie - New Crystal Structures 217, 9–10. URL: https://www.degruyter.com/document/doi/10.1524/ncrs.2002.217.jg.9/html, doi:10.1524/NCRS.2002.217.JG.9.

[15] Bullard, J.W., Jennings, H.M., Livingston, R.A., Nonat, A., Scherer, G.W., Schweitzer, J.S., Scrivener, K.L., Thomas, J.J., 2011. “Mechanisms of cement hydration.” Cement and Concrete Research 41, 1208–1223. URL: http://dx.doi.org/10.1016/j.cemconres. 2010.09.011, doi:10.1016/j.cemconres.2010.09.011.

[16] Castellote, M., Fernandez, L., Andrade, C., Alonso, C., 2009. “Chemical changes and phase analysis of OPC pastes carbonated at different CO2 concentrations.” Materials and Structures/Materiaux et Constructions doi:10.1617/s11527-008-9399-1.

[17] Chaix-Pluchery, O., Pannetier, J., Bouillot, J., Niepce, J.C., 1987. “Structural prereactional transformations in Ca(OH)2.” Journal of Solid State Chemistry 67, 225–234. doi:10.1016/ 0022-4596(87)90358-6.

[18] CHATTERJI, A.K., RAWAT, R.S., 1965. “Hydration of Portland Cement.” Nature 1965 207:4998 207, 713–715. URL: https://www.nature.com/articles/207713a0, doi:10. 1038/207713a0.

[19] Chatterji, S., Snyder, K.A., Marchand, J., 2002. “Depth profiles of carbonates formed during natural carbonation.” Cement and Concrete Research 32, 1923–1930. doi:10.1016/ S0008-8846(02)00908-0.

[20] Cheng, G., Zussman, J., IUCr, 1963. “The crystal structure of anhydrite (CaSO4).” urn:issn:0365-110X 16, 767–769. URL: //scripts.iucr.org/cgi-bin/paper?a03906, doi:10.1107/S0365110X63001997.

[21] Choi, J.I., Lee, Y., Kim, Y.Y., Lee, B.Y., 2017. “Image-processing technique to detect carbonation regions of concrete sprayed with a phenolphthalein solution.” Construction and Building

Materials 154, 451–461. URL: http://dx.doi.org/10.1016/j.conbuildmat.2017.07.205, doi:10.1016/j.conbuildmat.2017.07.205.

[22] De Weerdt, K., Plusquellec, G., Belda Revert, A., Geiker, M.R., Lothenbach, B., 2019. "Effect of carbonation on the pore solution of mortar." Cement and Concrete Research 118, 38–56. URL: https://doi.org/10.1016/j.cemconres.2019.02.004, doi:10.1016/ j.cemconres.2019.02.004.

[23] El-Hassan, H., Shao, Y., Journal, Z.G.A.M., 2013, U., . "Effect of Initial Curing on Carbonation Of Light weight Concrete Masonry Units."search.ebscohost.comURL:http://search.ebscohost.com/login.aspx?direct=true{&}profile=ehost{&}scope=site{&}authtype=crawler{&}jrnl=0889325X{&}AN=89187232{&}h=RGtfHMrwGSaUqnbbXSHRUv7pysa0Hawj9WOvzcx6H{%}2B1JDrYiKBeD9LJVM7J6LSe{%}2B05HhvUK1btADeOvIm02Y c.

[24] Feng, X., Garboczi, E.J., Bentz, D.P., Stutzman, P.E., Mason, T.O., 2004. "Estimation of the degree of hydration of blended cement pastes by a scanning electron microscope point-counting procedure." Cement and Concrete Research 34, 1787–1793. doi:10.1016/J.CEMCONRES.2004.01.014.

[25] Franc¸ois, M., Renaudin, G., Evrard, O., IUCr, 1998. "A Cementitious Compound with Composition 3CaO.Al2O3.CaCO3.11H2O." urn:issn:0108-2701 54, 1214–1217. URL: //scripts.iucr.org/cgi-bin/paper?sk1142, doi:10.1107/S0108270198004223.

[26] Han, J., Sun, W., Pan, G., Caihui, W., 2013. "Monitoring the evolution of accelerated carbonation of hardened cement pastes by X-ray computed tomography." Journal of materials in civil engineering 25, 347–354.

[27] Herrmann, H., Bucksch, H., 2014. Concrete Chemise. doi:10.1007/978-3-642-41714-6_ 33900.

[28] Jansen, D., Goetz-Neunhoeffer, F., Stabler, C., Neubauer, J., 2011. "A remastered external standard method applied to the quantification of early OPC hydration." Cement and Concrete Research 41, 602–608. doi:10.1016/J.CEMCONRES.2011.03.004.

[29] Jeong, J., Ram´ezani, H., Chuta, E., 2019. "Reactive transport numerical modeling of mortar carbonation: Atmospheric and accelerated carbonation." Journal of Building Engineering 23, 351–368. URL: https://doi.org/10.1016/j.jobe.2019.01.038, doi:10.1016/ j.jobe.2019.01.038.

[30] Jeong, J., Ram´ezani, H., Leklou, N., 2014. "Thermo-chemical heterogeneous hydration gradient modeling of concrete and aggregates size effect on ITZ." Thermochimica Acta 590, 165–180. doi:10.1016/J.TCA.2014.06.019.

[31] Jeong, J., Ram´ezani, H., Leklou, N., 2016. "Why does the modified Arrhenius' law fail to describe the hydration modeling of recycled aggregate? " Thermochimica Acta 626, 13–30. doi:10.1016/J.TCA.2016.01.001.

[32] Jeong, J., Ram´ezani, H., Leklou, N., Jeong, J., Ram´ezani, H., Leklou, N., 2017. "Porous-microdilatation theory for random crystallization: Monte Carlo simulation for delayed ettringite formation." Acta Mechanica 2017 228:9 228, 3223–3249. URL: https://link.springer.com/article/10.1007/s00707-017-1863-y, doi:10.1007/S00707-017-1863-Y.

[33] Jeong, J., Ram´ezani, H., Leklou, N., Mounanga, P., 2013. "Chemo-physical modeling of cement mortar hydration: Role of aggregates. Thermochimica Acta 564, 70–82. doi:10.1016/J.TCA.2013.03.034.

[34] Jeong, J., Ram´ezani, H., Papadakis, V.G., Colin, J., Izoret, L., 2021. "On \ce{CO2} sequestration in concrete aggregate via carbonation: simulation and experimental verification." European Journal of Environmental and Civil Engineering doi:10.1080/19648189.2021.1928555.

[35] Kamhi, S., IUCr, 1963. "On the structure of vaterite CaCO3. urn:issn:0365-110X 16, 770–772. URL: //scripts.iucr.org/cgi-bin/paper?a03907, doi:10.1107/S0365110X63002000.

[36] Kamimura, K., Sereda, P.J., Swenson, E.G., 2015. "Changes in weight and dimensions in the drying and carbonation of Portland cement mortars." http://dx.doi.org/10.1680/macr.1965.17.50.5 17, 5–14. URL: https://www.icevirtuallibrary.com/doi/abs/10.1680/macr.1965.17.50.5,doi:10.1680/MACR. 1965.17.50.5.

[37] Ll'Inets, A., Doklady, Y.M.....P., undefined 1985, . "Crystal structure of the rhombohedral modification of tricalcium silicate Ca3SiO5. ui.adsabs.harvard.edu URL: https://ui.adsabs.harvard.edu/abs/1985SPhD...30..191L/abstract.

[38] Maslen, E., Streltsov, V., Streltsova, N., IUCr, 1993. "X-ray study of the electron density in calcite, CaCo3. urn:issn:0108-7681 49, 636–641. URL: //scripts.iucr.org/cgi-bin/paper?as0621, doi:10.1107/S0108768193002575.

[39] Mather, B., Hime, W.G., 2002. "Amount of Water Required for Complete Hydration of Portland Cement." Concrete International 24, 56–58.

[40] Matschei, T., Lothenbach, B., Glasser, F.P., 2007. "The role of calcium carbonate in cement hydration." Cement and Concrete Research 37, 551–558. doi:10.1016/j.cemconres.2006.10.013.

[41] Mehta, P., Monteiro, P., 2014. "Concrete: microstructure, properties, and materials." URL:https://www.accessengineeringlibrary.com/binary/mheaeworks/a8a2d82a09d997cb/a23447d5355b9c16fe749ac698b56fbf08584d3422a5d81c9281c54449cc825a/ book-summary.pdf.

[42] Meller, N., Hall, C., Jupe, A.C., Colston, S.L., Jacques, S.D., Barnes, P., Phipps, J., 2004. "The paste hydration of brownmillerite with and without gypsum: A time resolved synchrotron

diffraction study at 30, 70, 100 and 150 °C." Journal of Materials Chemistry , 428–435doi:10.1039/b313215c.

[43] Monkman, S., Shao, Y., 2010. "Carbonation curing of slag-cement concrete for binding co 2 and improving performance." Journal of Materials in Civil Engineering 22, 296–304.

[44] Mousa, M.I., Mahdy, M.G., Abdel-Reheem, A.H., Yehia, A.Z., 2015. "Self-curing concrete types; water retention and durability." Alexandria Engineering Journal 54, 565–575. doi:10.1016/J.AEJ.2015.03.027.

[45] Ngala, V.T., Page, C.L., 1997. "Effects of carbonation on pore structure and diffusional properties of hydrated cement pastes." Cement and Concrete Research 27, 995–1007. doi:10.1016/S0008-8846(97)00102-6.

[46] Norman, R.L., Dann, S.E., Hogg, S.C., Kirk, C.A., 2013. "Synthesis and structural characterisation of new ettringite and thaumasite type phases: Ca6[Ga(OH)6·12H2O]2(SO4)3·2H2O and Ca6[M(OH)6·12H2O]2(SO4)2(CO3)2, M = Mn, Sn. Solid State Sciences 25, 110–117. doi:10.1016/J.SOLIDSTATESCIENCES.2013.08.006.

[47] Oh, S.I., Altan, T., Histon, E., 2013. "FEM modelling of materials processing and properties, 169URL:https://books.google.com/books/about/Applied{_}Finite{_}Element{_}Analysis.html?hl=fr{&}id=ypNRAAAAMAAJ.

[48] Otsu, N., 1979. "A threshold selection method from gray-level histograms. IEEE transactions on systems, man, and cybernetics 9, 62–66.

[49] Papadakis, V.G., Fardis, M.N., Vayenas, C.G., 1992. "Effect of composition, environmental factors and cement-lime mortar coating on concrete carbonation." Materials and Structures 25, 293–304. URL: http://dx.doi.org/10.1007/BF02472670, doi:10.1007/BF02472670.

[50] Papadakis, V.G., Vayenas, C.G., Fardis, M.N., 1989. "A reaction engineering approach to the problem of concrete carbonation." AIChE Journal 35, 1639–1650. URL: http://dx.doi.org/10.1002/aic.690351008, doi:10.1002/aic.690351008.

[51] Papadakis, V.G., Vayenas, C.G., Fardis, M.N., 1991. "Experimental investigation and mathematical modeling of the concrete carbonation problem." Chemical Engineering Science 46, 1333–1338. URL: http://www.sciencedirect.com/science/article/pii/000925099185060B, doi:10.1016/0009-2509(91)85060-B.

[52] Phung, Q.T., Maes, N., De Schutter, G., Jacques, D., Ye, G., 2013. "A methodology to study carbonation of cement paste and its effect on permeability." Proceedings of the 4th International Conference on Accelerated Carbonation for Environmental and Materials Engineering , 459–463URL: http://hdl.handle.net/1854/LU-3194191.

[53] Raheem, A.A., Soyingbe, A.A., Emenike, A.J., 2013. “Effect of Curing Methods on Density and Compressive Strength of Concrete.” Cement and Concrete Composites 3, 55–64.

[54] Ram´ezani, H., El-Hraiech, A., Jeong, J., Benhamou, C.L., 2012. “Size effect method application for modeling of human cancellous bone using geometrically exact Cosserat elasticity.” Computer Methods in Applied Mechanics and Engineering 237-240, 227–243. doi:10.1016/J.CMA.2012.05.002.

[55] Ram´ezani, H., Jeong, J., 2011. “Environmentally motivated modeling of hygrothermally induced stresses in the layered limestone masonry structures: Physical motivation and numerical modeling.” Acta Mechanica 2011 220:1 220, 107–137. URL: https://link.springer.com/article/10.1007/s00707-011-0463-5, doi:10.1007/S00707-011-0463-5.

[56] Ram´ezani, H., Mounanga, P., Jeong, J., Bouasker, M., 2013. “Role of cement paste composition on the self induced stress in early-age mortars: Application of the Cosserat size number.” Cement and Concrete Composites 39, 43–59. doi:10.1016/J.CEMCONCOMP.2013. 03.005.

[57] Redhammer, G.J., Tippelt, G., Roth, G., Amthauer, G., 2004. “Structural variations in the brownmillerite series Ca2(Fe2−xAlx)O5: Single-crystal X-ray diffraction at 25 °C and hightemperature X-ray powder diffraction (25 °C ≤ T ≤ 1000 °C).” American Mineralogist 89, 405–420. URL: https://www.degruyter.com/document/doi/10.2138/am-2004-2-322/ html, doi:10.2138/AM-2004-2-322.

[58] Rostami, V., Shao, Y., Boyd, A.J., 2011. “Carbonation Curing versus Steam Curing for Precast Concrete Production.” Journal of Materials in Civil Engineering 24, 1221–1229. URL: https://ascelibrary.org/doi/abs/10.1061/{%}28ASCE{%}29MT.1943-5533.0000462, doi:10.1061/(ASCE)MT.1943-5533.0000462.

[59] Rostami, V., Shao, Y., Boyd, A.J., 2012. “Carbonation Curing versus Steam Curing for Precast Concrete Production.” Journal of Materials in Civil Engineering 24, 1221–1229. doi:10.1061/(asce)mt.1943-5533.0000462.

[60] ROTHBAUER, R., ZIGAN, F., O’DANIEL, H., 1967. “Verfeinerung der Struktur des Bayerits, Al(OH)3. Zeitschrift fu¨r Kristallographie - Crystalline Materials 125, 317–331. URL:https://www.degruyter.com/document/doi/10.1524/zkri.1967.125.16.317/html, doi:10.1524/ZKRI.1967.125.16.317.

[61] Runvcevski, T., Dinnebier, R., Magdysyuk, O., Po¨llmann, H., IUCr, 2012. “Crystal structures of calcium hemicarboaluminate and carbonated calcium hemicarboaluminate from synchrotron powder diffraction data.” urn:issn:0108-7681 68, 493–500. URL: http: //scripts.iucr.org/cgi-bin/paper?eb5017, doi:10.1107/S010876811203042X.

[62] SASAKI, S., FUJINO, K., TAKEUCHI, Y., 1979. "X-Ray Determination of Electron-Density´ Distributions in Oxides, MgO, MnO, CoO, and NiO, and Atomic Scattering Factors of their Constituent Atoms." Proceedings of the Japan Academy, Series B 55, 43–48. doi:10.2183/PJAB.55.43.

[63] Scrivener, K., Ouzia, A., Juilland, P., Kunhi Mohamed, A., 2019. "Advances in understanding cement hydration mechanisms. " Cement and Concrete Research 124, 105823. URL: https://doi.org/10.1016/j.cemconres.2019.105823, doi:10.1016/j. cemconres.2019.105823.

[64] Scrivener, K.L., Juilland, P., Monteiro, P.J.M., 2015. "Advances in understanding hydration of Portland cement."Cement and Concrete Research 78, 38–56.

[65] Scrivener, K.L., Nonat, A., 2011. "Hydration of cementitious materials, present and future." Cement and Concrete Research 41, 651–665. URL: http://dx.doi.org/10.1016/ j.cemconres.2011.03.026, doi:10.1016/j.cemconres.2011.03.026.

[66] Scrivener, K.L., Snellings, R., Lothenbach, B., 2016. "A Practical Guide to Microstructural Analysis of Cementitious Materials." CRC Press, Taylor & Francis Group.

[67] Shah, V., Scrivener, K., Bhattacharjee, B., Bishnoi, S., 2018. "Changes in microstructure characteristics of cement paste on carbonation." Cement and Concrete Research 109, 184–197. URL: https://doi.org/10.1016/j.cemconres.2018.04.016, doi:10.1016/j. cemconres.2018.04.016.

[68] Sharma, D., Goyal, S., 2020. "Effect of accelerated carbonation curing on near surface properties of concrete." https://doi.org/10.1080/19648189.2019.1707714 URL: https://www.tandfonline.com/doi/abs/10.1080/19648189.2019.1707714, doi:10.1080/19648189. 2019.1707714.

[69] Tak´euchi, Y., Nishi, F., 1980. "Crystal-chemical characterization of the 3CaO·Al2O3—Na2O solid-solution series. Zeitschrift fu¨r Kristallographie - Crystalline Materials 152, 259– 308. URL: https://www.degruyter.com/document/doi/10.1524/zkri.1980.152.14.259/html, doi:10.1524/ZKRI.1980.152.14.259.

[70] Vijai, K., Kumutha, R., Vishnuram, B.G., 2010. "Effect of types of curing on strength of geopolymer concrete." International Journal of Physical Sciences 5, 1419–1423. URL:https://academicjournals.org/journal/IJPS/article-abstract/D33A2EE30426, doi:10.5897/IJPS.9000200.

[71] Wu, B., Ye, G., 2017. "Development of porosity of cement paste blended with supplementary cementitious materials after carbonation." Construction and Building Materials 145, 52– 61. doi:10.1016/J.CONBUILDMAT.2017.03.176.

[72] Yio, M.H., Phelan, J.C., Wong, H.S., Buenfeld, N.R., 2014. "Determining the slag fraction, water/binder ratio and degree of hydration in hardened cement pastes." Cement and Concrete Research 56, 171–181. doi:10.1016/J.CEMCONRES.2013.12.002.

[73] YOUNG, J.F., BERGER, R.L., BREESE, J., 1974. "Accelerated Curing of Compacted Calcium Silicate Mortars on Exposure to CO2." Journal of the American Ceramic Society doi:10.1111/j.1151-2916.1974.tb11420.x.

[74] Zienkiewicz, O.C., Taylor, R.L.R.L., Nithiarasu, P., Zienkiewicz, O.C., Zienkiewicz, O.C., 2005. "The finite element method for fluid dynamics , 435. "

[75] Zongjin, L., 2011. "Advanced concrete technology." Hoboken, New Jersey: John Wiley & Sons, Inc .

ACKNOWLEDGEMENTS

I would like to express my deepest gratitude to Professor Hyeong-Ki Kim, for his advice and continuous support through all stages of this research and my stay in South Korea. I am grateful for his advice and guidance that helped me through the experiment and thesis preparation. I feel honored to work and to study under such thoughtful and respected person.

I would like to express my sincere thanks to Dr. Hyo-kyoung Lee for her cooperative response in the experimental investigation and her limitless support in my stay in South Korea. I would like to acknowledge Dr. Jena Jeong and Dr. Hamidréza Ramézani, for their numerical model. It used to verify the experimental investigation in a better way with reasonable concepts.

My special thanks goes to my fellow lab mates and friends: Abel Shiferaw, Minuye Mesfin, Elsa Tadege, Jae Seong Ahn, Sang-Min Jeon, Jeong eun Kim, and Yu Jin Kim. I would like to extend my gratitude to my friend and former lab mate Dr. Million Tafesse. I thank you all for your valuable contribution and endless support.

I would like to thank you my family for their support and encouragement that brought me up to this stage. Finally I thank you my friends in South Korea, for making me to feel as I am in my home country.